

ELECTROCHEMICAL DETECTION OF DOPAMINE IN THE PRESENCE OF
EXCESS ASCORBIC ACID USING GLASSY CARBON ELECTRODES
MODIFIED WITH CONDUCTING POLYMERS

A THESIS SUBMITTED TO
THE GRADUATE SCHOOL OF NATURAL AND APPLIED SCIENCES
OF
MIDDLE EAST TECHNICAL UNIVERSITY

BY

SAMET ŞANLI

IN PARTIAL FULFILLMENT OF THE REQUIREMENTS
FOR
THE DEGREE OF MASTER OF SCIENCE
IN
POLYMER SCIENCE AND TECHNOLOGY

NOVEMBER 2018

Approval of the thesis:

**ELECTROCHEMICAL DETECTION OF DOPAMINE IN THE PRESENCE
OF EXCESS ASCORBIC ACID USING GLASSY CARBON ELECTRODES
MODIFIED WITH CONDUCTING POLYMERS**

submitted by **SAMET ŞANLI** in partial fulfillment of the requirements for the degree
of **Master of Science in Polymer Science and Technology Department, Middle
East Technical University** by,

Prof. Dr. Halil Kalıpçılar
Dean, Graduate School of **Natural and Applied Sciences**

Prof. Dr. Necati Özkan
Head of Department, **Polymer Science and Technology**

Prof. Dr. Ahmet M. Önal
Supervisor, **Polymer Science and Technology, METU**

Prof. Dr. Mürvet Volkan
Co-Supervisor, **Chemistry, METU**

Examining Committee Members:

Prof. Dr. Necati Özkan
Polymer Science and Technology, METU

Prof. Dr. Ahmet M. Önal
Polymer Science and Technology, METU

Prof. Dr. Mürvet Volkan
Chemistry, METU

Prof. Dr. Atilla Cihaner
Chem. Eng. and App. Chem., Atılım University

Assoc. Prof. Dr. İrem Erel Göktepe
Chemistry, METU

Date: 28.11.2018

I hereby declare that all information in this document has been obtained and presented in accordance with academic rules and ethical conduct. I also declare that, as required by these rules and conduct, I have fully cited and referenced all material and results that are not original to this work.

Name, Surname: Samet Şanlı

Signature:

ABSTRACT

ELECTROCHEMICAL DETECTION OF DOPAMINE IN THE PRESENCE OF EXCESS ASCORBIC ACID USING GLASSY CARBON ELECTRODES MODIFIED WITH CONDUCTING POLYMERS

Şanlı, Samet

Master of Science, Polymer Science and Technology

Supervisor: Prof. Dr. Ahmet M. Önal

[Co-Supervisor: Prof. Dr. Mürvet Volkan]

November 2018, 96 pages

In this study, the main goal was to prepare new modified electrodes to be used in the dopamine (DA) determination in the presence of ascorbic acid (AA). For this purpose, the surface of glassy carbon electrodes (GCE) were modified with poly(3,4-ethylenedioxythiophene) (PEDOT), polyoxometalate (POM) doped PEDOT, poly(9-amino fluorene) (P9AF) and poly(9-fluorene carboxylic acid) (PFCA) by using electrochemical polymerization method.

The modified electrodes were used as a working electrode in the presence of excess AA in DA determination using differential pulse voltammetry (DPV). The results showed that PEDOT-POM electrodes enhanced the current response of DA compared to that of PEDOT modified electrode. The effect of pH on the performance of POMs was evaluated.

Electrochemical oxidation of DA in the presence of AA on glassy carbon electrode modified with P9AF was also investigated. It was found that modified electrode with P9AF can separate the oxidation potential of AA and DA at pH=4 and pH=5 phthalate buffer media. On the other hand, PFCA modified GC electrode exhibited well-separated oxidation potentials for AA and DA in different buffer solutions. The limit

of detection of DA in the presence of 15 mM AA at pH=4 was calculated as 5.2 μ M in the concentration range from 0.03 mM to 1.5 mM. It was observed that the proposed electrode still has high stability when stored at dry ambient conditions for three days. Satisfactory results with good recovery values were obtained for the determination of DA in dopamine injection solution.

Keywords: Dopamine, Ascorbic Acid, Poly(3,4-Ethylenedioxythiophene), Poly(9-Amino Fluorene), Poly(9-Fluorene Carboxylic Acid)

ÖZ

İLETKEN POLİMERLER İLE MODİFİYE EDİLMİŞ CAMSI KARBON ELEKTROTLAR KULLANARAK AŞIRI ASKORBİK ASİT VARLIĞINDA DOPAMİNİN ELEKTROKİMYASAL TESPİTİ

Şanlı, Samet

Yüksek Lisans, Polimer Bilim ve Teknolojisi

Tez Danışmanı: Prof. Dr. Ahmet M. Önal

Ortak Tez Danışmanı: Prof. Dr. Mürvet Volkan

Kasım 2018, 96 sayfa

Bu çalışmada temel amaç, askorbik asit (AA) varlığında dopamin (DA) tayininde kullanılmak üzere yeni modifiye elektrotların hazırlanmasıdır. Bu amaçla camı karbon elektrotların yüzeyi poli(3,4-etilendioksitiyofen) (PEDOT), polioksometalat (POM) katkılı PEDOT, poli(9-amino floren) (P9AF) ve poli(9-floren karboksilik asit) (PFCA) ile elektrokimyasal polimerizasyon yöntemi kullanılarak modifiye edilmiştir. Modifiye elektrotlar çalışma elektodu olarak aşırı AA varlığında DA tayininde kullanılmıştır. Bu tayin için diferansiyel puls voltametri tekniği kullanılmıştır. Sonuçlar, PEDOT-POM elektrotların, PEDOT modifiye elektrotundakine kıyasla DA'nin akım cevabını arttırdığını göstermiştir. pH'ın POM'ların performansına etkisi değerlendirilmiştir.

P9AF ile modifiye edilmiş camı karbon elektrotlar kullanılarak AA varlığında DA'nin oksidasyonu da bu çalışmada araştırılmıştır. P9AF ile modifiye edilmiş elektrotun AA ve DA'nin oksidasyon potansiyelini pH=4 ve pH=5 ftalat tampon ortamlarında ayırabileceği bulunmuştur. Diğer taraftan, PFCA ile modifiye edilmiş GC elektrot farklı tampon çözeltilerde AA ve DA için iyi ayrılmış oksidasyon potansiyelleri sergilemiştir. pH=4'te 15 mM AA varlığında DA'nin tespit limiti, 0.03

mM ile 1.5 mM derişim aralıęında 5.2 μ M olarak hesaplanmıřtır. Önerilen elektrotun kuru ortam kořullarında üç gün boyunca saklandığında hala yüksek kararlılıęa sahip olduęu gözlenmiřtir. Dopamin enjeksiyon solüsyonunda DA tayini için iyi geri kazanım deęerleri ile tatmin edici sonuçlar elde edilmiřtir.

Anahtar Kelimeler: Dopamin, Askorbik Asit, Poli(3,4-Etilendioksitiyofen), Poli(9-Amino Floren), Poli(9-Floren Karboksilik Asit)

To my beloved Bêrivan,

ACKNOWLEDGMENTS

It is a pleasure to thank the many people who made this thesis possible.

I would first like to thank my supervisor Prof. Dr. Ahmet M. Önal for his patient guidance and supports through the learning process of this master thesis. I feel honored to have a chance to work with him.

I would also like to thank my co-supervisor Prof. Dr. Mürvet Volkan for her encouragement and valuable ideas.

I would like to thank my lab-mates Deniz Çakal, Merve Akbayrak, Elif Arabacı, Yalçın Boztaş and Deniz Eroğlu for their supports and friendship.

I wish to thank my co-workers Hasan Basri Boz, Muammer Kahraman, Ramazan Özdemir, Halil Yıldız and Muhammet Ballıkaya for their friendship and providing enjoyable working environment.

I am grateful to my friends Amine Çiçek and Devran Ceng Çelik for their encouragement and endless support.

I wish to thank my fiancée Berivan Uçar for all the emotional and moral support. I will be grateful forever for her love.

Lastly, I wish to thank my dear parents, Filiz Şanlı and Secaattin Şanlı for their continuous encouragement and endless support throughout my years of study

TABLE OF CONTENTS

ABSTRACT	v
ÖZ	vii
ACKNOWLEDGMENTS	x
TABLE OF CONTENTS	xi
LIST OF TABLES	xvi
LIST OF FIGURES	xvii
LIST OF SCHEMES	xxii
CHAPTERS	
1. INTRODUCTION	1
1.1. Conducting Polymers	2
1.1.1. Synthesis of Conducting Polymers	3
1.1.2. Applications of Conducting Polymers	4
1.1.3. Examples of Conducting Polymers.....	5
1.1.4. Conducting Polymers used for Electrode Modification in this Thesis	7
1.1.4.1. Poly(3,4-ethylenedioxythiophene)	7
1.1.4.2. Poly (9-fluorene carboxylic acid).....	7
1.1.4.3. Poly (9-amino fluorene)	7
1.2. Polyoxometalates (POMs).....	8
1.2.1. Polyoxometalates used for Electrode Modifications in this Thesis	11
1.2.1.1. Ammonium Salt of 18-Molybdo-2-Phosphate $(\text{NH}_4)_6\text{P}_2\text{Mo}_{18}\text{O}_{62}$	11
1.2.1.2. Tetrabutylammonium Salt of 12-Molybdo Silicate $[(\text{C}_4\text{H}_9)_4\text{N}]_4\text{SiMo}_{12}\text{O}_{40}$	11

1.2.1.3. 12-Molybdo Phosphoric Acid $H_3PMo_{12}O_{40}$	12
1.3. Biological Compounds used for Analyzing in this Thesis.....	12
1.3.1. Dopamine	12
1.3.2. Ascorbic Acid.....	14
1.4. Electroanalytical Techniques	15
1.4.1. Voltammetric Techniques	15
1.4.1.1. Cyclic Voltammetry (CV)	16
1.4.1.2. Differential Pulse Voltammetry (DPV)	18
1.5. Chemically Modified Electrodes (CME)	19
1.6. Application of Conducting Polymers to Chemical and Biochemical Sensors	20
1.7. Literature Survey related with Determination of DA in the presence of AA with Conducting Polymers.....	21
1.8. The Aim of This Study.....	24
2. EXPERIMENTAL	27
2.1. Materials.....	27
2.2. Preparation of Buffer Solutions	27
2.3. Apparatus	28
2.4. Electrochemical Techniques	29
2.5. Preparation of Modified Electrodes	30
2.5.1. Preparation of Poly(3,4-ethylenedioxythiophene) /GCE, (PEDOT)/GCE	30
2.5.2. Preparation of PEDOT- $(NH_4)_6P_2Mo_{18}O_{62}$ /GCE, (PEDOT- P_2Mo_{18})/GCE	30
2.5.3. Preparation of PEDOT- $(TBA)_4SiMo_{12}O_{40}$ /GCE, (PEDOT- $SiMo_{12}$)/GCE	30

2.5.4. Preparation of PEDOT-H ₃ PMo ₁₂ O ₄₀ /GCE, (PEDOT-PMo ₁₂)/GCE.....	31
2.5.5. Preparation of Poly (9-amino fluorene)/GCE, (P9AF)/GCE.....	31
2.5.6. Preparation of Poly (9-fluorene carboxylic acid)/GCE, (PFCA)/GCE.....	31
2.6. Determination of AA and DA by DPV Technique	31
2.6.1. Preparation of Calibration Studies at Different pHs Values.....	31
3. RESULTS AND DISCUSSION.....	33
3.1. Electrochemical Polymerization and Behavior of PEDOT and PEDOT/POMs	33
3.1.1. Electrochemical Polymerization and Mechanism of PEDOT Formation.	33
3.1.2. Electrochemical Polymerization and Electrochemical Behavior of PEDOT-(NH ₄) ₆ P ₂ Mo ₁₈ O ₆₂	35
3.1.3. Electrochemical Polymerization and Electrochemical Behavior of PEDOT-(TBA) ₄ SiMo ₁₂ O ₄₀	38
3.1.4. Electrochemical Polymerization and Electrochemical Behavior of PEDOT-H ₃ PMo ₁₂ O ₄₀	40
3.2. Comparison of the Electrochemical Performances of PEDOT and PEDOT POMs modified electrodes for the measurement of DA Signal.....	42
3.2.1. Comparison of the Electrochemical Performances of PEDOT/GC and PEDOT-(NH ₄) ₆ P ₂ Mo ₁₈ O ₆₂ /GC (PEDOT-P ₂ Mo ₁₈)/GC electrodes for the measurement of DA Signal.....	42
3.2.2. Comparison of the Electrochemical Performances of PEDOT/GC and PEDOT-(TBA) ₄ SiMo ₁₂ O ₄₀ /GC (PEDOT-SiMo ₁₂)/GC electrodes for the measurement of DA Signal.....	45
3.2.3. Comparison of the Electrochemical Performances of PEDOT/GC and PEDOT-H ₃ PMo ₁₂ O ₄₀ /GC (PEDOT-PMo ₁₂)/GC electrodes for the measurement of DA Signal	46

3.3. Electrochemical Polymerization and Electrochemical Behavior of Poly (9-amino fluorene)	49
3.4. Characterization of P9AF Film	52
3.4.1. Spectroelectrochemical Property of P9AF Film	52
3.4.2. Fourier Transform Infrared Spectroscopy (FT-IR) of 9AF and P9AF.....	53
3.5. Electrocatalytic Oxidation of DA in the Presence of AA at the P9AF/GCE..	54
3.6. Electrochemical Polymerization and Electrochemical Behavior of Poly (9-fluorene carboxylic acid)	56
3.7. Optimization of the Polymerization Conditions	59
3.7.1. 9-Fluorene Carboxylic Acid Oxidation in Different Electrolytic Solutions	59
3.7.2. Effect of the Amount of Trifluoroacetic Acid (TFA) in the Electrolytic Solution for the Electrochemical Behavior of AA and DA.....	60
3.7.3. Effect of Number of Polymerization Cycles on PFCA Film.....	61
3.8. Characterization Studies of PFCA Film.....	62
3.8.1. Spectroelectrochemical Behavior of PFCA Film.....	62
3.8.2. Fourier Transform Infrared Spectroscopy (FT-IR) of FCA and PFCA ...	63
3.9. Electrocatalytic Oxidation of DA in the Presence of AA at the PFCA/GCE .	64
3.9.1. Electrochemical Behavior of AA and DA on BARE/GCE and PFCA/GCE in Different Media	65
3.9.2. Effect of pH on the peak currents and peak potentials of DA and AA	70
3.9.3. Effect of Scan Rate.....	73
3.9.4. Effect of Polymer Coating on Oxidation Potential of AA and DA Compared to that of Bare Electrode.....	75
3.9.5. Stability of PFCA/GCE.....	76

3.10. Comparison of the performances of PEDOT/GCE, P9AF/GCE and PFCA/GCE in terms of their electrochemical responses for AA and DA	77
3.11. Analysis of DA in Real Sample	80
4. CONCLUSIONS	83
REFERENCES.....	85

LIST OF TABLES

TABLES

Table 1.1. Comparison of chemical and electrochemical polymerization techniques to form conducting polymer (CP) [8].	4
Table 3.1. Comparison of the response characteristics of different modified electrodes for the determination of DA in the presence of AA	80
Table 3.2. Determination of DA in dopamine hydrochloride injection ampoule.	81

LIST OF FIGURES

FIGURES

Figure 1.1. Polaron and bipolaron formation in a heterocyclic polymer. X=S, N, or O [7].	3
Figure 1.2. Some examples of the intrinsically conducting polymers [6].	6
Figure 1.3. Structural formula of monomers used in this thesis a) EDOT b) FCA and c) 9AF	8
Figure 1.4. The Keggin structure [28].	9
Figure 1.5. The chemical structure of $P_2W_{18}O_{62}^{6-}$ (Dawson-Type) [30].	10
Figure 1.6. Schematic diagram of three-electrode system.	16
Figure 1.7. A triangular waveform potential excitation signal with switching potentials between 0.8 and -0.2 V versus saturated calomel electrode (SCE) as a reference electrode [60].	17
Figure 1.8. Cyclic voltammogram of 6 mM $K_3Fe(CN)_6$ in 1M KNO_3 at 50 mV/s, where E_{pa} and E_{pc} are anodic and cathodic peak potentials, i_{pa} and i_{pc} are anodic and cathodic peak currents, respectively [60].	18
Figure 1.9. The excitation waveform of the DPV.	19
Figure 1.10. The generic illustration of modified electrode [63].	20
Figure 1.11. The schematic diagram of a biosensor. A biological sensing element like enzyme, antibody detects a biochemical signal from the analyte and the signal is transferred to the transducer such as a conducting polymer [7].	21
Figure 2.1. Three-electrode cell system	29
Figure 3.1. Voltammetric generation of PEDOT film in acetonitrile solution containing 10 mM EDOT and 33 mM $LiClO_4$. Scan rate was 100 mV/s. Inset: 1 st cycle.	34
Figure 3.2. Voltammetric generation of PEDOT-P_2Mo_{18} film was carried in a solution containing 0.5 mM $(NH_4)_6P_2Mo_{18}O_{62}$ in deionized water and 10 mM EDOT in acetonitrile (1:1 by volume). Scan rate was 100 mV/s.	36

Figure 3.3. First and fourth cycles of electropolymerization process in a solution containing 0.5 mM $(\text{NH}_4)_6\text{P}_2\text{Mo}_{18}\text{O}_{62}$ in deionized water and 10 mM EDOT in acetonitrile (1:1 by volume). Scan rate was 100 mV/s.....	37
Figure 3.4. Cyclic voltammograms of Bare GCE , (PEDOT)/GCE and (PEDOT-P_2Mo_{18})/GCE in 0.2 M $\text{H}_2\text{SO}_{4(\text{aq})}$ solution. Scan rate was 100 mV/s.....	38
Figure 3.5. Voltammetric generation of PEDOT-SiMo₁₂ film was carried out in a solution containing 2.5 mM $(\text{TBA})_4\text{SiMo}_{12}\text{O}_{40}$ and 50 mM EDOT in acetonitrile (1:1 by volume). Scan rate was 100 mV/s.	39
Figure 3.6. Cyclic voltammogram of PEDOT-SiMo₁₂ film in 0.2 M $\text{H}_2\text{SO}_{4(\text{aq})}$ solution. Scan rate was 100 mV/s.....	40
Figure 3.7. Voltammetric generation of PEDOT-PMo₁₂ film was carried out in a solution containing 0.5 mM $\text{H}_3\text{PMo}_{12}\text{O}_{40}$, 10 mM EDOT in acetonitrile and 0.2 M $\text{H}_2\text{SO}_{4(\text{aq})}$ (2:2:1, respectively). Scan rate was 100 mV/s.	41
Figure 3.8. Differential pulse voltammograms of PEDOT-PMo₁₂ and PEDOT modified electrodes in 0.2 M $\text{H}_2\text{SO}_{4(\text{aq})}$ solution.	42
Figure 3.9. Comparison differential pulse voltammograms of PEDOT/GCE and PEDOT-P_2Mo_{18}/GCE for 1 mM and 10 mM dopamine solutions in 0.2 M $\text{H}_2\text{SO}_{4(\text{aq})}$	43
Figure 3.10. Differential pulse voltammograms of blanks and 10 mM DA at the PEDOT-P_2Mo_{18}/GCE electrode in different media.	44
Figure 3.11. Differential pulse voltammograms of 10 mM dopamine at the PEDOT/GCE in 0.2 M $\text{H}_2\text{SO}_{4(\text{aq})}$ and pH=4 phthalate buffer solution containing 0.1 M $\text{KCl}_{(\text{aq})}$	44
Figure 3.12. Comparison differential pulse voltammograms of PEDOT/GCE and PEDOT-SiMo₁₂/GCE in 10 mM DA solution containing 0.2 M $\text{H}_2\text{SO}_{4(\text{aq})}$	45
Figure 3.13. Comparison differential pulse voltammograms of PEDOT/GCE and PEDOT-SiMo₁₂/GCE for 1 mM dopamine solution in pH=7 phosphate buffer containing 0.1 M $\text{KCl}_{(\text{aq})}$	46
Figure 3.14. Comparison of differential pulse voltammograms of PEDOT/GCE and PEDOT-PMo₁₂/GCE for 1 mM dopamine solution in 0.2 M $\text{H}_2\text{SO}_{4(\text{aq})}$	47

Figure 3.15. Comparison differential pulse voltammograms of PEDOT/GCE and PEDOT-PMo₁₂/GCE for 1 mM dopamine solution in pH=4 phthalate buffer solution containing 0.1 M KCl _(aq)	48
Figure 3.16. The response of PEDOT/GCE to the 30 mM AA and 15 mM DA in 0.2 M H ₂ SO _{4(aq)} solution.	49
Figure 3.17. Voltammetric generation of P9AF film in boron trifluoride diethyl etherate (BFEE) and trifluoroacetic acid (TFA) mixture (70/30; v/v) containing 25 mM 9-aminofluorene . Scan rate was 100 mV/s. Inset: 1 st cycle.....	50
Figure 3.18. Cyclic voltammogram of P9AF/GCE in monomer free DCM containing 0.1 M TBAPF ₆ solution. Scan rate was 100 mV/s.....	52
Figure 3.19. The changes in the electronic absorption spectra of electrochemically obtained P9FA film recorded in DCM containing TBAPF ₆ as a function of applied potentials between -0.3 V and +1.3 V.....	53
Figure 3.20. FTIR spectra of 9AF and P9AF a) in the range of 3600-700 cm ⁻¹ b) in the range of 800-1600 cm ⁻¹ c) in the range of the 700-800 cm ⁻¹	54
Figure 3.21. Differential pulse voltammograms of AA and DA in pH=4 and pH=5 phthalate buffer solution containing 0.1 M KCl _(aq) at modified P9AF/GCE . AA and DA concentrations are 30 mM and 3 mM , respectively.	55
Figure 3.22. Differential pulse voltammograms of 30 mM AA and 3 mM DA in 0.2 M H ₂ SO ₄ (pH<1) and pH=7.4 phosphate buffer solution containing 0.1 M KCl _(aq) at modified P9AF/GCE	56
Figure 3.23. Voltammetric generation of PFCA in boron trifluoride diethyl etherate (BFEE) -trifluoroacetic acid (TFA) mixture (70/30; v/v) containing 25 mM 9-fluorenicarboxylic acid . Scan rate was 100 mV/s. Inset: shows 1 st cycle.....	57
Figure 3.24. Cyclic voltammogram of PFCA/GCE in monomer free BFEE - TFA mixture (70/30; v/v). Scan rate was 100 mV/s.....	59
Figure 3.25. 25 mM FCA oxidation potentials in different electrolytic solutions....	60
Figure 3.26. Effect of TFA amount in electrolytic solution for the quality of PFCA film. 15 mM AA and 3 mM DA in pH=4 phthalate buffer containing 0.1 M KCl _(aq) solution.....	61

Figure 3.27. Effect of number of cycles used in the polymerization of FCA in terms of its response to 30 mM AA and 3 mM DA in pH=5 phthalate buffer containing 0.1 M $\text{KCl}_{(\text{aq})}$. Inset: Signal intensity versus number of polymerization cycles.....	62
Figure 3.28. The changes in the electronic absorption spectra of electrochemically obtained PFCA film recorded in BFEE/TFA (70/30; v/v) mixture as a function of applied potentials between 0.0 V and +1.2 V.....	63
Figure 3.29. a) FT-IR spectra of FCA and PFCA . b) The region between 1200 cm^{-1} and 550 cm^{-1} of the spectra of FCA and PFCA is given in an enlarged scale.....	64
Figure 3.30. Differential pulse voltammogram of 15 mM AA and 3 mM DA mixture at bare GCE in 0.2 M $\text{H}_2\text{SO}_{4(\text{aq})}$ solution.	65
Figure 3.31. a) Differential pulse voltammogram of 0.3-15.0 mM DA in the presence of 15.0 mM AA in 0.2 M $\text{H}_2\text{SO}_{4(\text{aq})}$ solution. b) Calibration plot of DA	66
Figure 3.32. Differential pulse voltammogram of 15.0 mM AA and 3.0 mM DA mixture at bare GCE in pH=4 phthalate buffer containing 0.1 M $\text{KCl}_{(\text{aq})}$ solution.	67
Figure 3.33. a) Differential pulse voltammogram of 0.03-1.50 mM DA in the presence of 15.0 mM AA in pH=4 phthalate buffer solution containing 0.1 M $\text{KCl}_{(\text{aq})}$. b) Calibration plot of DA	68
Figure 3.34. The differential pulse voltammogram of 15 mM AA and 3 mM DA mixture at bare GCE in pH=5 phthalate buffer solution containing 0.1 M $\text{KCl}_{(\text{aq})}$ solution.	69
Figure 3.35. a) Differential pulse voltammogram of 0.015-3.0 mM DA in the presence of 15.0 mM AA in pH=5 phthalate buffer solution containing 0.1 M $\text{KCl}_{(\text{aq})}$ solution. b) Calibration plot of DA	70
Figure 3.36. Differential pulse voltammograms mixture of 15.0 mM AA and 0.30 mM DA in different media.....	72
Figure 3.37. Effect of pH on (a) 0.30 mM DA peak current and (b) 0.30 mM DA peak potential.....	72
Figure 3.38. (a) Cyclic voltammograms of 1.0 mM DA between 40 and 320 mV s^{-1} in pH=4 phthalate buffer containing 0.1 M $\text{KCl}_{(\text{aq})}$. (b) The plot of oxidation peak current vs square root of scan rate.	74

Figure 3.39. The comparison of cyclic voltammograms of **PFCA/GCE** and **BARE/GCE** before and after the immersion in **1.0 mM DA** solution. The CVs recorded in pH=4 phthalate buffer solution containing 0.1 M $\text{KCl}_{(\text{aq})}$. Scan rate is 100 mV/s.75

Figure 3.40. Differential pulse voltammograms of **10.0 mM AA** and **1.0 mM DA** in pH=4 phthalate buffer solution containing 0.1 M $\text{KCl}_{(\text{aq})}$ on **BARE/GCE**.76

Figure 3.41. Stability test of the **PFCA/GCE**. The solution was **15.0 mM AA** and **1.5 mM DA** in pH=4 phthalate buffer solution containing 0.1 M $\text{KCl}_{(\text{aq})}$77

Figure 3.42. (a) The comparison of the responses of **P9AF/GCE** and **PFCA/GCE** to the **15.0 mM AA** and **3.0 mM DA** in pH=5 phthalate buffer solution containing 0.1 M $\text{KCl}_{(\text{aq})}$. (b) For clarity DPV of the **P9AF/GCE** is presented in a larger scale.78

Figure 3.43. The comparison response of **PEDOT/GCE** and **PFCA/GCE** to the **15 mM AA** and **0.15 mM DA** in pH=5 phthalate buffer solution containing 0.1 M $\text{KCl}_{(\text{aq})}$79

LIST OF SCHEMES

SCHEMES

Scheme 1.1. Electrochemical oxidation of dopamine.....	13
Scheme 1.2. The oxidation process of AA.....	14
Scheme 3.1. The proposed oxidative electrochemical polymerization of EDOT [83]	37
Scheme 3.2. Possible mechanism for the electrochemical polymerization of 9AF [86].....	52
Scheme 3.3. Possible mechanism for the electrochemical polymerization of FCA [86].....	59
Scheme 3.4. Various forms of DA as a function of pH [92].....	74

CHAPTER 1

INTRODUCTION

Electroanalytical techniques are widely used for detecting important chemicals such as dopamine, ascorbic acid, urea and many others [1]. Although low cost of the electroanalytical techniques is an advantage, sometimes low sensitivity and selectivity [1] might be an important drawback of these techniques. One way of improving selectivity and sensitivity is to use modified electrodes. Modified electrodes can be prepared by using chemical or electrochemical techniques to produce suitable objectives [2]. They carry different chemical or electrochemical properties as compared to unmodified electrodes. Generally, electrode modification is considered necessary not only for providing selectivity and sensitivity of the electrodes but also for improving the electrocatalytic properties [2], especially in electroanalytical chemistry. Modified electrodes are also used for energy conversion and developing electrochromic devices [1].

As the day goes on, the demand for simple, rapid and inexpensive analytical methods to determine trace concentrations of biologically important compounds is increasing [2]. Ascorbic acid, glucose, uric acid and the catecholamines (epinephrine, norepinephrine and dopamine) can be given as examples for these biologically important compounds. Electroanalytical techniques utilizing modified electrodes are particularly useful for these applications. Modifying the surface of electrodes provides role of chemical sensor and biosensor to detect biologically or clinically important compounds.

Recently, conducting polymers have attracted much interest in the determination of biologically important molecules. Electrode modification with conducting polymers

provide great ease for the fabrication of sensors because of immobilization of biomolecules and rapid electron transfer features of conducting polymers [3].

1.1. Conducting Polymers

Until the discovery of Alan MacDiarmid, Hideki Shirakawa, and Alan Heeger [4], all carbon-based polymers were accepted as insulators because of their very poor electrical conductivities. In the 1800s, to impart electrical conductivity, carbon black which is naturally conductive was added to natural rubber. In the 1930s, natural rubber filled with acetylene black and it was used as an antistatic device [4]. In the year 1975, polysulfurnitride (SN)_x was discovered and an increase in its conducting properties was observed by doping with an electron acceptor such as bromine [4]. In the late 1970s, Alan MacDiarmid, Hideki Shirakawa, and Alan Heeger, found that the electrical conductivity of polyacetylene could also be increased by doping with an electron donor such as sodium naphthalide or an electron acceptor such as I₂, and AsF₅ [5]. This discovery catches scientific community's attention to new conducting polymers.

Conducting polymers carry π - electron in their backbone and these electrons provide electrical conductivity. π - conjugated system of conducting polymers alternates along the polymer chain between single and double bonds [3]. Conducting polymers do not show any conductivity in their neutral state. Their conductivity appears from the formation of charge carriers, in the form of charged polarons or bipolarons, upon oxidizing (p-doping) or reducing (n-doping) and movement of these charge carriers along the conjugated backbone [6]. In Figure 1.1, polaron and bipolaron formations upon oxidation (p-type doping) can be seen.

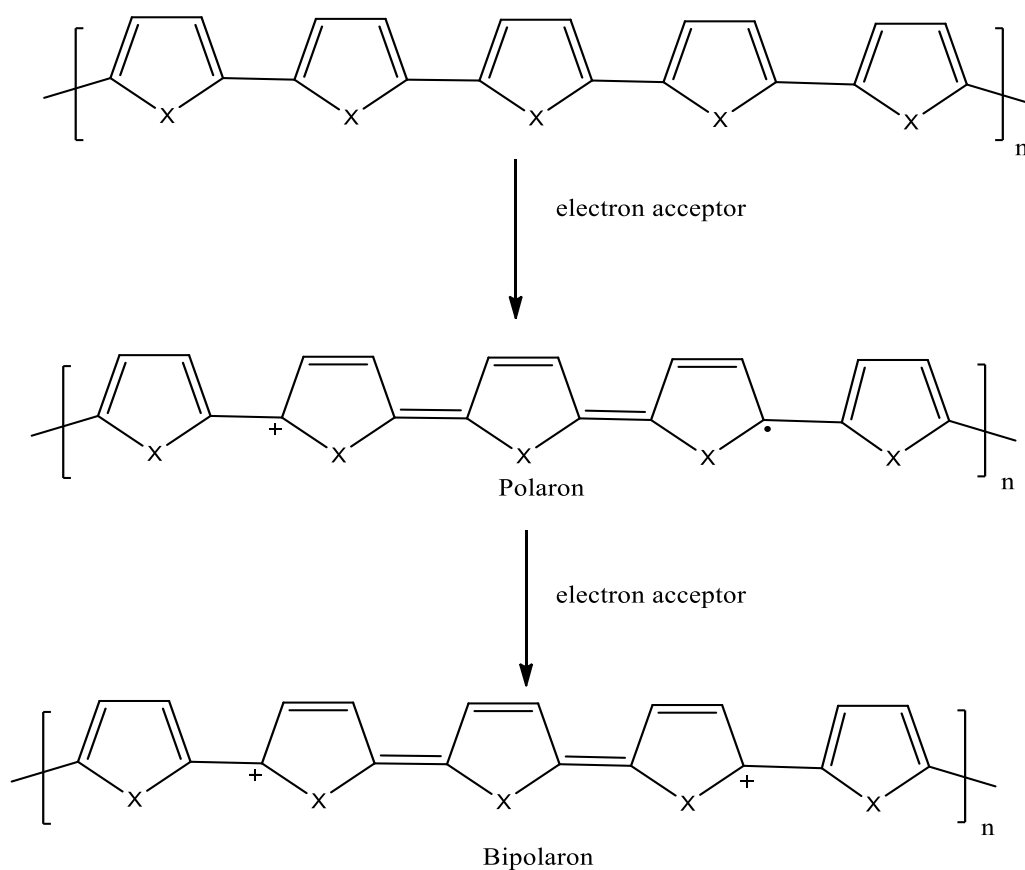


Figure 1.1. Polaron and bipolaron formation in a heterocyclic polymer. X=S, N, or O [7].

1.1.1. Synthesis of Conducting Polymers

The most widely used technique for the synthesis of conducting polymers (CP) is oxidation of monomers, either chemical or electrochemical oxidation, to form a cation radical which might react with a neutral monomer molecule to form dimeric radical-cation. Subsequent addition of this active species leads to formation of polymer chains. Electrochemical polymerizations are mostly preferred because of its simplicity and reproducibility. Moreover, electrochemical polymerization can be carried out at room temperature and film thickness can be controlled by changing current or potential with time [3]. Comparison of electrochemical and chemical polymerizations is given in Table 1.1.

Table 1.1. Comparison of chemical and electrochemical polymerization techniques to form conducting polymer (CP) [8].

Polymerization approach	Advantages	Disadvantages
Chemical polymerization	<p>Larger-scale production possible.</p> <p>Post-covalent modification of bulk CP possible.</p> <p>More options to modify CP backbone covalently.</p>	<p>Difficulty in making thin films</p> <p>More complex synthesis</p>
Electrochemical polymerization	<p>Thin film synthesis possible</p> <p>Ease of synthesis</p> <p>Simultaneous doping during polymer formation</p>	<p>Difficult to remove film from the electrode surface</p> <p>Post-covalent modification of bulk CP is difficult</p>

1.1.2. Applications of Conducting Polymers

After the discovery of conducting polymers in the end of the 1970s, many scientists have been concentrating to find applications for the newly discovered conducting polymers [9].

Many conducting polymers are used for construction of electronic nano-device investigations including field effect transistors (FETs) [10], light emitting diodes (LEDs) [11] because of their high electrical conductivities, mechanical flexibilities and low cost. Moreover, conductivity of conducting polymers may be changed by incorporating them with metals, semiconductors and carbon nanomaterials. These incorporated materials are applicable especially for FETs and LEDs studies [12].

Conducting polymers have also been widely used as chemical sensors, optical sensors and biosensors due to their electrical and optical properties changing reversibly on doped/dedoped states [6,13-15]. Conducting polymers play important role in sensing biomolecules due to their speed and sensitivity. Therefore, conducting polymers provide convenience in medical diagnostics [16].

Energy is the most important problem for the world because of exhausting fossil fuels and conducting polymers also find application areas in solar cells, fuel cells and supercapacitors due to their high capacitance values [12].

Nowadays, biomedical engineering plays important role on human health. Most biological cells exhibit sensitivity towards electrical impulses. The electrical properties of conducting polymers make them suitable candidates for tissue engineering, since they can be used for modulating cellular activities. Moreover, conducting polymer nanostructures are good candidates as artificial muscles because conducting polymers swell with increasing oxidation. The entry of counter anions into the polymer causes the structural change of the polymer backbone and volume. That's why this electromechanical property makes conducting polymers potential candidate in making polymer-based artificial muscles [17].

1.1.3. Examples of Conducting Polymers

Conducting polymers are subdivided into two basic types which are intrinsically conducting polymers and extrinsically conducting polymers. Intrinsically conducting polymers conduct electricity. However, extrinsically conducting polymers are composites which are composed of a conductive material such as carbon black is embedded in a non-conducting polymer such as polyethylene and the resulting composite conducts electricity. The polymer acts as the binder to hold the conducting material [18]. Some of the examples of intrinsically conducting polymers are shown in Figure 1.2.

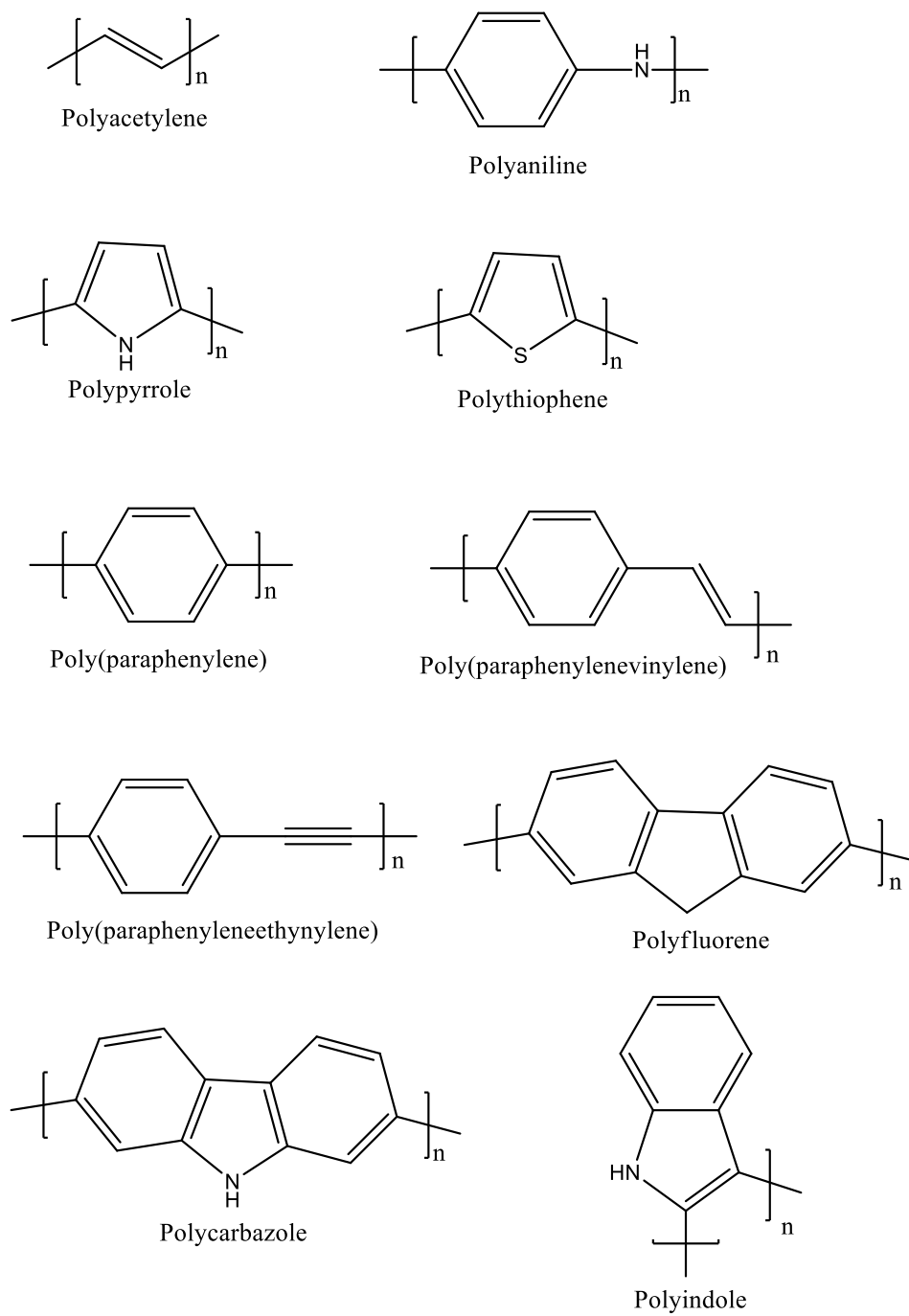


Figure 1.2. Some examples of the intrinsically conducting polymers [6].

1.1.4. Conducting Polymers used for Electrode Modification in this Thesis

1.1.4.1. Poly(3,4-ethylenedioxythiophene)

Poly(3,4-ethylenedioxythiophene), also known as PEDOT, is obtained from 3,4-ethylenedioxythiophene or EDOT. PEDOT has many advantages in terms of optical transparency in its conducting state and high stability in the oxidized state. The synthesis of PEDOT and its derivatives from EDOT based monomers can be realized by oxidative chemical or electrochemical polymerization methods. Mostly, FeCl₃ is used as an oxidizing agent for chemical polymerization. Electrochemical polymerization of EDOT, on the other hand, is more practical since reasonable amount of polymer can be obtained from small amount of monomer in a short time period [19].

1.1.4.2. Poly (9-fluorene carboxylic acid)

Among various conducting polymers, polyfluorenes find wide variety of application areas such as in light emitting diodes and electrochromic devices [20, 21]. Poly (9-fluorene carboxylic acid) (PFCA) is found in polyfluorene family and can be prepared via anodic oxidation of 9-fluorene carboxylic acid (FCA). However, anodic oxidation of monomer is not easy in common neutral solvents due to high oxidation potential of FCA. To overcome this difficulty, different solvents containing boron trifluoride diethyl etherate, trifluoroacetic acid or mixture of both were used to lower the oxidation potential of monomer during its electrochemical polymerization [22, 23].

1.1.4.3. Poly (9-amino fluorene)

Poly (9-amino fluorene) (P9AF) is also found in polyfluorene family and is easily obtained by the direct anodic oxidation of 9-amino fluorene (9AF). The substitution of the C (9) position with amino group in the polyfluorene backbone gives good solubility in water and this solubility in water provides convenience for applications of blue-light emitting studies. Fan et al. found that doped P9AF films in water were

blue-light emitter [24]. The structural formulas of monomers used in this thesis are shown in Figure 1.3.

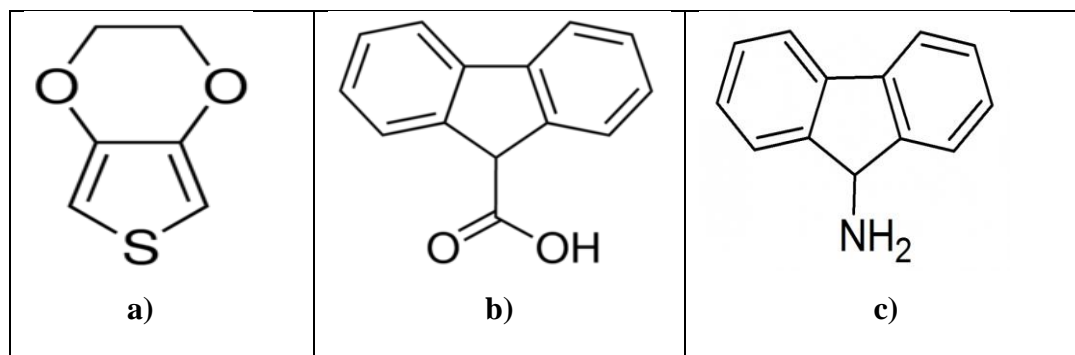


Figure 1.3. Structural formula of monomers used in this thesis **a)** EDOT **b)** FCA and **c)** 9AF

1.2. Polyoxometalates (POMs)

Recently, catalytic redox activity of polyoxometalates (POMs) have drawn attention because of important characteristic features such as high stability of most of their redox states, having possibility of adjusting redox potential by changing hetero ions and/or the addenda ions without affecting their structure, possibility of incorporating various transition metal cations into the polyoxometalate structure. Moreover, POMs make possible multiple electron transfer [25].

Countless polyoxometalates have been prepared and characterized. However, the limited number of POMs, which are Keggin-Type heteropolyanions, Dawson-Type heteropolyanions, Mixed-Addenda heteropolyanions and Transition Metal-Substituted heteropolyanions, are known to give good results for electrocatalytic effect [25].

Keggin-Type structure is the best-known structure of heteropolyanions. The general structure of the Keggin-Type heteropolyanion is $[XM_{12}O_{40}]^{n-}$, where X symbolizes heteroatom such as Si, P etc. and M symbolizes addenda atoms such as W, Mo etc. [26]. In this structure, one heteroatom is surrounded by four oxygen atoms.

Heteroatom is located centrally and 12 MO₆ units cage of it. In 1934, J.F. Keggin explored the structure of Keggin-Type heteropolyanions by using X-Ray diffraction technique [27]. In Figure 1.4, the Keggin Type structure is shown.

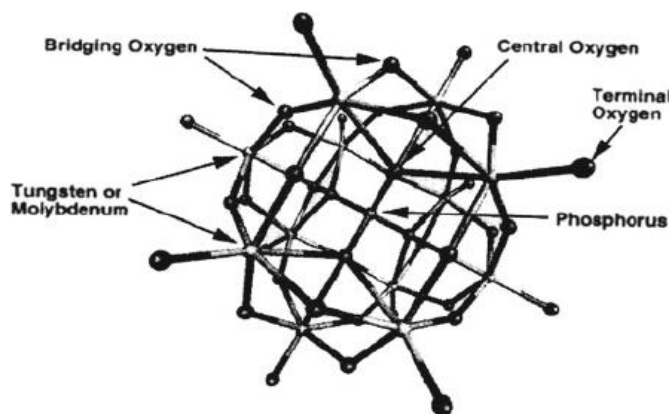


Figure 1.4. The Keggin structure [28].

The chemical formulation of Dawson-type structure is $[X_2M_{18}O_{62}]^{n-}$ where X symbolizes heteroatom such as As, P etc. and M symbolizes addenda atoms such as W, Mo etc. The first crystallographic study of Dawson-type structure was made in 1952 by Dawson [29]. The structure has two identical half units which is XM_9O_{31} and they are linked through oxygen atoms [30]. The structure of $P_2W_{18}O_{62}^{6-}$ is shown in Figure 1.5.

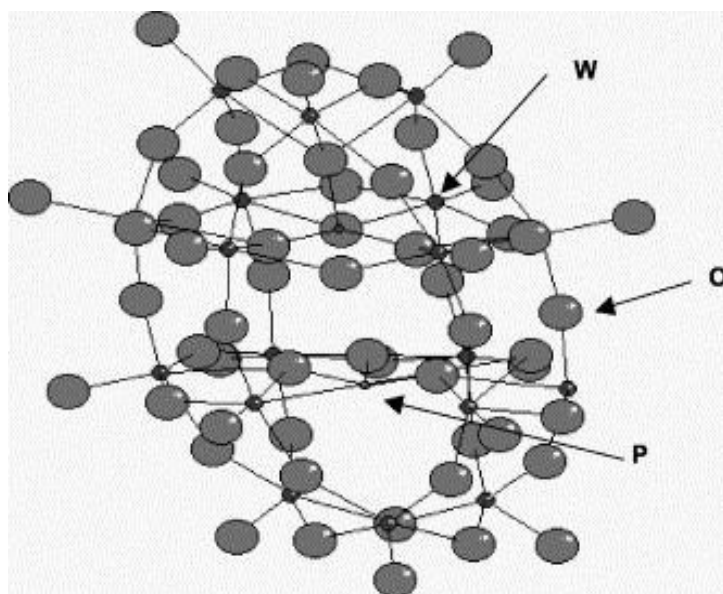


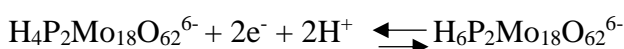
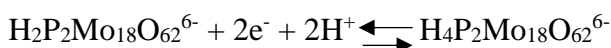
Figure 1.5. The chemical structure of $P_2W_{18}O_{62}^{6-}$ (Dawson-Type) [30].

In recent years, electrocatalytic effect of conducting polymer doped with POMs have drawn great attention. POM doped conducting polymers show electrochemical properties of both for POM and polymer matrix. Generally, a conducting polymer acts as a carrier for catalytically active species in these composite materials [31]. Many studies can be found about immobilization of POMs into the polymeric matrix such as polypyrrole, polythiophene, polyaniline etc. The immobilization of POMs into the polymer matrix is achieved either by chemical or electrochemical methods in a monomer-POMs solution. Heteropolyanions are entrapped into the polymeric matrix by electrostatic interaction with polymer which is pre-formed on the electrode surface or POMs are immobilized simultaneously with the electropolymerization method [25]. The working electrode is covered with the conducting polymer and POM when the suitable oxidation potential is applied, and this modified working electrode can be used for many electrocatalytic studies [32]. For example, Dong and Liu showed that polypyrrole and Dawson-type tungstophosphate modified electrode has catalytic effect on the reduction of oxygen [33]. Pham et al. studied catalytic effect of a phosphomolybdic anion doped poly(5-amino-1-naphthol) on the reduction of chlorate anions [34].

1.2.1. Polyoxometalates used for Electrode Modifications in this Thesis

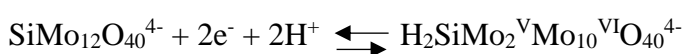
1.2.1.1. Ammonium Salt of 18-Molybdo-2-Phosphate $(\text{NH}_4)_6\text{P}_2\text{Mo}_{18}\text{O}_{62}$

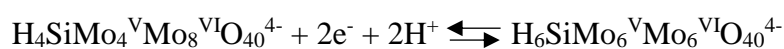
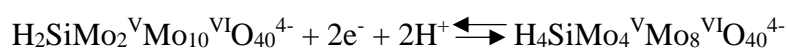
Molybdenum based Dawson type heteropolyanions have drawn great attention because of their catalytic properties. For example, Wijesekera et al. patented catalytic oxidation of alkanes to unsaturated carboxylic acids by using phospho-molybdic compounds [35]. The heteroblu formed by chemical reduction of $(\text{NH}_4)_6\text{P}_2\text{Mo}_{18}\text{O}_{62}$ was first described by Wu (Wu, 1920). $(\text{NH}_4)_6\text{P}_2\text{Mo}_{18}\text{O}_{62}$ have several one electron reductions in organic or aqueous solvents if no protonation accompanies the reductions. The one-electron reductions of $\text{P}_2\text{Mo}_{18}\text{O}_{62}^{6-}$ are converted to two electron reductions by addition of acids. $\text{P}_2\text{Mo}_{18}\text{O}_{62}^{6-}$ have three two electrons and one four electrons reductions which are shown below in acidic solution [25]:



1.2.1.2. Tetrabutylammonium Salt of 12-Molybdo Silicate $[(\text{C}_4\text{H}_9)_4\text{N}]_4\text{SiMo}_{12}\text{O}_{40}$

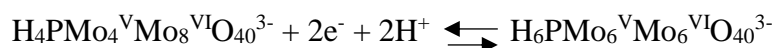
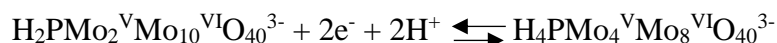
$\text{SiMo}_{12}\text{O}_{40}^{4-}$ can be reduced in aqueous acid solutions such as HCl, HClO_4 , H_2SO_4 , HNO_3 , etc. $\text{SiMo}_{12}\text{O}_{40}^{4-}$ is usually found in combination with organic ammonium cations. $\text{SiMo}_{12}\text{O}_{40}^{4-}$ heteropolyanion adopts the Keggin structure [37]. Its organic ammonium forms are insoluble in water. Electrocatalytic effect of $\text{SiMo}_{12}\text{O}_{40}^{4-}$ has drawn great attention. As an example, Wang et al. observed that modified carbon paste electrodes with $\text{SiMo}_{12}\text{O}_{40}^{4-}$ nanoparticles have electrocatalytic effect on reduction of nitrite in acidic solution [38]. The $\text{SiMo}_{12}\text{O}_{40}^{4-}$ anions are unstable in neutral and basic aqueous solutions because of several hydrolysis process. The electrochemical behavior of $\text{SiMo}_{12}\text{O}_{40}^{4-}$ is summarized below [39]:





1.2.1.3. 12-Molybdo Phosphoric Acid $\text{H}_3\text{PMo}_{12}\text{O}_{40}$

Many voltammetric studies show that 12-molybdo phosphoric acid is easily hydrolyzed in aqueous solutions. However, addition of some organic solvent can prevent hydrolysis. Thus, voltammetric studies are usually carried out in mixed organic-aqueous solvents containing acid because neutral or basic aqueous solutions is not suitable [25]. 12-molybdo phosphoric acid in acidic solutions containing organic solvents undergoes several two electron reductions to yield mixed valence Mo (V) and Mo (VI) species [40]. 12-molybdo phosphoric acid is used in many studies for its electrocatalytic properties. For example, Wang et al. showed electrocatalytic effect of 12-molybdo phosphoric acid on the oxidation of ascorbic acid in acidic solution [41]. The electrochemical behavior of $\text{PMo}_{12}\text{O}_{40}^{3-}$ ion is summarized below [42]:



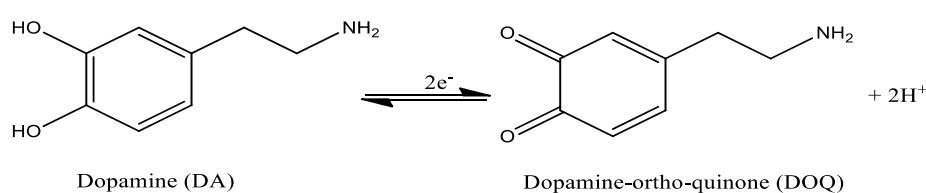
1.3. Biological Compounds used for Analyzing in this Thesis

1.3.1. Dopamine

Dopamine (DA) or 3,4-dihydroxyphenethylamine is a very important organic chemical for brain and body. DA belongs to the family of catecholamine and is synthesized from L-DOPA by removing a carboxyl group. L-DOPA is synthesized in the brain and kidneys. Dopamine is a kind of neurotransmitter which transmits a signal from one neuron to the other neuron. Dopamine provides desire and motivation from the point of pharmacology [43]. Several important diseases are related to the dopamine level in human nervous system. For example, Parkinson's disease is arising from

destruction of dopamine neurons. High levels of dopamine also cause schizophrenia [44].

The measurement of dopamine level in biological systems is very important. In recent years, many techniques have been developed for the determination of dopamine in biological samples. The common analytical techniques have been used for the determination of DA like high performance liquid chromatography (HPLC), capillary electrophoresis and fluorescence [45-47]. However, these methods take time and are very expensive. Electrochemical activity of dopamine, on the other hand, makes its detection possible via electrochemical measurements. Therefore, electrochemical techniques provide a great facility in terms of time and cost. The electrochemical oxidation of dopamine in aqueous solution includes two-electron process with transfer of two protons [48]. The typical oxidation of dopamine to dopamine-ortho-quinone is shown in Scheme 1.1.



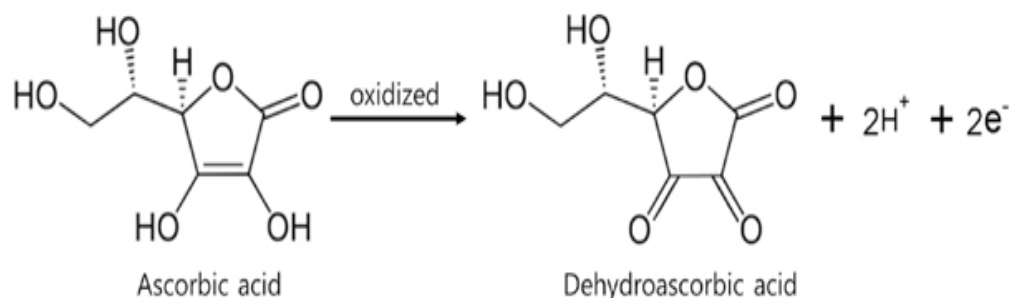
Scheme 1.1. Electrochemical oxidation of dopamine

The main problem for determination of dopamine by using electrochemical methods is interfering substances such as ascorbic acid. Ascorbic acid coexists with dopamine in vivo and its oxidation potential is very close to that of dopamine. In recent years, various methods have been proposed for increasing sensitivity and eliminating interference effect of ascorbic acid in dopamine determination. There are several reports about simultaneous determination of ascorbic acid and dopamine in the literature [49-51].

1.3.2. Ascorbic Acid

Ascorbic Acid (AA), also known as Vitamin C, is a water-soluble antioxidant. Ascorbic acid is an unstable and easily oxidized compound. Since human body cannot synthesize vitamin C, it should be taken from the outside as a supplement. Ascorbic acid is very important compound for functioning of body system. It provides lower blood cholesterol and participates in the synthesis of amino acids. It plays a role for tissue growth and wound healing. As an antioxidant, the most important role of ascorbic acid in body is to prevent harmful effects of free radicals. For these reasons, ascorbic acid is used for treatment of diabetes, cataracts, heart diseases, cancer and so on. Deficiency of ascorbic acid in the body system causes anemia, muscle degeneration, poor wound healing, many infections etc. [52].

Many analytical techniques as in the case of dopamine have been proposed to determine ascorbic acid such as spectrophotometric or chromatographic methods [53, 54]. The electrochemically active nature of AA gives opportunity to electrochemical techniques which are in great demand for the determination of AA due to rapidity and low cost. The oxidation mechanism of AA involves oxidation of hydroxyl group to carbonyl groups in furan ring of AA [55]. According to the literature, the oxidation process of AA involves two electrons and two protons in acidic medium. However, at pH higher than the first pK_a (4.17) of ascorbic acid, the oxidation mechanism includes the loss of single proton and two electrons (Raj, Tokuda, & Ohsaka, 2001). The oxidation process of ascorbic acid is shown in Scheme 1.2.



Scheme 1.2. The oxidation process of AA

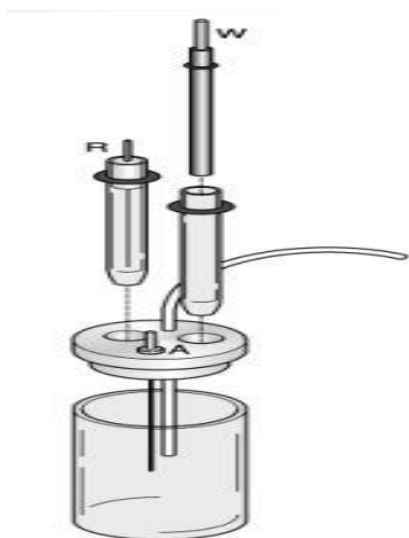
1.4. Electroanalytical Techniques

Electroanalytical techniques are a class of analytical techniques which depend on measuring the potential and/or current of solution of the analyte in an electrochemical cell and provide low detection limits. The instrumentation of electroanalytical techniques is also inexpensive in comparison with the other analytical instruments [57]. Main branches of electroanalytical techniques are potentiometry, coulometry and voltammetry [58]. Voltammetric techniques were used in this study.

1.4.1. Voltammetric Techniques

Voltammetric techniques depend on the measurement of current (i) in an electrochemical cell as a function of applied potential (E). Voltammetry is commonly used for analytical, inorganic, physical, and biological studies of oxidation and reduction process, adsorption process on surfaces and electron transfer mechanisms at surfaces of modified electrodes [58]. Voltammetric techniques provide several advantages in terms of analytical approach such as excellent sensitivity, large useful linear concentration range, rapid analysis time, a wide range of temperatures, and determination of several analytes simultaneously. Voltammetry gives opportunity to analytical chemists for quantitative determination of several dissolved organic and inorganic substances (Kounaves, 1997).

A typical voltammetric experiment is carried out in an electrochemical cell which consists of sample dissolved in a solvent, supporting electrolyte, a working electrode, a counter electrode and a reference electrode (Kounaves, 1997). The analyte oxidation/reduction process takes place at the surface of working electrode and its potential with respect to potential of the reference electrode (constant potential) is controlled throughout the experiment. The current in the cell passes between the working electrode and the counter electrode (Skoog, West, Holler, & Crouch, 2003). The schematic diagram of three-electrode system of an electrochemical cell is shown in Figure 1.6.



A: Counter Electrode
W: Working Electrode
R: Reference Electrode

Figure 1.6. Schematic diagram of three-electrode system.

1.4.1.1. Cyclic Voltammetry (CV)

Cyclic voltammetric technique is widely used for the study of the redox process and reaction intermediates rather than quantitative determinations. This technique depends on monitoring the current as a function of applied potential to the working electrode both in positive and/or negative direction at a constant scan rate (Kounaves, 1997). Typical excitation signal for cyclic voltammetry and cyclic voltammogram of 6 mM $\text{K}_3\text{Fe}(\text{CN})_6$ in 1 M KNO_3 is shown in Figure 1.7 and Figure 1.8, respectively.

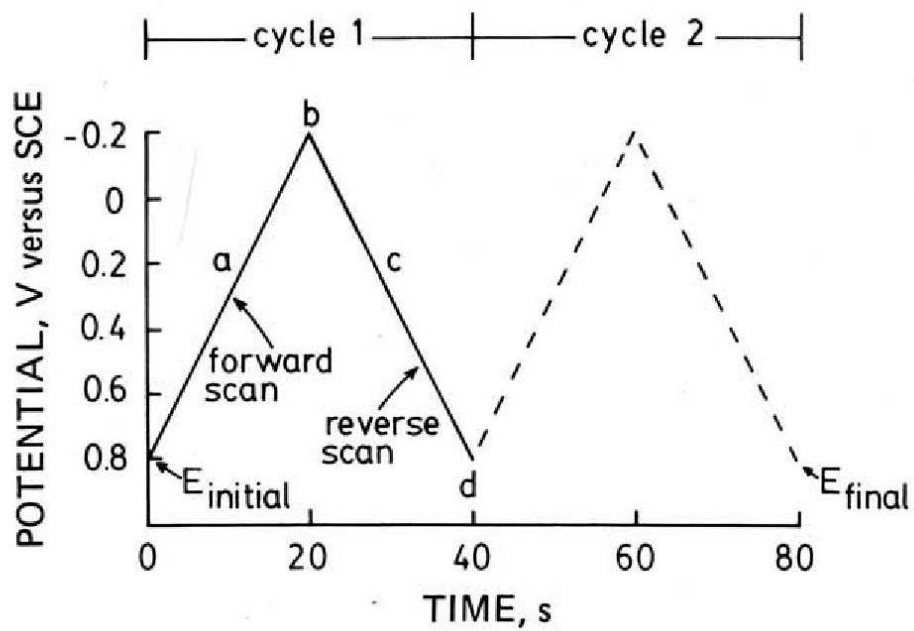


Figure 1.7. A triangular waveform potential excitation signal with switching potentials between 0.8 and -0.2 V versus saturated calomel electrode (SCE) as a reference electrode [60].

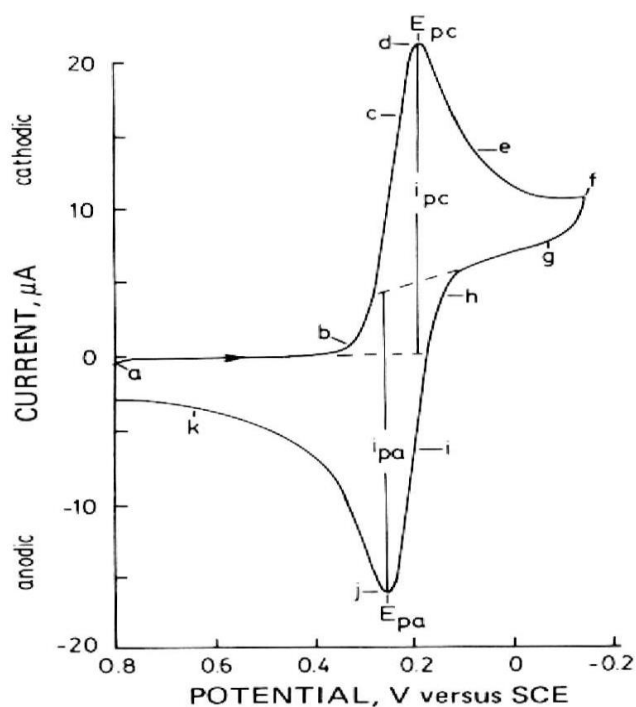


Figure 1.8. Cyclic voltammogram of 6 mM $K_3Fe(CN)_6$ in 1M KNO_3 at 50 mV/s, where E_{pa} and E_{pc} are anodic and cathodic peak potentials, i_{pa} and i_{pc} are anodic and cathodic peak currents, respectively [60].

The cathodic current increases until the surface concentration of $Fe^{III}(CN)_6^{3-}$ diminishing at the electrode surface between (b) and (d) as shown in Figure 1.8 [60]:



The anodic current, on the other hand, increases between (i) and (j) until the surface concentration of $Fe^{II}(CN)_6^{4-}$ diminishing in Figure 1.8 because of the strong oxidant property of electrode [60]:



1.4.1.2. Differential Pulse Voltammetry (DPV)

DPV provides several advantages for analytical measurements when compared to other electrochemical techniques. DPV technique has excellent sensitivity, where the potential is changing linearly with time (potential linear sweep) superimposed by the

potential pulses of the amplitude between 10 and 100 mV for several milliseconds [61]. Current is measured at two points for per pulse, where the first point (1) before the application of pulse and the second point (2) at the end of the pulse. The difference between the two sampled currents is plotted against the staircase potential and leads to a peak shaped waveform [62]. The excitation waveform of the differential pulse voltammetry is shown in Figure 1.9.

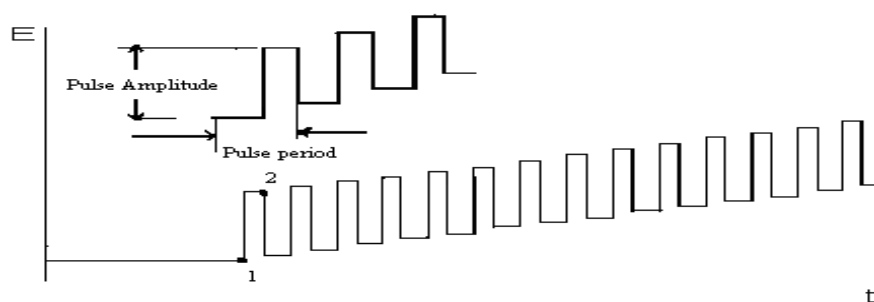


Figure 1.9. The excitation waveform of the DPV.

1.5. Chemically Modified Electrodes (CME)

Electrode surfaces are modified for special studies because of inability of bare conductive electrodes. Modification provides selectivity, sensitivity, chemical and electrochemical stability, and resistance to fouling [63]. CME is defined as coating of a conducting or semi-conducting material with a monomolecular, multi-molecular, ionic, or polymeric film which cause altering the electrochemical, optical, and other properties of the interface [64, 65]. The generic illustration of CME is shown in Figure 1.10.

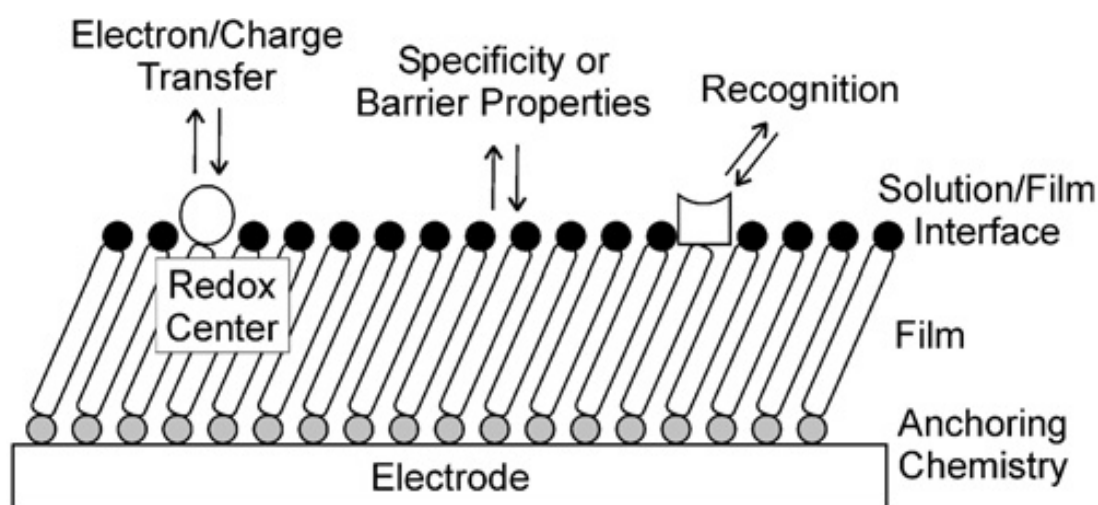


Figure 1.10. The generic illustration of modified electrode [63].

Modification of the bare conductive electrodes is performed by several different techniques such as adsorption, self-assembled layers, covalent bonding and electropolymerization, etc. Surface modification plays very important role in terms of catalytic role in electroanalytical applications [66].

1.6. Application of Conducting Polymers to Chemical and Biochemical Sensors

A chemical sensor is a self-contained analytical device which provides direct information about concentration of the analyte. Chemical sensors depend on two functions which are recognition and transduction. In a chemical sensor, recognition and transduction are integrated in the same device. However, recognition function depends on biochemical or biological mechanisms in a biosensor which is also a chemical sensor [67]. A biosensor is a device which has a biological sensing element connected or integrated within a transducer. The purpose of a biosensor is to produce a digital electronic signal which is directly proportional to the analyte concentration [3]. The role of the transducer in a biosensor is to convert the biochemical signal to an electronic signal [9]. Conducting polymers (CPs) are extensively used as transducers that integrate the signals produced by biological sensing elements (biomolecule) such as enzymes and antibodies [7]. The schematic diagram of a simple biosensor is shown in Figure 1.11.

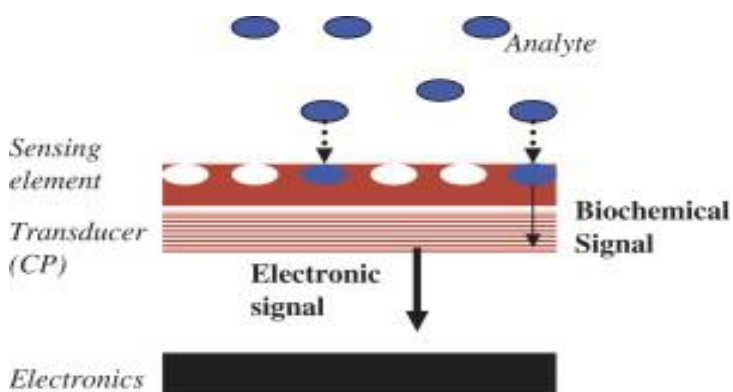


Figure 1.11. The schematic diagram of a biosensor. A biological sensing element like enzyme, antibody detects a biochemical signal from the analyte and the signal is transferred to the transducer such as a conducting polymer [7].

Importance of conducting polymers to sensors in diagnostics to measure vital analytes make sense in scientific field because of its improvement speed and sensitivity [3]. For example, dopamine (DA) is a vital compound and is found in central and peripheral nervous systems. Sarac et al. have investigated modified polycarbazole/carbon fiber microelectrode for sensor applications to detect DA concentration [68].

1.7. Literature Survey related with Determination of DA in the presence of AA with Conducting Polymers

Dopamine (DA) is an important neurotransmitter molecule of catecholamine and its concentration level is very important for central nervous system. Its abnormal level causes to several brain disorders such as Parkinson's disease and schizophrenia [69]. For this reason, determination of DA in the presence of interference substances is the main goal for electrochemical analysis. DA coexists with ascorbic acid (AA) in the central nervous system and its electrochemical detection in the presence of AA reduces its sensitivity and selectivity since its oxidation potential is close to that of AA [50].

Conducting polymer films have drawn a great attention for favorable effects of them on detection of DA in the presence of AA. Some of the conducting polymers have

pendant groups (amine or carboxylic acid) which may interact with the analyte or interferent molecules and results in better separation of the oxidation potential of AA and DA [70-72].

Rubianes et al. showed that a melanin-type polymer film electropolymerized on glassy carbon electrode (GCE) can be used for dopamine quantification in the presence of large excess of ascorbic acid and 3,4-dihydroxyphenyl acetic acid (dopac). The resulting polymer film exhibits permselectivity except anionic species such as potassium ferricyanide, ascorbic acid, dopac and uric acid and cationic dopamine can be oxidized at the polymer-modified electrode. Detection limit was found as 5.0 nM in the presence of 1.0×10^{-3} M AA. This study also showed that the use of ascorbic acid in the measurement solution enhances the dopamine oxidation signal due to the reduction of dopaminequinone by ascorbic acid [73]. In another study, Roy et al. synthesized poly (N, N-dimethylaniline) (PDMA) on GCE and this modified electrode was used for detection of DA in the presence of AA. PDMA film in its oxidized state is positive and AA exists as the negatively charged ion in the neutral solution. DA, on the other hand, exists as the positively charged ion. Therefore, electrostatic interaction between PDMA and AA causes a cathodic shift of the AA oxidation potential as compared to bare GCE. However, oxidation potential of DA anodically shifts due electrostatic repulsion between DA and PDMA. Square wave voltammetric measurements showed that oxidation potential of AA and DA were separated about 300 mV. PDMA coated electrode detected 0.2 μ M DA in the presence of 1000 times higher concentration of AA which is close to the physiological level [74]. Lin et al. synthesized p-nitrobenzenazo resorcinol (NBAR) polymer film on GCE for the determination of dopamine level in the presence of AA and uric acid (UA) in pH 4.0 phosphate buffer solution. A linear range of 5.0×10^{-6} to 2.5×10^{-5} M and a detection limit of 3×10^{-7} M was reported. The study also showed that modified electrode exhibits excellent selectivity for DA in 30 times and 3 times higher concentrations of AA and UA, respectively, than that of DA concentration. Three well-defined separated voltammetric peaks were observed in cyclic voltammetry for DA, AA and UA at

potentials 0.390, 0.195 and 0.559 V, respectively [72]. Recently, Zheng et al. obtained a polymer film of 4-aminobutyric acid (P-4-ABA) on GCE. The results in cyclic voltammetry (CV), differential pulse voltammetry (DPV) and electrochemical impedance spectroscopy (EIS) showed that polymeric film has electrocatalytic effect for the oxidation of AA, DA and UA. The peak separations between AA and DA, DA and UA, AA and UA at modified electrode 208, 136 and 344 mV, respectively, were observed by using DPV method. The detection limits for AA, DA and UA were calculated as 5.0, 1.0 and 0.5 μM , respectively. Moreover, the modified electrode showed good results for determination of AA, DA and UA in human urine samples [75]. Conducting polymer films incorporated with nanoparticles also provide different approach. Khudaish et al. obtained a novel surface material on glassy carbon electrode. 2,4,6-triaminopyrimidine (TAP) was polymerized and its polymer form (PTAP) was decorated with gold nanoparticles (AuNPs). The resulting modified electrode (AuNPs-PTAP/GCE) sensor showed electrocatalytic effect towards electrochemical detection of dopamine (DA). The sensor showed an excellent sensitivity and selectivity for dopamine with the detection limit of 0.017 μM in solution which contains large amounts of ascorbic acid (AA) and uric acid (UA). This modified electrode showed good recovery in the presence of AA and UA for DA (97.6 %) in the presence of AA and DA in serum [76].

Polyoxometalates (POMs) have drawn great attention in electrocatalytic studies because of high stability of most of their redox states and the possibility to change their redox potentials by changing the heteroions and/or the addenda ions without changing their structure. The POMs can be attached to the electrode surfaces by entrapping them into polymer matrix [77]. Balamurugan et al. studied electrocatalytic reduction of bromate ion and oxidation of ascorbic acid by using silicomolybdate-doped PEDOT modified electrode in strong acid medium [78]. In another study, Zhang et al. prepared polyaniline (PANI) doped with silicotungstic acid (SiW_{12}) and carbon nanotubes (CNTs) on glassy carbon electrode with single-step electropolymerization for the determination of ascorbic acid (AA). The investigation

showed that this modified electrode has an electrocatalytic oxidation of AA with 0.51 μM as a limit of detection [79]. Xu et al. prepared a novel electrochemical sensor with phosphotungstic acid (PTA) and poly(ethyleneimine) (PEI) on indium tin oxide electrode (ITO) through layer-by-layer technique. The electrocatalytic effect of PEI/PTA multilayer modified electrode was investigated by using ascorbic acid and H_2O_2 in 0.1 M NaAc-HAc buffer (pH 5.0). The results showed that response of reduction peak of film increased gradually with the increase of H_2O_2 concentration in the range from 3.5×10^{-3} to 3.5×10^{-2} mg/mL with a correlation coefficient R^2 of 0.9964 which means that there is an electrocatalytic reduction effect of modified electrode on H_2O_2 . Similarly, oxidation peak of modified electrode increased with the addition of ascorbic acid [80]. Only one study has been made about incorporation of conducting polymer and polyoxometalate for investigation of electrocatalytic effect to DA by poly(luminol)/ $\text{PMo}_{12}\text{O}_{40}^{3-}$ hybrid film [81].

1.8. The Aim of This Study

The determination of dopamine (DA) in the presence of ascorbic acid (AA) requires sensitive and selective methods. Voltammetric methods have important role for the detection of DA and AA, simultaneously because of simplicity and rapidity. However, direct redox reactions of these species are irreversible at bare electrodes and required high over potentials for their detections. Moreover, direct redox reactions of these compounds take place at very similar potentials so that sensitivity and selectivity of the method decreases [72].

In this work the main goal was to prepare new modified electrodes to be used in the dopamine determination in the presence of ascorbic acid. For this purpose, GCEs were modified by electrodeposition of PEDOT in the presence of polyoxometalates. The modified electrodes, PEDOT-(NH_4) $_6\text{P}_2\text{Mo}_{18}\text{O}_{62}$ /GCE, PEDOT-[(C_4H_9) $_4\text{N}$] $_4\text{SiMo}_{12}\text{O}_{40}$ /GCE and PEDOT- $\text{H}_3\text{PMo}_{12}\text{O}_{40}$ /GCE were investigated in point of response to dopamine signal. The effect of pH of electrolytic solution on DA detection was also investigated. In the second part of this study, a polymerized film of

9-aminofluorene was prepared on the surface of GCE by electropolymerization. Cyclic voltammetry (CV) and differential pulse voltammetry (DPV) were used to study the electrochemical properties of the modified electrodes. Electrocatalytic effect of poly (9-amino fluorene) modified GCE was studied for the oxidation of ascorbic acid and dopamine in different pH media. Characterization studies of poly (9-amino fluorene) film were made by using UV-VIS spectrophotometer and Fourier Transform Infrared spectroscopy (FT-IR). The final part was related to the synthesis of poly (9-fluorene carboxylic acid) on GCE. The effect polymerization conditions, such as number of cycles, the electrolytic solution etc., on the DA and AA oxidation was also investigated. After optimization studies poly(9-fluorene carboxylic acid), modified electrode was used to detect and to produce calibration plots for DA in the presence of AA in different pH media. UV-VIS spectrophotometer and FT-IR were used for characterization of poly(9-fluorene carboxylic acid) film.

CHAPTER 2

EXPERIMENTAL

2.1. Materials

Monomers, 3,4-ethylenedioxythiophene, fluorene-9-carboxylic acid (97%), and 9-aminofluorene hydrochloride (98%) were purchased from Sigma Aldrich Chemicals and used as received. Trifluoroacetic acid (Merck), boron trifluoride diethyl etherate (Sigma-Aldrich), acetonitrile (ACN, 99.9%, Sigma-Aldrich), dichloromethane (CH_2Cl_2 , 99.8%, Sigma-Aldrich), lithium perchlorate (LiClO_4 , 95%, Sigma-Aldrich), tetrabutylammonium hexafluorophosphate (TBAPF₆, 98%, Sigma-Aldrich), potassium chloride (KCl, 99.8%, Sigma-Aldrich) and sulfuric acid (H_2SO_4 , 95%, Sigma-Aldrich) were used without any further purification. L-Ascorbic acid (99%, Sigma-Aldrich) and dopamine hydrochloride (98%, Sigma-Aldrich) solutions were prepared in different pH media. Dopamine hydrochloride injection (40 mg. mL⁻¹, Vem İlaç Sanayi ve Ticaret Ltd. Şti.) ampoule was used with dilution. Buffer solutions for different pHs were prepared from sodium hydroxide (NaOH, 97%, Merck), potassium hydrogen phthalate ($\text{C}_8\text{H}_5\text{KO}_4$, Merck) and potassium dihydrogen phosphate (KH_2PO_4 , Merck). $(\text{NH}_4)_6\text{P}_2\text{Mo}_{18}\text{O}_{62} \cdot 13\text{H}_2\text{O}$, $[(\text{C}_4\text{H}_9)_4\text{N}]_4\text{SiMo}_{12}\text{O}_{40}$ and $\text{H}_3\text{PMo}_{12}\text{O}_{40} \cdot 29\text{H}_2\text{O}$ polyoxometalates were donated by Andriy B. Vishnikin (Department of Analytical Chemistry, Dnepropetrovsk National University, Ukraine).

2.2. Preparation of Buffer Solutions

All solutions used in this study were prepared by using deionized water (18 MΩ) which was obtained by Millipore water purification system. Different buffer solutions were prepared, and their pHs were controlled by using PHM210 pH meter. 0.2 M H_2SO_4 was prepared for acidic medium studies. Phthalate buffer solution (pH=4) from Fisher Scientific Company was used directly. 45.2 mL of 0.1 M NaOH solution was

added to 100 mL 0.1 M potassium hydrogen phthalate and made up to 200 mL with deionized water to obtain pH=5 phthalate buffer medium. 58.2 mL and 78.2 mL of 0.1 M NaOH solution were added to 100 mL 0.1 M potassium dihydrogen phosphate to obtain pH=7 and pH=7.4 phosphate buffer media, respectively. Finally, solutions were made up to 200 mL with deionized water for desired pH values. 0.1 M KCl solution in all pH media (except acidic medium) was used as a supporting electrolyte for the electrochemical detection of ascorbic acid (AA) and dopamine (DA).

2.3. Apparatus

All electrochemical measurements were conducted using Gamry PCI4/300 potentiostat-galvanostat. A conventional three-electrode cell system comprising of 0.07 cm² glassy carbon electrode (GCE) as a working electrode (bare or modified), Ag/AgCl (in 3 M NaCl aqueous solution) as a reference electrode and a platinum wire as a counter electrode were used (Figure 2.1) for all electrochemical studies. Carbon electrodes have been widely preferred in the electroanalysis of neurotransmitters because of its biocompatibility with tissue and having low residual current in comparison to the metal electrodes [74]. Before performing the electrochemical measurements, GCE surface was cleaned by using 0.05 μm alumina polishing suspension and then thoroughly rinsed with ethanol and distilled water. Finally, electrode was also cleaned electrochemically by cycling the potential between -0.7 and 1.7 V at the scan rate of 100 mV/s for 20 cycles in 0.2 M H₂SO₄ solution.

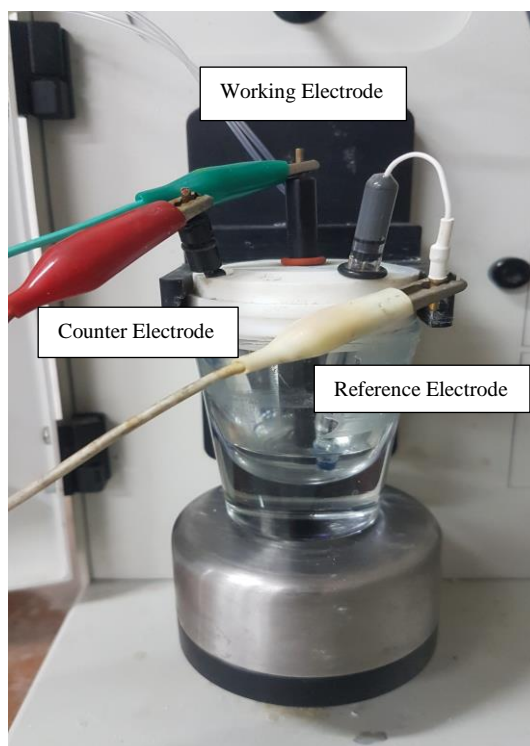


Figure 2.1. Three-electrode cell system

Spectroelectrochemical measurements were performed by using a Carry 60 model UV-VIS spectrophotometer combined with Gamry PCI4/300 potentiostat-galvanostat. FTIR spectra were recorded by Nicolet İS10. All measurements were conducted at room temperature.

2.4. Electrochemical Techniques

Cyclic voltammetry (CV) and differential pulse voltammetry (DPV) techniques were used for electrochemical measurements in this study. Electropolymerization of monomers and behavior of modified surfaces were investigated by using CV technique. Scan limits were adjusted according to monomers used for electrochemical polymerization. However, scan rate and step size were adjusted fixedly after optimization studies to 100 mV/s and 10 mV, respectively. Generally, the DPV technique is considered to be more sensitive than the CV technique due to the

elimination of the non-faradaic current [82]. For this reason, individual or simultaneous determination and calibration studies of ascorbic acid (AA) and dopamine (DA) were performed by using DPV technique. Initial and final potentials were adjusted according to each medium, but the other parameters were optimized for the best result. As a result of optimization studies, step size, pulse time and pulse size were fixed to 5 mV, 0.2 s and 20 mV, respectively.

2.5. Preparation of Modified Electrodes

2.5.1. Preparation of Poly(3,4-ethylenedioxythiophene) /GCE, (PEDOT)/GCE

10 mM EDOT monomer solution was prepared in acetonitrile containing 33 mM LiClO₄ as a supporting electrolyte. EDOT was electropolymerized onto GCE by cycling the potential between -0.2 and 1.4 V at a scan rate of 100 mV/s for 20 cycles.

2.5.2. Preparation of PEDOT- (NH₄)₆P₂Mo₁₈O₆₂/GCE, (PEDOT-P₂Mo₁₈)/GCE

Modified PEDOT-Polyoxometalates surfaces onto the GCE was prepared with one-step procedure. In other words, electropolymerization is carried out in a solution which contains monomer and polyoxometalate. P₂Mo₁₈O₆₂⁶⁻ containing PEDOT film was obtained on glassy carbon by potential cycling for 15 cycles at 100 mV/s from -0.2 to 1.3 V. The solution contained 0.5 Mm (NH₄)₆P₂Mo₁₈O₆₂ in deionized water and 10 mM EDOT in acetonitrile (1:1 by volume). P₂Mo₁₈O₆₂⁶⁻ also acted as a supporting electrolyte therefore, LiClO₄ was not added.

2.5.3. Preparation of PEDOT-(TBA)₄SiMo₁₂O₄₀/GCE, (PEDOT-SiMo₁₂)/GCE

The bare GCE was immersed into the 50 mM EDOT and 2.5 mM (TBA)₄SiMo₁₂O₄₀ solution in acetonitrile (1:1 by volume) and electropolymerization was started by cycling the potential between -0.2 and 1.4 V at a scan rate of 100 mV/s for 20 cycles. No extra supporting electrolyte was used since SiMo₁₂O₄₀⁴⁻ also acted as a supporting electrolyte.

2.5.4. Preparation of PEDOT-H₃PMo₁₂O₄₀/GCE, (PEDOT-PMo₁₂)/GCE

Surface modification onto GCE was carried out in a mixture of 0.5 Mm H₃PMo₁₂O₄₀, 10 mM EDOT in acetonitrile and 0.2 M H₂SO₄ solution (2:2:1 by volume, respectively) by cycling the potential between -0.2 and 1.4 V at a scan rate of 100 mV/s for 20 cycles. 0.2 M H₂SO₄ solution was used as a supporting electrolyte.

2.5.5. Preparation of Poly (9-amino fluorene)/GCE, (P9AF)/GCE

The surface of GCE was modified by electro-oxidation of 9-aminofluorene (9AF). The modified electrode was prepared by cycling the electrode potential between 0.2 and 1.4 V (20 cycles) at the scan rate of 100 mV/s in boron trifluoride diethyl etherate (BFEE)-trifluoroacetic acid (TFA) (70/30, v/v) solution containing 25 mM 9-aminofluorene.

2.5.6. Preparation of Poly (9-fluorene carboxylic acid)/GCE, (PFCA)/GCE

25 mM solution of 9-fluorene carboxylic acid (FCA) was prepared by dissolving appropriate amount of FCA in boron trifluoride diethyl etherate (BFEE)-trifluoroacetic acid (TFA) (70/30, v/v) solution. FCA was electropolymerized onto the GCE by potential cycling between 0.2 and 1.3 V for 20 cycles at a scan rate of 100 mV/s

2.6. Determination of AA and DA by DPV Technique

Modified electrodes were used for the investigation of electrocatalytic effect on ascorbic acid and dopamine oxidation. The calibration studies were performed by using PFCA/GCE in the presence of excess amount AA at various pH values. All solutions were prepared daily at room temperature.

2.6.1. Preparation of Calibration Studies at Different pHs Values

pH<1 medium calibration study: The analytical curve for dopamine was obtained over the concentration range from 0.3 mM to 15 mM in the presence of 15 mM

ascorbic acid in 0.2 M H₂SO₄ solution. Initial and final potentials were adjusted to 0.0 and 0.9 V, respectively.

pH=4 medium calibration study: The analytical curve for dopamine was obtained over the concentration range from 0.03 mM to 1.5 mM in the presence of 15 mM ascorbic acid in pH=4 phthalate buffer containing 0.1 M KCl solution. The reliability of method was tested by using dopamine hydrochloride injection ampoule (40 mgmL⁻¹). Dopamine hydrochloride injection ampoule (40 mgmL⁻¹) diluted solutions (5x10⁻⁵ M and 9x10⁻⁵ M) was also prepared with pH=4 phthalate buffer containing 0.1 M KCl solution and the reliability was tested on calibration plot only dopamine solutions (from 0.02 mM to 0.1 mM). Initial and final potentials were fixed to 0.0 and 0.6 V, respectively.

pH=5 medium calibration study: The analytical curve for dopamine was obtained over the concentration range from 0.015 mM to 3 mM in the presence of 15 mM ascorbic acid in pH=5 phthalate buffer containing 0.1 M KCl solution. Initial and final potentials were adjusted to 0.0 and 0.6 V, respectively.

CHAPTER 3

RESULTS AND DISCUSSION

3.1. Electrochemical Polymerization and Behavior of PEDOT and PEDOT/POMs

3.1.1. Electrochemical Polymerization and Mechanism of PEDOT Formation

Electrodeposition of **PEDOT** film on GCE was achieved by voltammetric potential cycling as described in Experimental section. Figure 3.1 illustrates the 1st cycle of the voltammogram (Figure 3.1 inset) and growth of **PEDOT** film on glassy carbon electrode through repetitive cycling between -0.2 and + 1.4 V vs Ag/AgCl. As seen from the Figure 3.1, the oxidation onset of **EDOT** appears at about +1.15 V vs Ag/AgCl. After 20 cycles, a deep blue polymer film was observed on GCE.

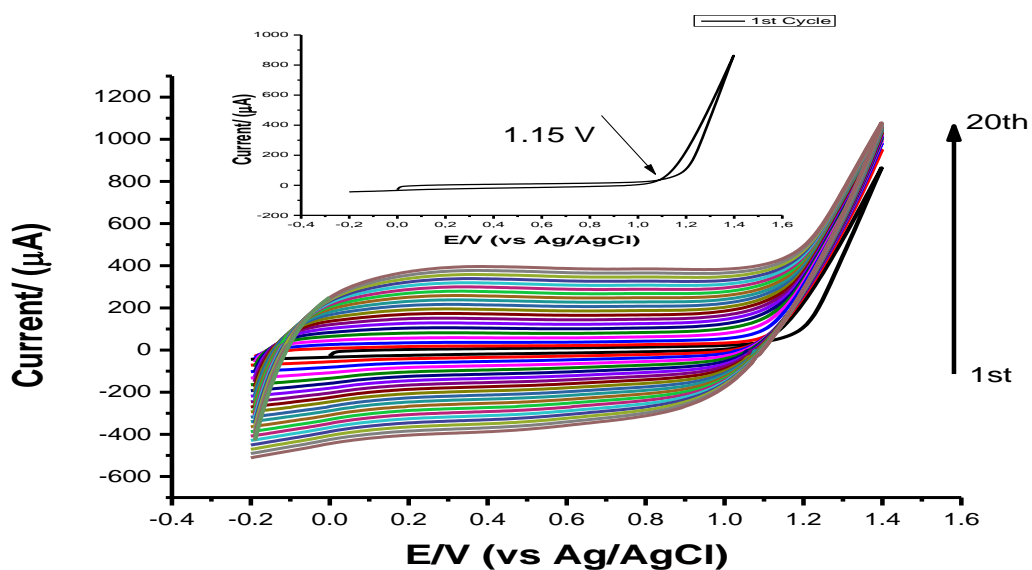
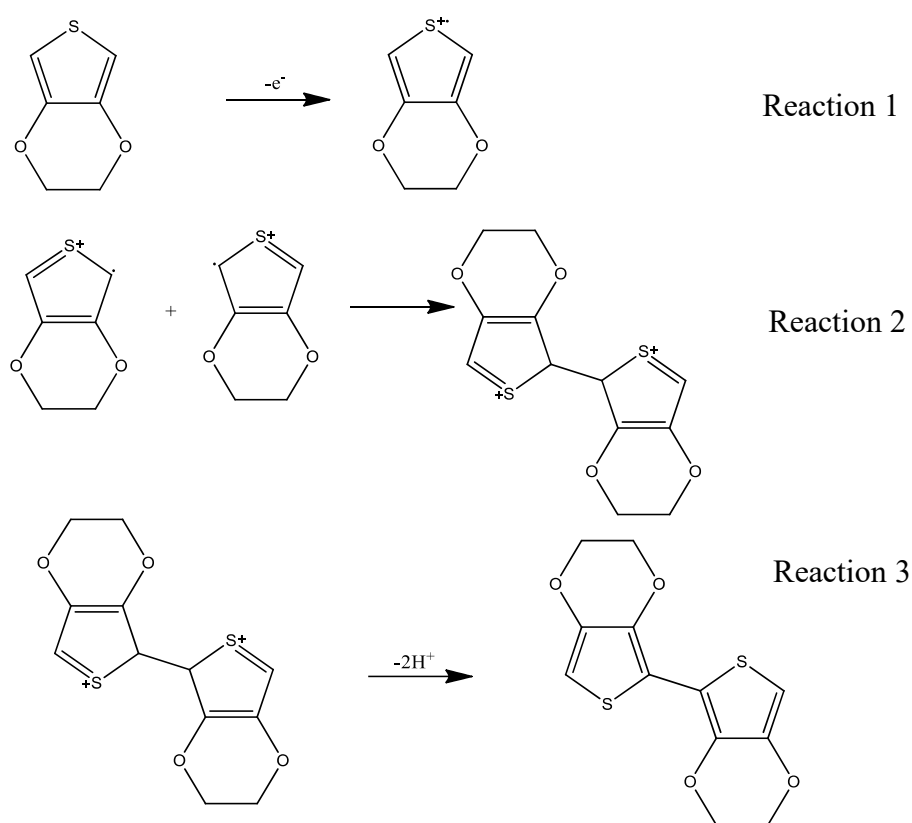


Figure 3.1. Voltammetric generation of **PEDOT** film in acetonitrile solution containing 10 mM **EDOT** and 33 mM LiClO_4 . Scan rate was 100 mV/s. Inset: 1st cycle.

As it is already reported [83] electrochemical oxidative polymerization of **EDOT** follows the mechanism depicted in Scheme 3.1. Upon one electron transfer to the working electrode, radical cations are formed (Reaction 1). The radical cations couple in the subsequent step (Reaction 2) to form cationic dimers which becomes neutral dimer upon deprotonation (Reaction 3). Further oxidation and coupling of dimers many times result in the formation of polymeric chain.



Scheme 3.1. The proposed oxidative electrochemical polymerization of EDOT [83].

3.1.2. Electrochemical Polymerization and Electrochemical Behavior of PEDOT-(NH₄)₆P₂Mo₁₈O₆₂

Composite film of **PEDOT** with a Dawson type heteropolyanion **P₂Mo₁₈O₆₂⁶⁻**, (**P₂Mo₁₈**) was achieved on GCE by voltammetric potential cycling in the modification solution as described in Experimental section. Figure 3.2 shows the growth of the **PEDOT-P₂Mo₁₈** film on GCE.

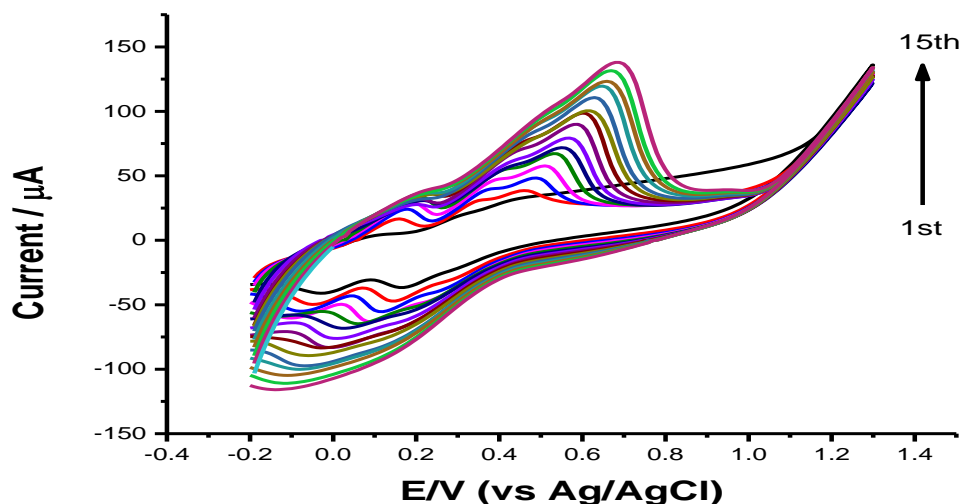


Figure 3.2. Voltammetric generation of **PEDOT-P₂Mo₁₈** film was carried in a solution containing 0.5 mM **(NH₄)₆P₂Mo₁₈O₆₂** in deionized water and 10 mM **EDOT** in acetonitrile (1:1 by volume). Scan rate was 100 mV/s.

It is expected that polymer was generated on the electrode surface simultaneously with polyoxometalates due to electrostatic interaction between negatively charged polyoxometalates and positively charged polymer in its doped state [77]. To show the redox peaks clearly, as an indication of incorporation of **P₂Mo₁₈O₆₂⁶⁻** polyanion into the polymer matrix, first and fourth cycles of electropolymerization are given in Figure 3.3. The three redox peaks present in the cyclic voltammogram obtained after the 4th cycle is characteristic for **P₂Mo₁₈O₆₂⁶⁻** anion and clearly shows incorporation of this anion into the polymer matrix. With increasing cycle number these peaks approach each other and after the 15th cycle they appear in the form of a single broad peak.

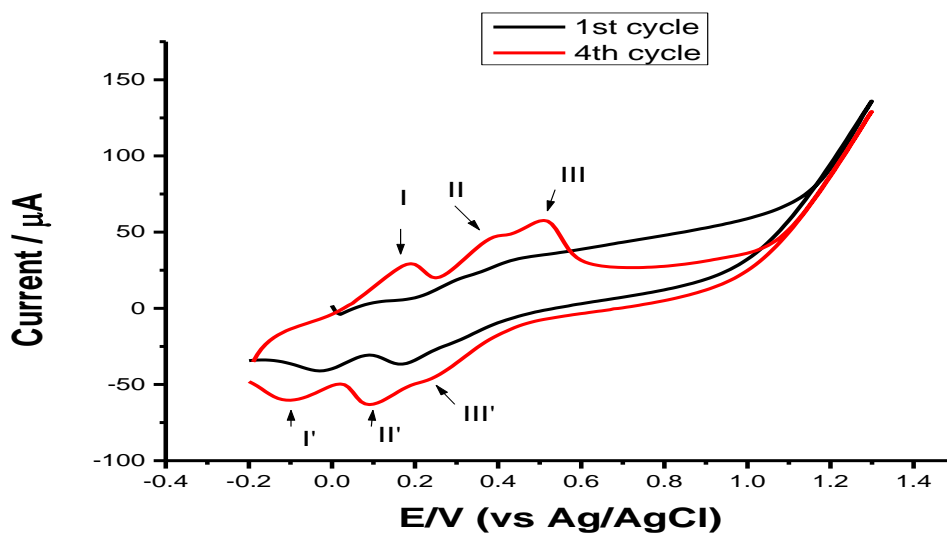


Figure 3.3. First and fourth cycles of electropolymerization process in a solution containing 0.5 mM $(\text{NH}_4)_6\text{P}_2\text{Mo}_{18}\text{O}_{62}$ in deionized water and 10 mM EDOT in acetonitrile (1:1 by volume). Scan rate was 100 mV/s.

In Figure 3.4, comparison of electrochemical behavior of **bare GCE**, **(PEDOT)/GCE** and **(PEDOT- P_2Mo_{18})/GCE** in 0.2 M H_2SO_4 solution are given. An inspection of Figure 3.4 reveals that the cyclic voltammogram of hybrid film, **(PEDOT- P_2Mo_{18})/GCE**, is totally different from the **bare GCE** and **(PEDOT)/GCE** due to presence of characteristic redox peaks (I-IV and I'-IV') of $\text{P}_2\text{Mo}_{18}\text{O}_{62}^{6-}$ heteropolyanion [25].

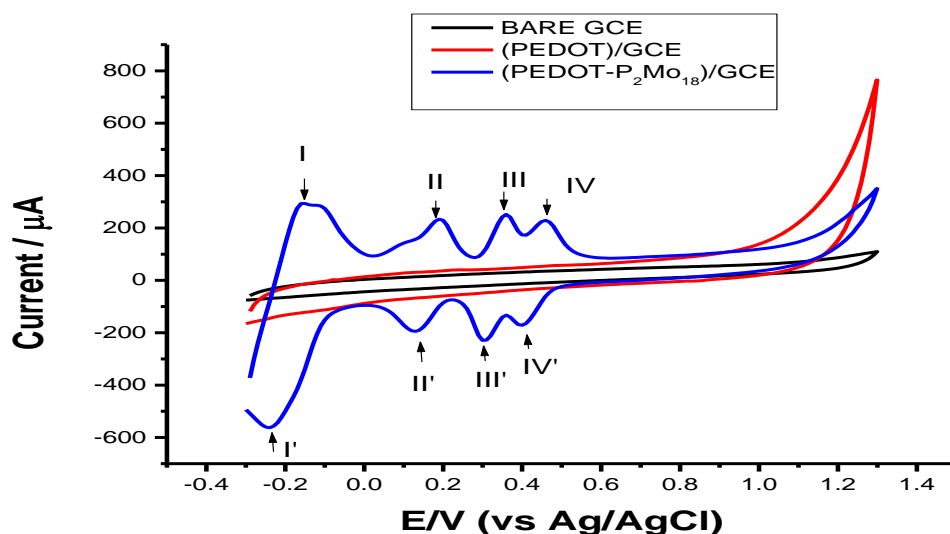


Figure 3.4. Cyclic voltammograms of **Bare GCE**, **(PEDOT)/GCE** and **(PEDOT-P₂Mo₁₈)/GCE** in 0.2 M H₂SO_{4(aq)} solution. Scan rate was 100 mV/s.

3.1.3. Electrochemical Polymerization and Electrochemical Behavior of PEDOT-(TBA)₄SiMo₁₂O₄₀

The electrochemical synthesis of **PEDOT-(TBA)₄SiMo₁₂O₄₀** (**PEDOT-SiMo₁₂**) was carried out by repetitive cycling as described in the experimental section and the cyclic voltammograms recorded during successive scans were depicted in Figure 3.5. Repetitive cycling between -0.2 and 1.4 V revealed the formation of new peaks indicating both the formation of electroactive polymers on the electrode surface and incorporation of **SiMo₁₂O₄₀⁴⁻** polyanion into the polymer matrix.

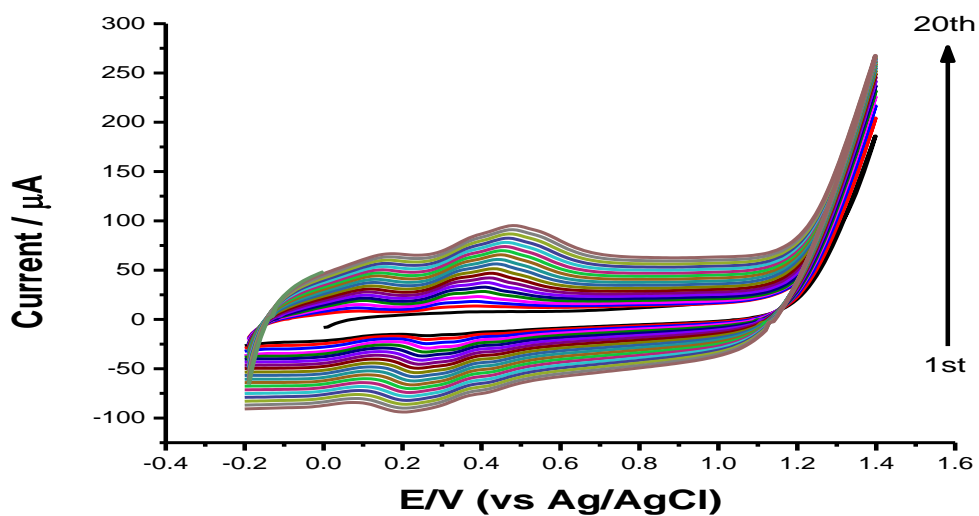


Figure 3.5. Voltammetric generation of **PEDOT-SiMo₁₂** film was carried out in a solution containing 2.5 mM **(TBA)₄SiMo₁₂O₄₀** and 50 mM **EDOT** in acetonitrile (1:1 by volume). Scan rate was 100 mV/s.

After 20 repetitive cycles, the **PEDOT-SiMo₁₂** film coated electrode was washed with ACN to remove any unreacted monomer and oligomeric species. The redox behavior of polymer film, **PEDOT-SiMo₁₂**, was investigated by recording the cyclic voltammograms in 0.2 M $\text{H}_2\text{SO}_{4(\text{aq})}$ solution in Figure 3.6. As seen from the Figure 3.6, modified electrode exhibited three reversible peaks at $E_{1/2} = -0.05$, $E_{1/2} = 0.191$ and $E_{1/2} = 0.278$ (I-III and I'-III') in accordance with the reported values [78].

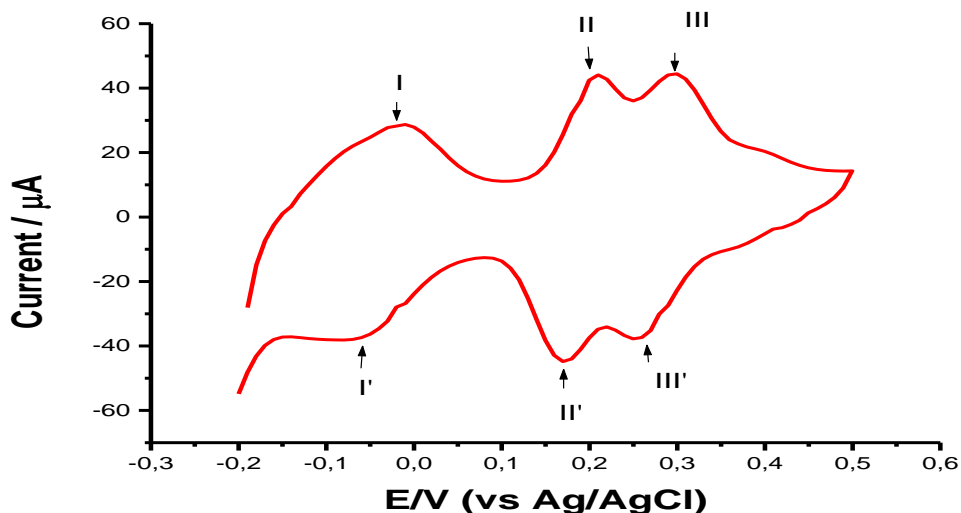


Figure 3.6. Cyclic voltammogram of **PEDOT-SiMo₁₂** film in 0.2 M H₂SO_{4(aq)} solution. Scan rate was 100 mV/s.

3.1.4. Electrochemical Polymerization and Electrochemical Behavior of PEDOT-H₃PMo₁₂O₄₀

The PEDOT polymer film, doped with **H₃PMo₁₂O₄₀**, (**PEDOT-PMo₁₂**) was synthesized on GCE via potential cycling in acetonitrile solution containing **EDOT** and **H₃PMo₁₂O₄₀** as described in the experimental section. The cyclic voltammograms recorded during repetitive cycling were given in Figure 3.7. The increase in the peak currents with increasing number of cycling indicated the formation of well-adhered film on the working electrode surface.

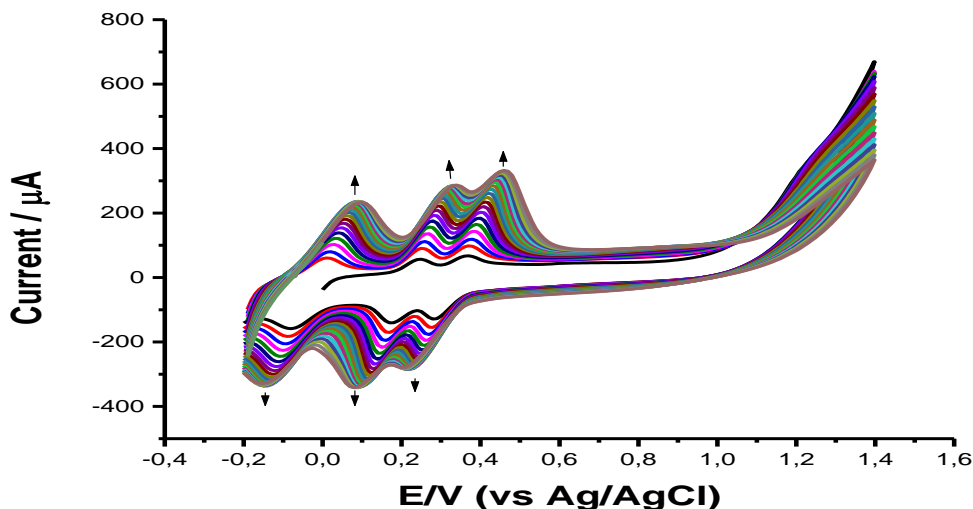


Figure 3.7. Voltammetric generation of **PEDOT-PMo₁₂** film was carried out in a solution containing 0.5 mM **H₃PMo₁₂O₄₀**, 10 mM **EDOT** in acetonitrile and 0.2 M **H₂SO_{4(aq)}** (2:2:1, respectively). Scan rate was 100 mV/s.

It is known that, 12-molybdo phosphoric acid (**H₃PMo₁₂O₄₀**) is both a strong acid and a strong oxidizing agent. Due to this property, it was effectively used to initiate chemical polymerization of pyrrole [84]. Thus, the chemical polymerization of PEDOT with **H₃PMo₁₂O₄₀** were also tried by mixing **H₃PMo₁₂O₄₀** with **EDOT** in acetonitrile. A sudden color change from light yellow to blue was noted in the solution due to direct electron transfer between **EDOT** and **H₃PMo₁₂O₄₀**. However, we did not observe any precipitation, indicating formation of **PEDOT**, therefore we gave up further studies on this issue.

The electrochemical behavior of **PEDOT** and **PEDOT-PMo₁₂** modified electrode in 0.2 M **H₂SO₄** solution were investigated by recording differential pulse voltammograms and the results were given in Figure 3.8. Three well-defined oxidation peaks characteristics of **PMo₁₂O₄₀³⁻** anion were observed at 0,363, 0,193 and -0,03 V (III, II and I, respectively) in the case of **PEDOT-PMo₁₂** modified electrode.

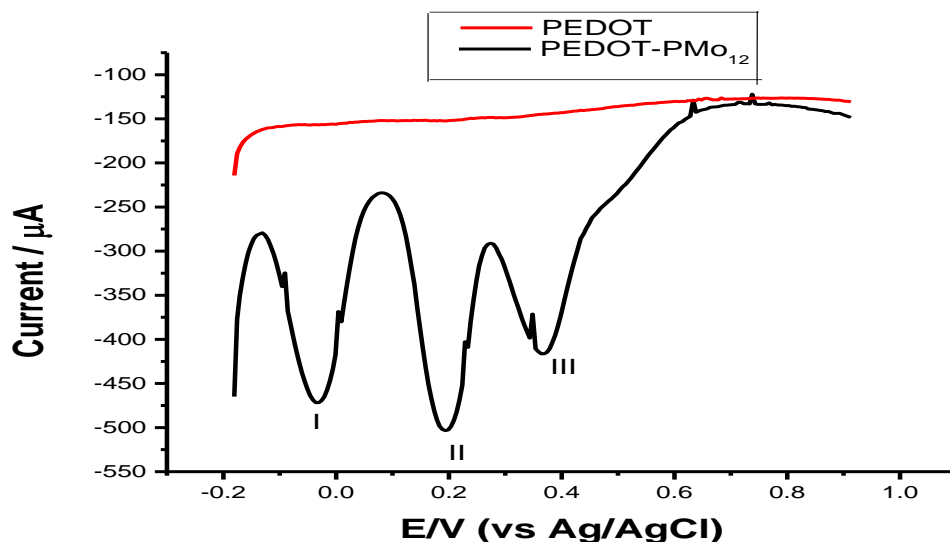


Figure 3.8. Differential pulse voltammograms of **PEDOT-PMo₁₂** and **PEDOT** modified electrodes in 0.2 M H₂SO_{4(aq)} solution.

3.2. Comparison of the Electrochemical Performances of PEDOT and PEDOT POMs modified electrodes for the measurement of DA Signal

The modified **PEDOT** and three different **PEDOT-POMs** electrodes on glassy carbon surface were compared in terms of **dopamine** oxidation current signal by using differential pulse voltammetric technique. Working conditions were described in the Experimental Section.

3.2.1. Comparison of the Electrochemical Performances of PEDOT/GC and PEDOT-(NH₄)₆P₂Mo₁₈O₆₂/GC (PEDOT-P₂Mo₁₈)/GC electrodes for the measurement of DA Signal

Figure 3.9 shows DPVs of **PEDOT/GCE** and **PEDOT-P₂Mo₁₈/GCE** for the determination of **1 mM** and **10 mM dopamine** solutions in 0.2 M H₂SO₄ acidic medium. As it is seen from Figure 3.9, besides characteristic oxidation peaks of **P₂Mo₁₈O₆₂⁶⁻** anion, (0.184, 0.354 and 0.486 V vs Ag/AgCl) a new peak at around 0.550 V was observed signaling the oxidation of **DA**. **Dopamine** response of **PEDOT-P₂Mo₁₈/GCE** was found to be 1.3 and 2.8 times higher than that of **PEDOT/GCE** for

10 mM and **1 mM DA** solutions, respectively. Since changing concentration level of DA did not influence characteristic peaks of heteropolyanion, it can be concluded that heteropolyanion remains unaffected from the presence of analyte.

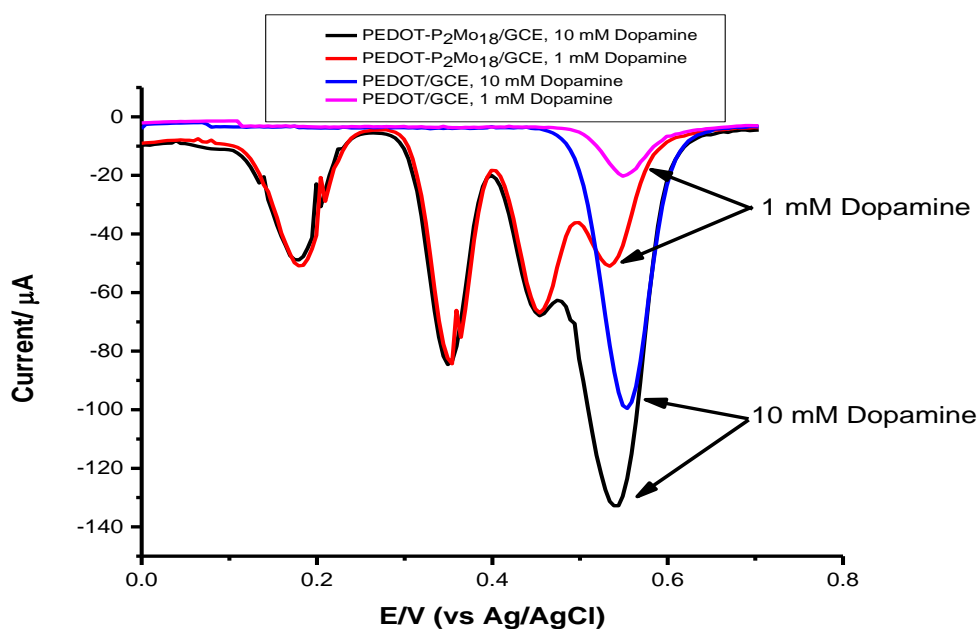


Figure 3.9. Comparison differential pulse voltammograms of **PEDOT/GCE** and **PEDOT-P₂Mo₁₈/GCE** for **1 mM** and **10 mM dopamine** solutions in **0.2 M H₂SO₄(aq)**.

The effect of pH on the potential and anodic peak current was also investigated in pH=4 phthalate buffer solution containing **10 mM DA** and 0.1 M KCl. An inspection of Figure 3.10 clearly shows that the peak current due to **DA** oxidation drastically decreases at pH=4 solution. The decrease in the peak current might be due to decrease in the protonation level of heteropolyanion. Furthermore, **DA** anodic current signal was not seen clearly with **PEDOT-P₂Mo₁₈/GCE** due to the overlapping of one of the oxidation peaks of **P₂Mo₁₈O₆₂⁶⁻** anion and **DA** oxidation peak. Moreover, dopamine current signal on **PEDOT/GCE** also decreased at pH=4 buffer as compared to the **dopamine** current in acidic medium and the oxidation peak potential of **DA** cathodically shifted from 0.553 to 0.409 V (See Figure 3.11).

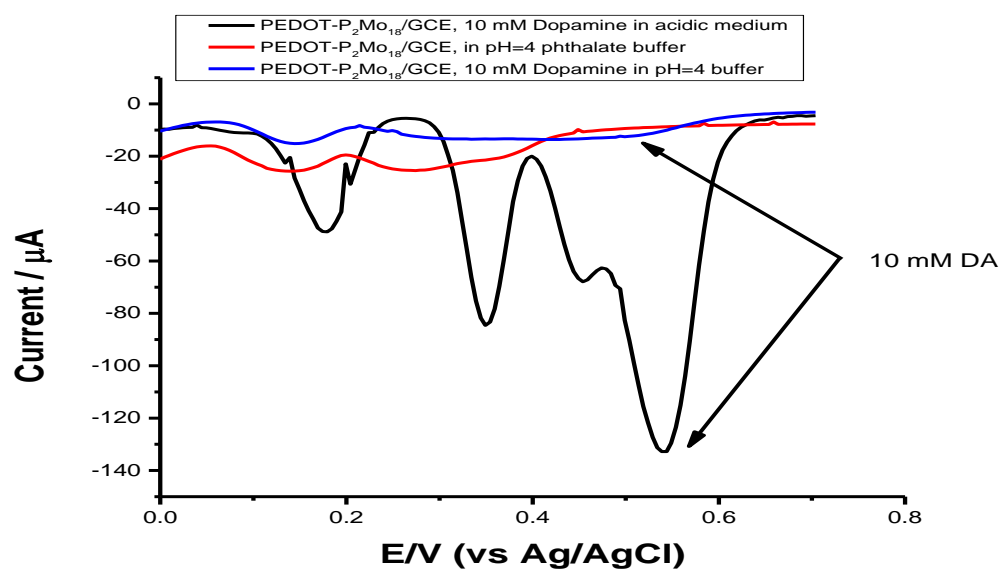


Figure 3.10. Differential pulse voltammograms of blanks and **10 mM DA** at the **PEDOT-P₂Mo₁₈/GCE electrode** in different media.

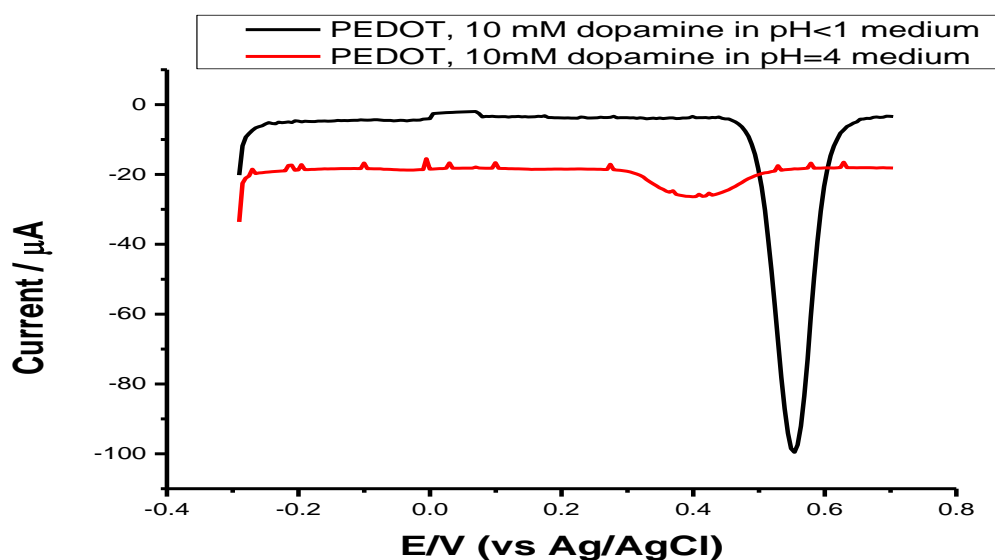


Figure 3.11. Differential pulse voltammograms of **10 mM dopamine** at the **PEDOT/GCE** in 0.2 M H₂SO_{4(aq)} and pH=4 phthalate buffer solution containing 0.1 M KCl_(aq).

3.2.2. Comparison of the Electrochemical Performances of PEDOT/GC and PEDOT-(TBA)₄SiMo₁₂O₄₀ /GC (PEDOT-SiMo₁₂)/GC electrodes for the measurement of DA Signal

DA response of PEDOT/GCE and PEDOT-SiMo₁₂/GCE modified electrodes were investigated in 10 mM DA solution containing 0.2 M H₂SO₄ and the resulting voltammograms were depicted in Figure 3.12. As seen from the Figure, PEDOT-SiMo₁₂/GCE exhibits the three characteristic peaks of heteropolyanion at -0,07 V, 0,06 V and 0,3 V vs Ag/AgCl. The peak observed at 0.569 V was assigned to DA oxidation which was appeared at 0.572 V in the case of PEDOT/GCE. Furthermore approximately 2.7 times higher peak current was observed in the case of PEDOT-SiMo₁₂/GCE.

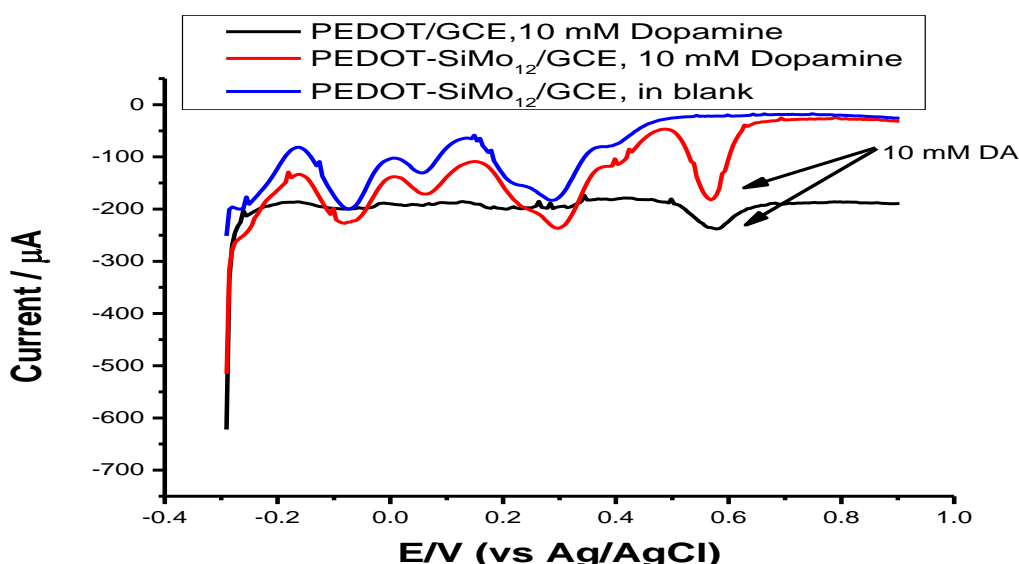


Figure 3.12. Comparison differential pulse voltammograms of PEDOT/GCE and PEDOT-SiMo₁₂/GCE in 10 mM DA solution containing 0.2 M H₂SO_{4(aq)}.

The effect of pH on the electrode response and the oxidation potential of DA was also investigated by recording differential pulse voltammogram in the pH=7 phosphate buffer solution containing 1 mM DA and 0.1 M KCl (See Figure 3.13). A close inspection of Figure 3.13 reveals that the increase in the pH shifts the DA oxidation

peak to lower potential site as expected from Nernst equation. On the other hand, a drastic decrease was observed in the **DA** peak current compared to that of the same concentration of dopamine in acidic condition (see Figure 3.12). It is important to note that at this pH value the characteristic peaks of heteropolyanion were not noticeable due to instability of $\text{SiMo}_{12}\text{O}_{40}^{4-}$ anions in neutral medium [39].

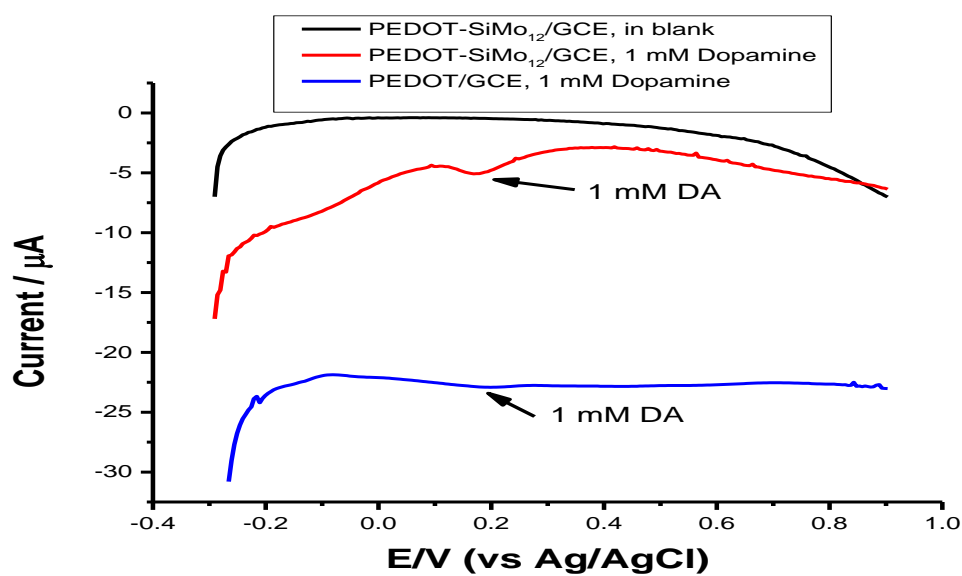


Figure 3.13. Comparison differential pulse voltammograms of **PEDOT/GCE** and **PEDOT-SiMo₁₂/GCE** for **1 mM dopamine** solution in pH=7 phosphate buffer containing 0.1 M $\text{KCl}_{(\text{aq})}$.

3.2.3. Comparison of the Electrochemical Performances of **PEDOT/GC** and **PEDOT-H₃PMo₁₂O₄₀/GC (PEDOT-PMo₁₂)/GC** electrodes for the measurement of **DA** Signal

The DPVs given in Figure 3.14 show the oxidation peak of **1mM DA** in 0.2 M H_2SO_4 solution obtained using **PEDOT/GCE** and **PEDOT-PMo₁₂/GCE** modified electrodes. The oxidation peak of **DA** appeared at 0.540 V and 0.532 V for **PEDOT/GCE** and **PEDOT-PMo₁₂/GCE**, respectively. Furthermore, characteristic redox peaks of $\text{PMo}_{12}\text{O}_{40}^{3-}$ anion appearing at -0.033 V, 0.197 V and 0.352 V confirmed the existence of $\text{PMo}_{12}\text{O}_{40}^{3-}$ anion in the polymer matrix. **Dopamine**

response of **PEDOT-PMo₁₂/GCE** was found to be 1.4 times higher than that of **PEDOT/GCE** for **1 mM DA** solution.

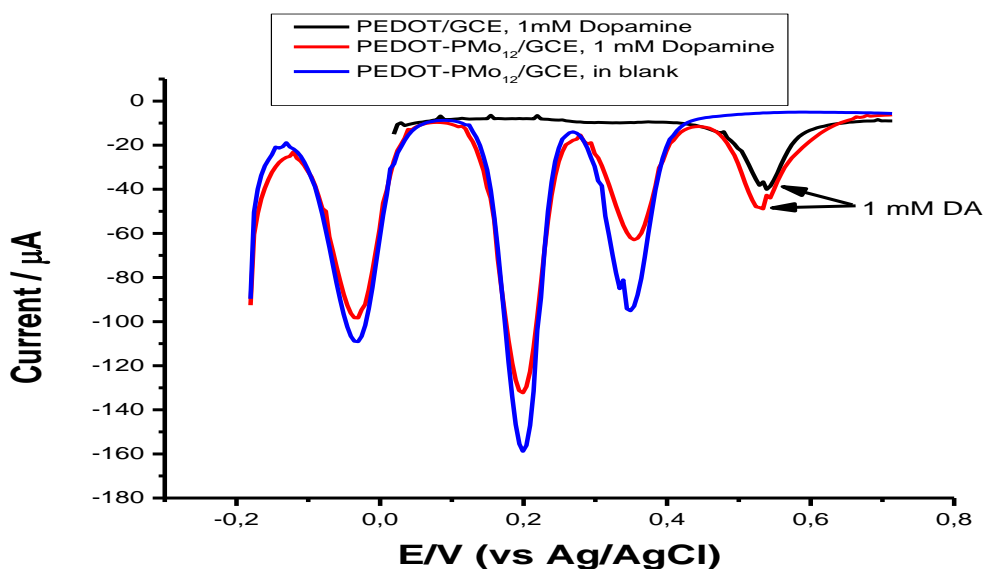


Figure 3.14. Comparison of differential pulse voltammograms of **PEDOT/GCE** and **PEDOT-PMo₁₂/GCE** for **1 mM dopamine** solution in **0.2 M H₂SO_{4(aq)}**.

The effect of pH on the electrochemical oxidation of **DA** for **PEDOT/GCE** and **PEDOT-PMo₁₂/GCE** was also investigated in pH=4 phthalate buffer solution containing 0.1 M KCl. Since **PMo₁₂O₄₀³⁻** anions undergo hydrolytic decomposition in neutral and basic aqueous solutions [85], a decrease in the characteristic oxidation peaks of **PMo₁₂O₄₀³⁻** was also observed at pH=4 buffer solution (See Figure 3.15). Due to expected cathodic shift of **DA** oxidation peak with increasing pH, the 3rd oxidation peak of **PMo₁₂O₄₀³⁻** anion coincides with **DA** oxidation peak which makes quantitative **DA** determination difficult. Moreover, **DA** oxidation peak current at **PEDOT-PMo₁₂/GCE** was 1.5 times higher than peak current at **PEDOT/GCE**.

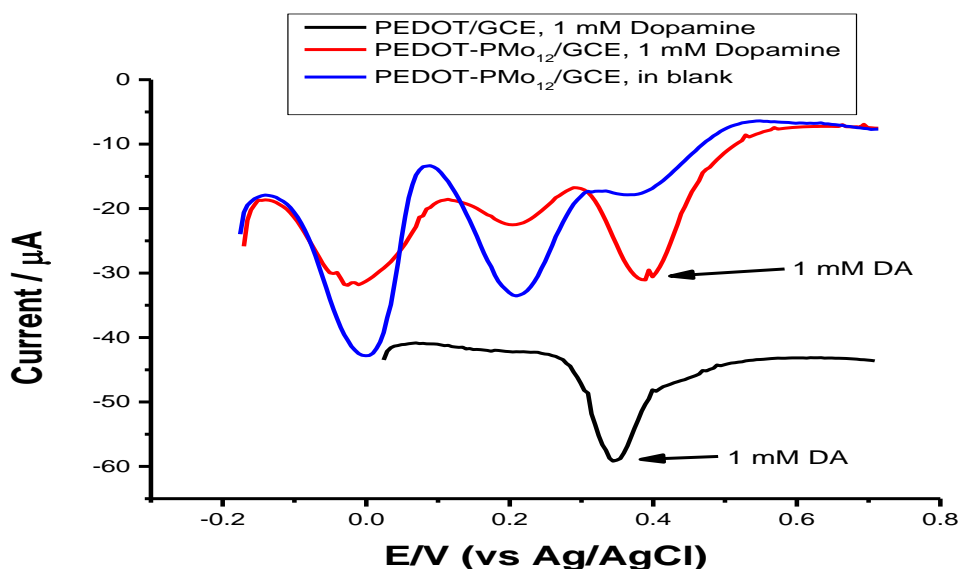


Figure 3.15. Comparison differential pulse voltammograms of **PEDOT/GCE** and **PEDOT-PMo₁₂/GCE** for **1 mM dopamine** solution in pH=4 phthalate buffer solution containing 0.1 M KCl_(aq).

In this study, three kinds of polyoxometalates were immobilized into the PEDOT polymeric matrix by electrochemical polymerization to investigate electrocatalytic effect of POMs for DA oxidation. It is found that, although POM doped PEDOT/GC electrodes did not show any catalytic shifting in the oxidation potential of DA, they exhibited slightly higher oxidation peak currents as compared to PEDOT/GC electrode. However, instability of POMs used in this work at pH values greater than 1 was an important limitation for this study. Because, studies on biological compounds (i.e DA and AA used in this study) make sense at higher pHs. It is also important to mention that, although Balamurgan A. reported that SiMo₁₂O₄₀⁴⁻ doped PEDOT film has an electrocatalytic effect on the oxidation of AA [78] we found similar electrocatalytic effect by using PEDOT alone to modify the GC electrode (Figure 3.16). Therefore, the cathodic shift in the oxidation potential of AA was not due to SiMo₁₂O₄₀⁴⁻ but due to PEDOT used to modify the GC electrode. On the other hand, there are several reports on the electrocatalytic effect of polyoxometalates doped conducting polymer electrodes producing more meaningful results for the reduction

of chlorate [34], bromate [78] and nitrite [81]. Therefore, we decided to use poly(9-amino fluorene) and poly(9-fluorene carboxylic acid) conducting polymers to modify GCE and use these electrodes in DA and AA determination.

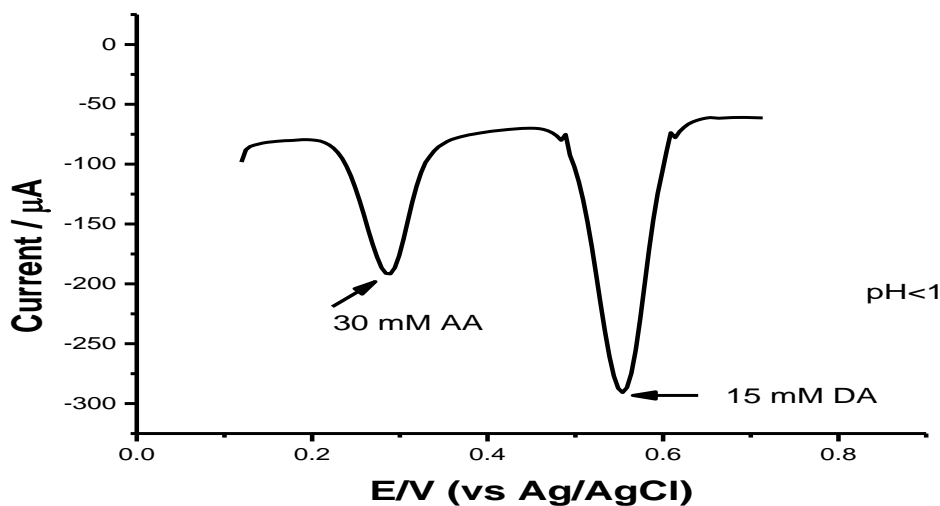


Figure 3.16. The response of PEDOT/GCE to the 30 mM AA and 15 mM DA in 0.2 M $\text{H}_2\text{SO}_{4(\text{aq})}$ solution.

3.3. Electrochemical Polymerization and Electrochemical Behavior of Poly (9-amino fluorene)

Figure 3.17 shows repetitive cyclic voltammograms of 25 mM **9-aminofluorene (9AF)** obtained in boron trifluoride diethyl etherate (BFEE) and trifluoroacetic acid (TFA) mixture (70/30; v/v) with GCE as described in the experimental section. As it is seen from the inset of Figure 3.17, on-set for the oxidation of **9AF** was observed at about 1.16 V. It is also noted that using BFEE as solvent yielded better polymer film quality, as compared to ACN solvent [24]. A possible mechanism for the electrochemical polymerization of **9AF** similar to the one reported previously for poly(fluorene-9-acetic acid) [86] is given in Scheme 3.2

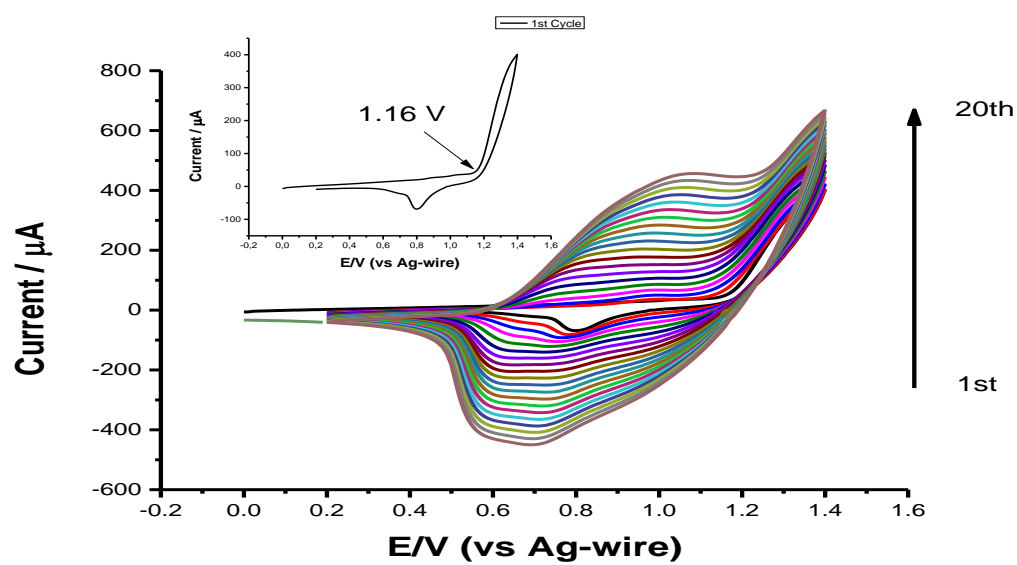
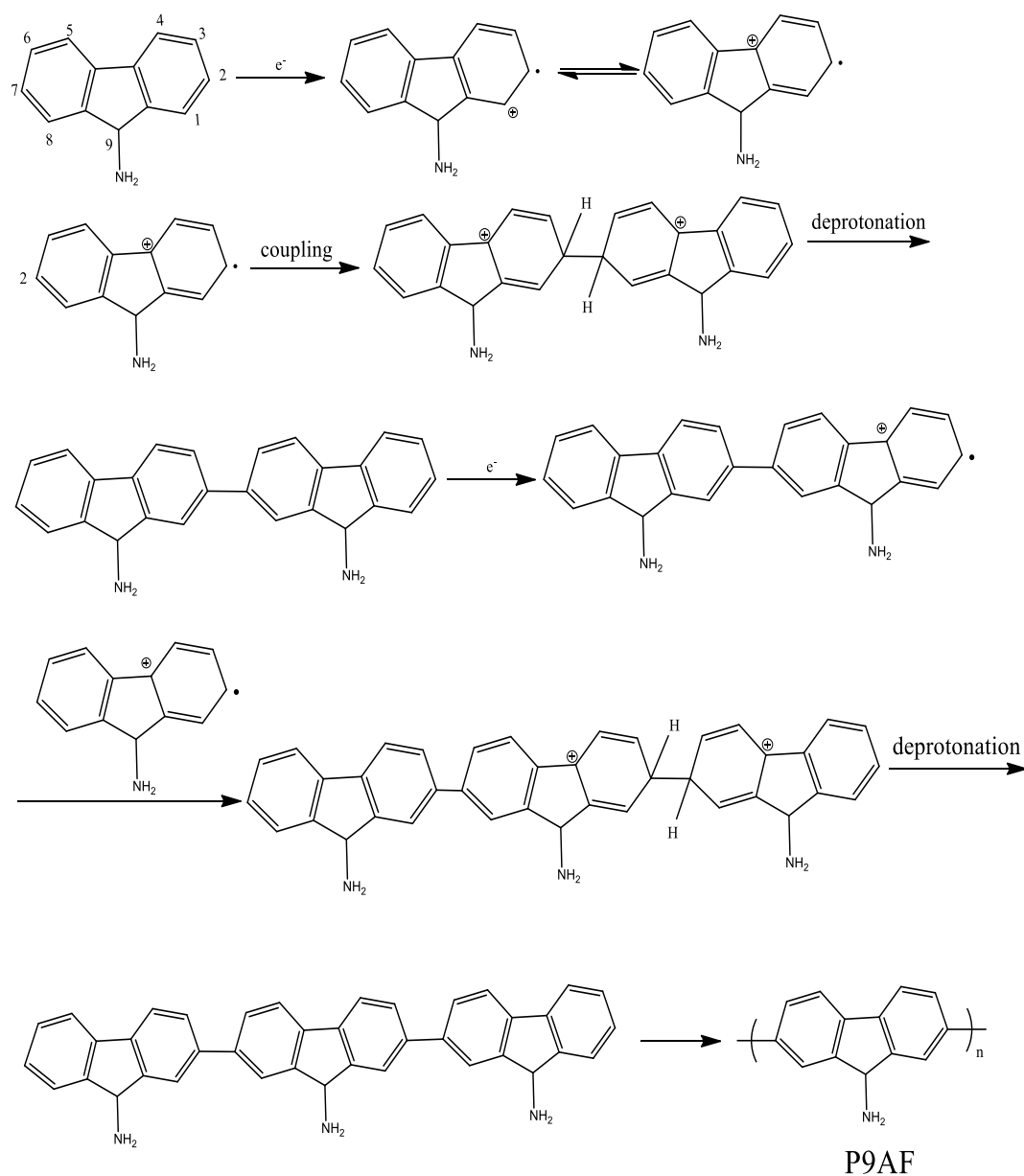


Figure 3.17. Voltammetric generation of **P9AF** film in boron trifluoride diethyl etherate (BFEE) and trifluoroacetic acid (TFA) mixture (70/30; v/v) containing 25 mM **9-aminofluorene**. Scan rate was 100 mV/s. Inset: 1st cycle.



Scheme 3.2. Possible mechanism for the electrochemical polymerization of **9AF** [86].

The electrochemistry of deposited **P9AF** film on GCE was studied in DCM containing TBAPF₆ monomer free mixture. Similar to the literature [24], Figure 3.18 shows two anodic peaks centered at the 0.8 V and 1.0 V.

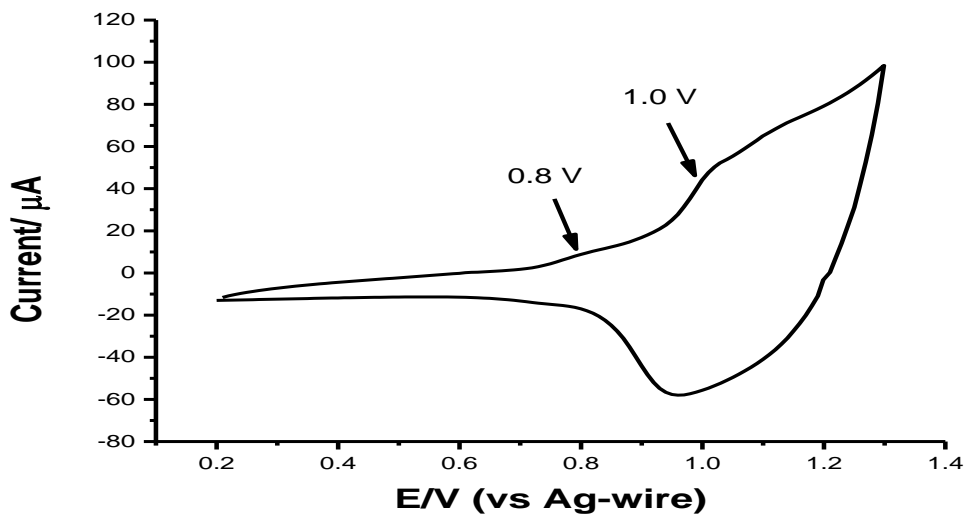


Figure 3.18. Cyclic voltammogram of **P9AF/GCE** in monomer free DCM containing 0.1 M TBAPF₆ solution. Scan rate was 100 mV/s.

3.4. Characterization of P9AF Film

3.4.1. Spectroelectrochemical Property of P9AF Film

P9AF film was electrodeposited on the indium tin oxide (ITO) electrode and its spectroelectrochemical behavior was investigated by recording the electronic absorption spectra at various applied potentials in dichloromethane (DCM)-tetrabutylammonium hexafluorophosphate (TBAPF₆) solvent-electrolyte couple. Polymer film showed an absorbance band at 329 nm due to $\pi \rightarrow \pi^*$ transition in its neutral state. This band decreases with an increase in potential which is accompanied with the appearance of two new bands at 470 nm and 1050 nm due to the formation of charge carriers. The isosbestic point which is observed at 402 nm clearly indicates one step reaction due to the formation of charge carriers.

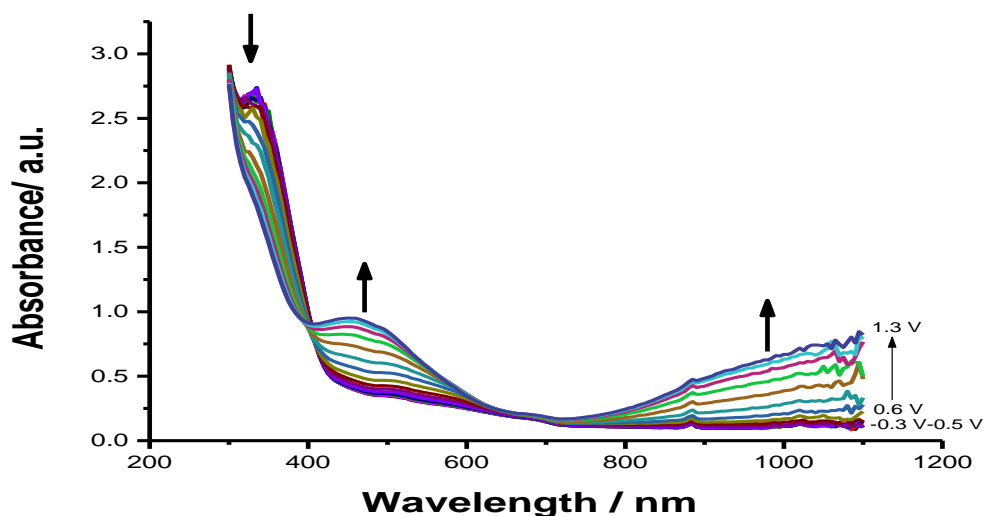


Figure 3.19. The changes in the electronic absorption spectra of electrochemically obtained **P9FA** film recorded in DCM containing TBAPF₆ as a function of applied potentials between -0.3 V and +1.3 V.

3.4.2. Fourier Transform Infrared Spectroscopy (FT-IR) of 9AF and P9AF

Figure 3.20 shows FT-IR spectra of monomer **9AF** and its corresponding polymer film, **P9AF**. Since ammonium ion form of **9-aminofluorene hydrochloride (9AF)** salt was used as the monomer, the characteristic N-H stretching peaks did not appear in the FTIR spectrum of the monomer. The peaks located at 735 cm⁻¹ and 761 cm⁻¹ are typical for 1,2-disubstituted benzene ring.

In the case of FTIR spectrum of **P9AF** film, since the salt form is not present in the polymer matrix, characteristic primary amine N-H stretching were observed at 3586 cm⁻¹ and 3200 cm⁻¹. The peaks at about 1455 cm⁻¹ and 1612 cm⁻¹ were due to elongation and deformation vibrations of N-H bond. Moreover, the appearance of a new peak at 781 cm⁻¹ is due to C-H stretching for 1,2,4-trisubstituted benzene ring and proves that polymerization proceeded via 2,7-positions.

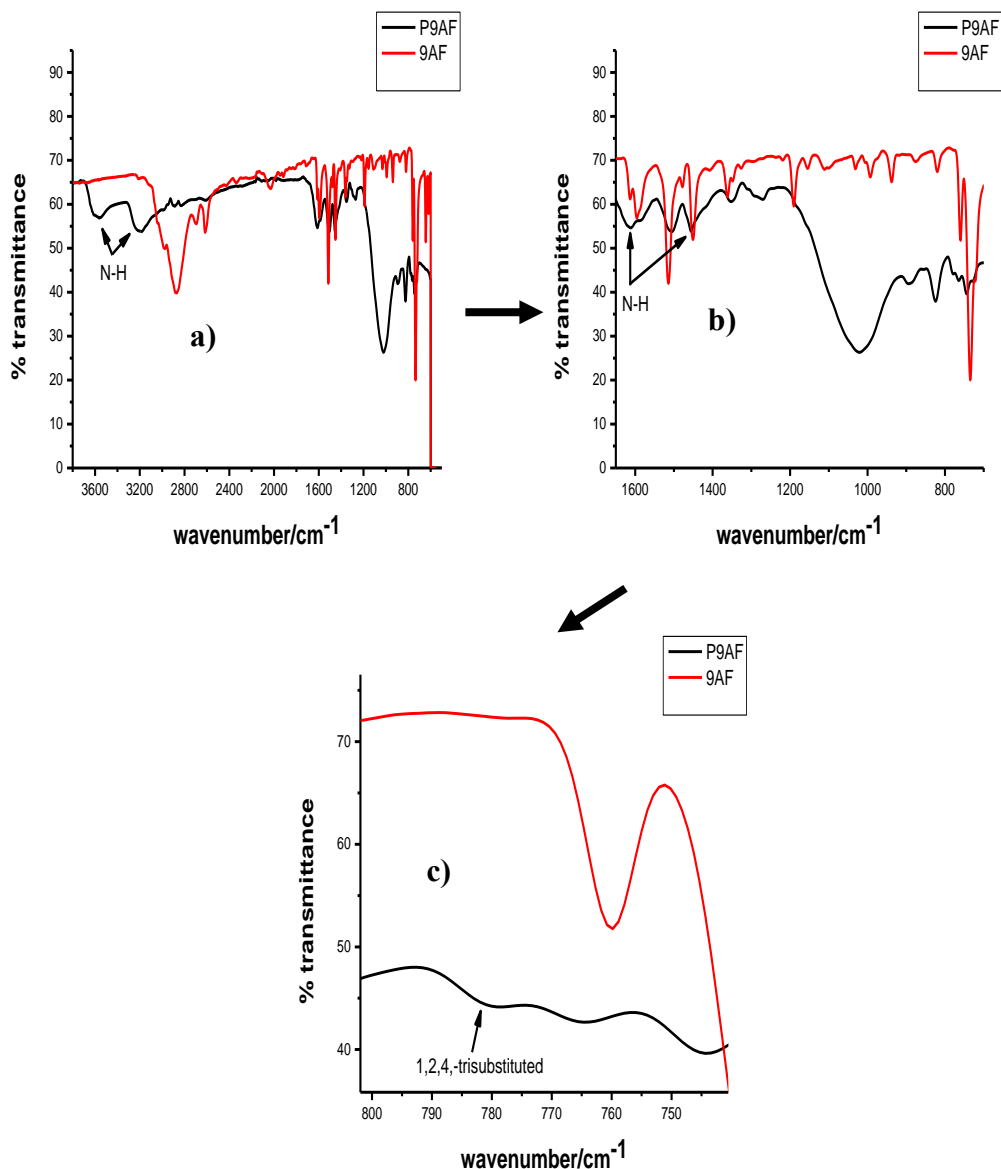


Figure 3.20. FTIR spectra of **9AF** and **P9AF** **a)** in the range of 3600-700 cm^{-1} **b)** in the range of 800-1600 cm^{-1} **c)** in the range of the 700-800 cm^{-1} .

3.5. Electrocatalytic Oxidation of DA in the Presence of AA at the P9AF/GCE

The mixture of **ascorbic acid (AA)** and **dopamine (DA)** in different pH medium were analyzed for investigating the electrocatalytic effect of modified **P9AF/GCE** by using DPV technique. Figure 3.21 demonstrates that **P9AF/GCE** has electrocatalytic effect

on **3.0 mM DA** in the presence of **30.0 mM AA** in pH=4.0 phthalate buffer containing 0.1 M KCl and pH=5 phthalate buffer containing 0.1 M KCl_(aq) medium, respectively. In pH=4.0 solution, **AA** and **DA** oxidation peak potentials were centered at 0.175 V and 0.375 V, respectively. In pH=5.0 phthalate medium, oxidation peak potentials were located at 0.152 V and 0.339 V for **AA** and **DA**, respectively. Although the peak separation is reasonable for determination of **DA** in the presence **AA**, the peak currents were not high enough for a sensible determination of **DA**. Acidic and neutral medium on the other hand, did not give satisfactory results for **AA** and **DA** mixture on **P9AF/GC** modified electrode. Figure 3.22 shows that the oxidation peaks of **30 mM AA** and **3 mM DA** in pH<1 (0.2 M H₂SO₄) and pH=7.4 buffer solutions are overlapping as in the case with **bare/GCE** (it will be shown on the following pages) at 0.421 V and 0.306 V, respectively.

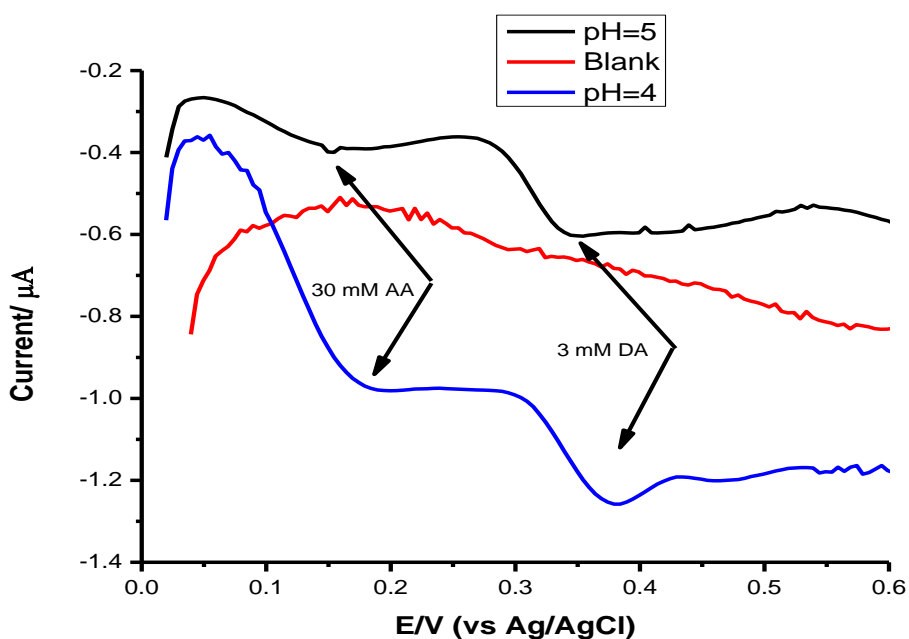


Figure 3.21. Differential pulse voltammograms of **AA** and **DA** in pH=4 and pH=5 phthalate buffer solution containing 0.1 M KCl_(aq) at modified **P9AF/GCE**. **AA** and **DA** concentrations are **30 mM** and **3 mM**, respectively.

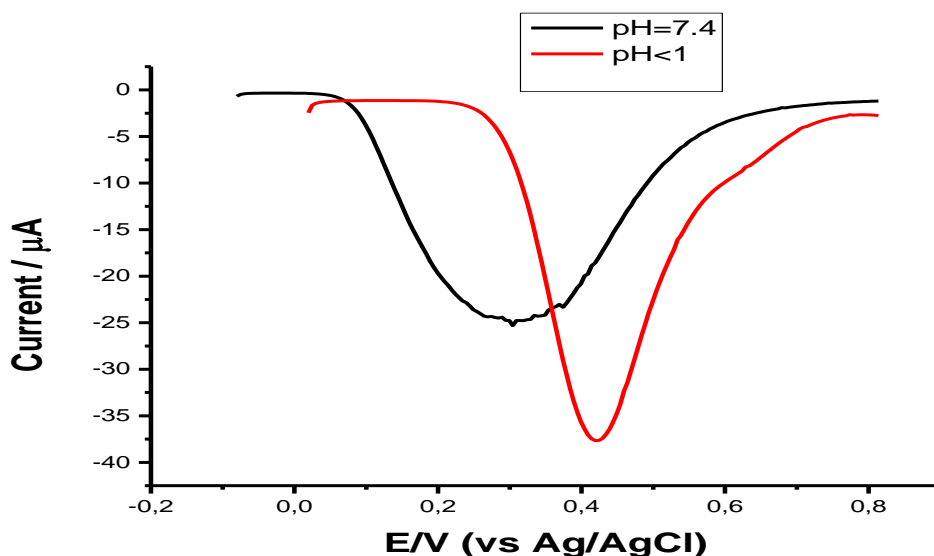


Figure 3.22. Differential pulse voltammograms of **30 mM AA** and **3 mM DA** in **0.2 M H₂SO₄ (pH<1)** and **pH=7.4 phosphate buffer solution** containing **0.1 M KCl_(aq)** at modified **P9AF/GCE**.

3.6. Electrochemical Polymerization and Electrochemical Behavior of Poly (9-fluorene carboxylic acid)

Electrochemical polymerization of **9-fluorene carboxylic acid (FCA)** was achieved in BFEE and TFA mixture via repetitive cycling and the resulting voltammograms are shown in Figure 3.23. As it is seen from the inset of Figure 3.23, the onset of **FCA** oxidation appeared at about 1.0 V. Upon repetitive cycling, the peak currents increased with the increasing number of scans indicating the polymer film formation on GCE. After 20 cycles between +0.2 and 1.3 V, a brown polymeric film was observed on the working electrode surface. As in the case of electrochemical polymerization of **9AF**, BFEE and TFA mixture was found to give better polymer film on GCE as compared to acetonitrile/LiClO₄ solvent/electrolyte couple. A possible mechanism, similar to the poly (fluorene-9-acetic acid) [86], for the electrochemical polymerization of **FCA** is shown in Scheme 3.3.

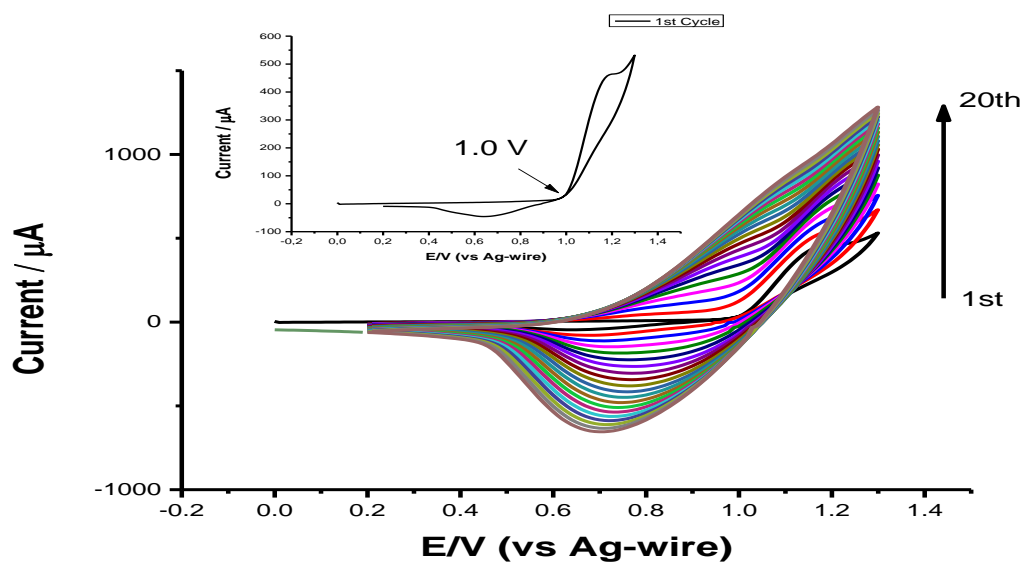
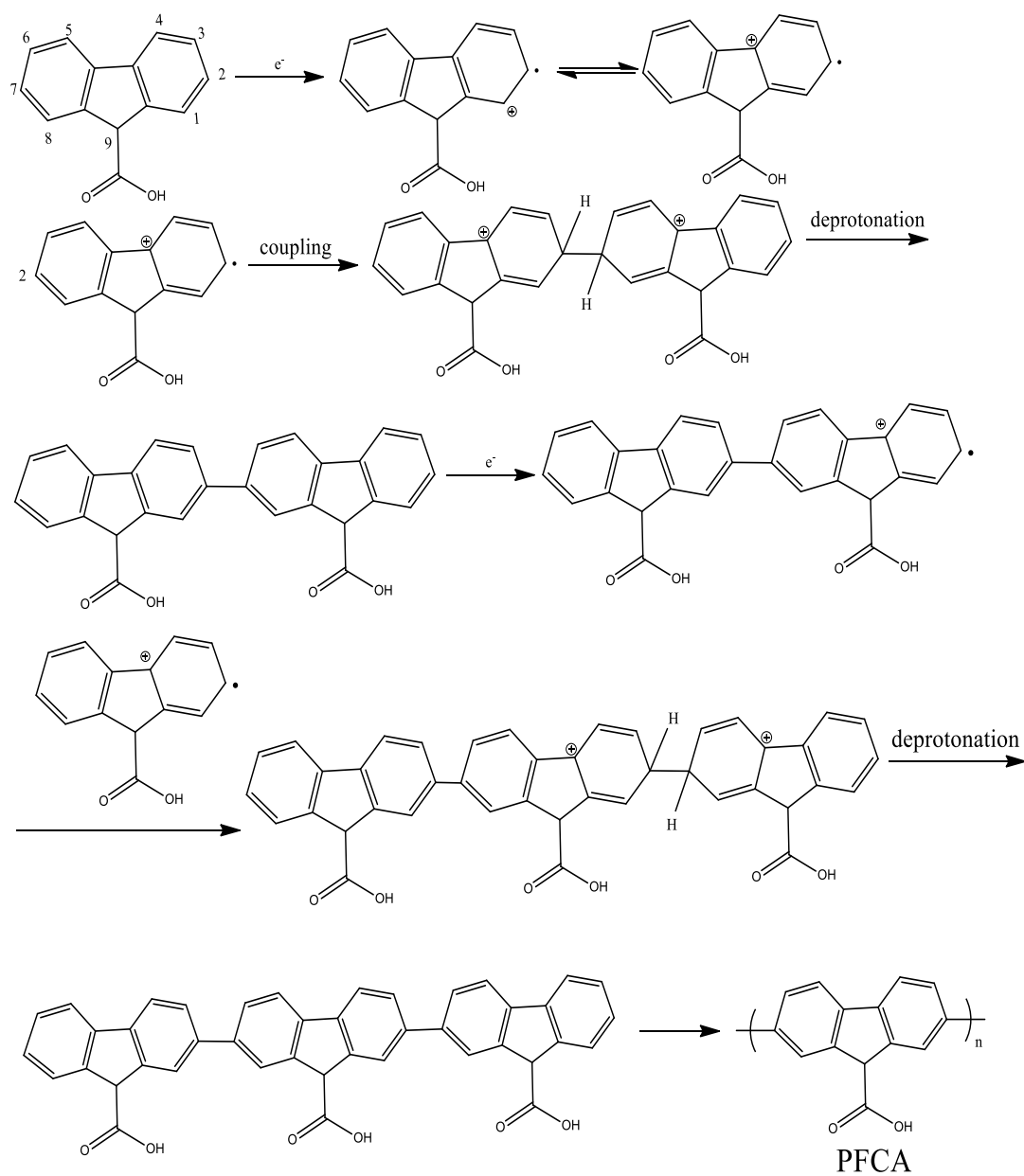


Figure 3.23. Voltammetric generation of **PFCA** in boron trifluoride diethyl etherate (BFEE) -trifluoroacetic acid (TFA) mixture (70/30; v/v) containing 25 mM **9-fluorenicarboxylic acid**. Scan rate was 100 mV/s. Inset: shows 1st cycle.



Scheme 3.3. Possible mechanism for the electrochemical polymerization of **FCA** [86].

The electrochemical behavior of the **PFCA** film was studied in monomer free BFEE - TFA mixture by recording the cyclic voltammogram in the range of 0.0 V to 1.3 V (See Figure 3.24). Similar to the previously reported cyclic voltammogram of **PFCA**,

broad anodic and cathodic peaks were observed corresponding to doping and dedoping of the polymer film [22].

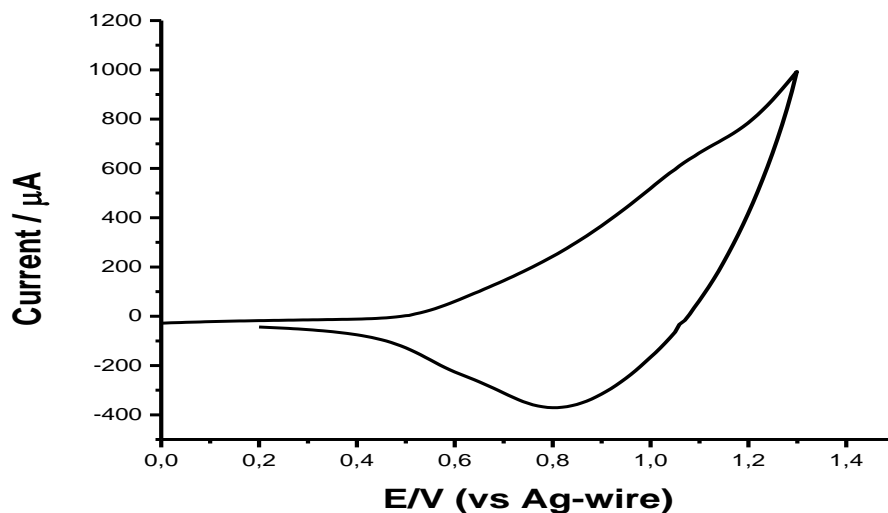


Figure 3.24. Cyclic voltammogram of **PFCA/GCE** in monomer free BFEE - TFA mixture (70/30; v/v). Scan rate was 100 mV/s.

3.7. Optimization of the Polymerization Conditions

3.7.1. 9-Fluorene Carboxylic Acid Oxidation in Different Electrolytic Solutions

In order to find the suitable medium for the electrochemical polymerization of **FCA**, DPV of the monomer was recorded in three different solvent-electrolyte mixtures and the resulting voltammograms are shown in Figure 3.25. The oxidation potential of **FCA** was found to be at about +1.65 V in acetonitrile-LiClO₄ solvent-electrolyte mixture. When the voltammogram of **FCA** was recorded in pure BFEE, as a middle Lewis acid, the oxidation potential was drastically lowered to 1.17 V due to lowering aromatization energy [87]. Besides, it is also reported that the presence of TFA in BFEE reduces the overoxidation effect and provides the formation of high-quality polymer films [22]. Therefore, BFEE - TFA mixture (70/30; v/v) was chosen as an electrolytic solution for the polymerization of **9-fluorene carboxylic acid**.

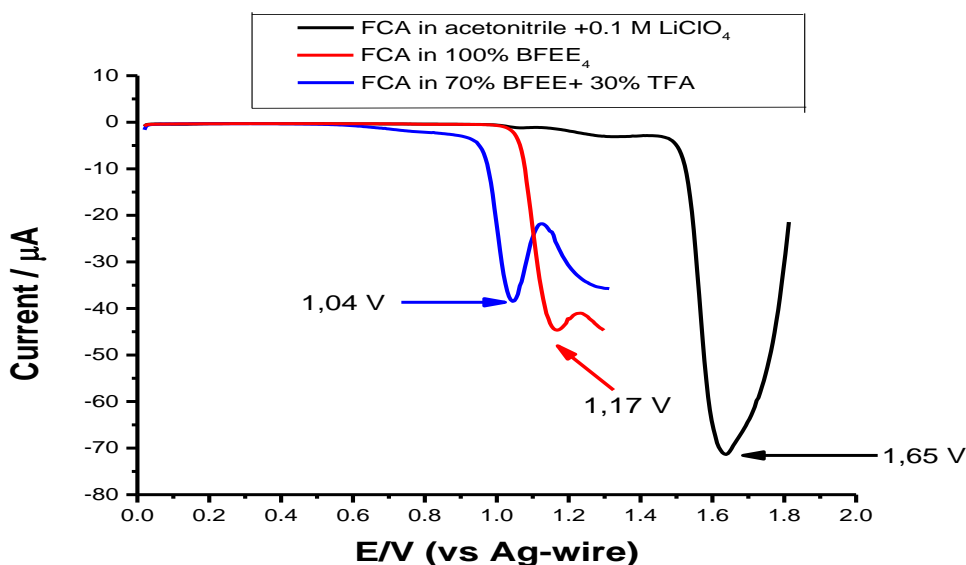


Figure 3.25. 25 mM FCA oxidation potentials in different electrolytic solutions.

3.7.2. Effect of the Amount of Trifluoroacetic Acid (TFA) in the Electrolytic Solution for the Electrochemical Behavior of AA and DA

Although BFEE -TFA mixture (70/30; v/v) was used as the electrolytic solution for FCA polymerization on GCE due to the important role of TFA on the film quality, we have also synthesized PFCA in a different volume ratio (40/60; v/v) of BFEE -TFA mixture. The response of three polymer film modified electrodes were tested in 15 mM AA and 3 mM DA solution in Figure 3.26. As seen from the Figure 3.26, PFCA film prepared in pure BFEE gave a low signal for DA oxidation together with an ill-defined signal for AA oxidation. When the PFCA polymer film was prepared in BFEE-TFA mixture (70/30; v/v) not only the signal intensity increased but also two clear peaks were observed corresponding to AA and DA oxidation. Since the polymer film prepared in the mixture containing more TFA (BFEE/TFA; 40/60; v/v) did not further improve AA and DA signals; therefore, the volume ratio (70/30; v/v) of BFEE-TFA mixture was preferred as electrolyte for PFCA modified electrode studies.

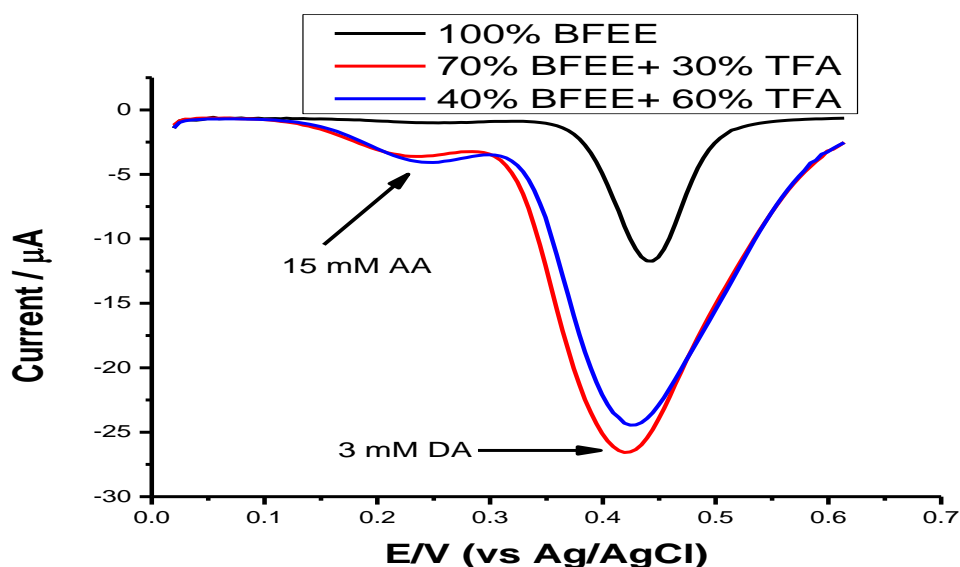


Figure 3.26. Effect of TFA amount in electrolytic solution for the quality of **PFCA** film. **15 mM AA** and **3 mM DA** in pH=4 phthalate buffer containing 0.1 M $\text{KCl}_{(\text{aq})}$ solution.

3.7.3. Effect of Number of Polymerization Cycles on PFCA Film

As it is written in part 3.6, **FCA** was electropolymerized via repetitive cycling. Since increasing number of cycles increases the film thickness, we have also investigated the effect of number of cycles used in the polymerization of **FCA** in terms of its response to **AA** and **DA**. As seen from Figure 3.27, the signal intensity both for **AA** and **DA** was found to increase with increasing number polymerization cycles up to 20 cycles. Surprisingly a lower signal intensity was observed when the polymer film was obtained via 25 repetitive cycles. This might be most probably due to formation of fractures on the polymer film.

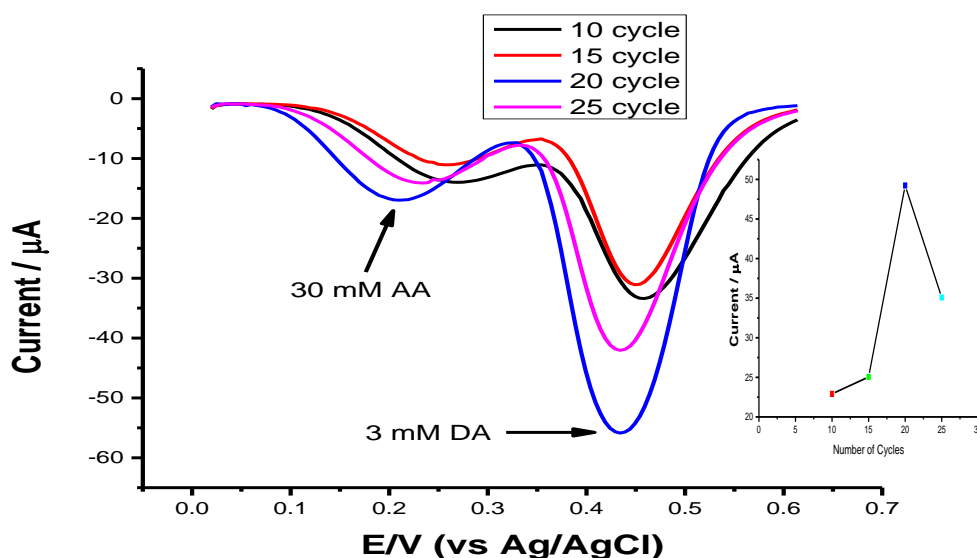


Figure 3.27. Effect of number of cycles used in the polymerization of **FCA** in terms of its response to **30 mM AA** and **3 mM DA** in pH=5 phthalate buffer containing 0.1 M $\text{KCl}_{(\text{aq})}$. Inset: Signal intensity versus number of polymerization cycles.

3.8. Characterization Studies of PFCA Film

3.8.1. Spectroelectrochemical Behavior of PFCA Film

To investigate spectroelectrochemical behavior of **PFCA**, the polymer film was electrodeposited on ITO-glass working electrode via repetitive potential cycling. After 20 cycles, the polymer film was washed with the monomer-free electrolyte solution and placed into cuvettes for subsequent spectroelectrochemical investigations. Electro-optical properties were investigated by monitoring the changes in absorption spectra as a function of applied potential in monomer-free solution (BFEE-TFA (70/30; v/v) and the related spectra recorded for **PFCA** were shown in Figure 3.28. As it is seen from the Figure 3.28, the polymer film showed an absorption band at 328 nm in its the neutral state due to $\pi \rightarrow \pi^*$ transition. Upon increasing the potential, the intensity of the $\pi \rightarrow \pi^*$ transition bands decreased simultaneously with concomitant absorption bands appearing at 487 nm and 900 nm during oxidation of **PFCA** due to

the formation of charge carriers. The isosbestic point which is observed at 394 nm clearly indicates one step reaction due to the formation of charge carriers [23].

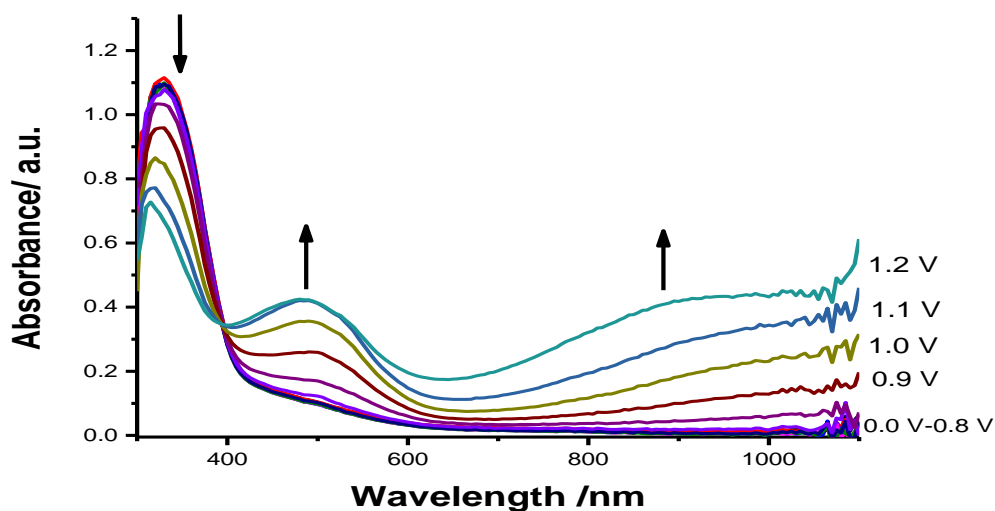


Figure 3.28. The changes in the electronic absorption spectra of electrochemically obtained **PFCA** film recorded in BFEE/TFA (70/30; v/v) mixture as a function of applied potentials between 0.0 V and +1.2 V.

3.8.2. Fourier Transform Infrared Spectroscopy (FT-IR) of FCA and PFCA

Figure 3.29 shows FT-IR spectra of the monomer (**FCA**) and its corresponding polymer film (**PFCA**). The presence of strong peak at around 1700 cm^{-1} due to the C=O group in the FTIR spectra of both monomer and its corresponding polymer indicates that this group remains intact during electrochemical polymerization of the monomer. The C-H stretching peak that appeared at 730 cm^{-1} , present in the spectrum of monomer, is characteristic for 1,2-disubstituted benzene ring and it lost its intensity in the spectrum of polymer film. The new C-H stretching peak, which appeared at 830 cm^{-1} in the spectrum of polymer, is characteristic for 1,2,4-trisubstituted benzene ring and proves that polymerization occurs via 2,7-positions [88]. The intense peak at around 1050 cm^{-1} in the spectrum of **PFCA** may be related with BF_3 [89].

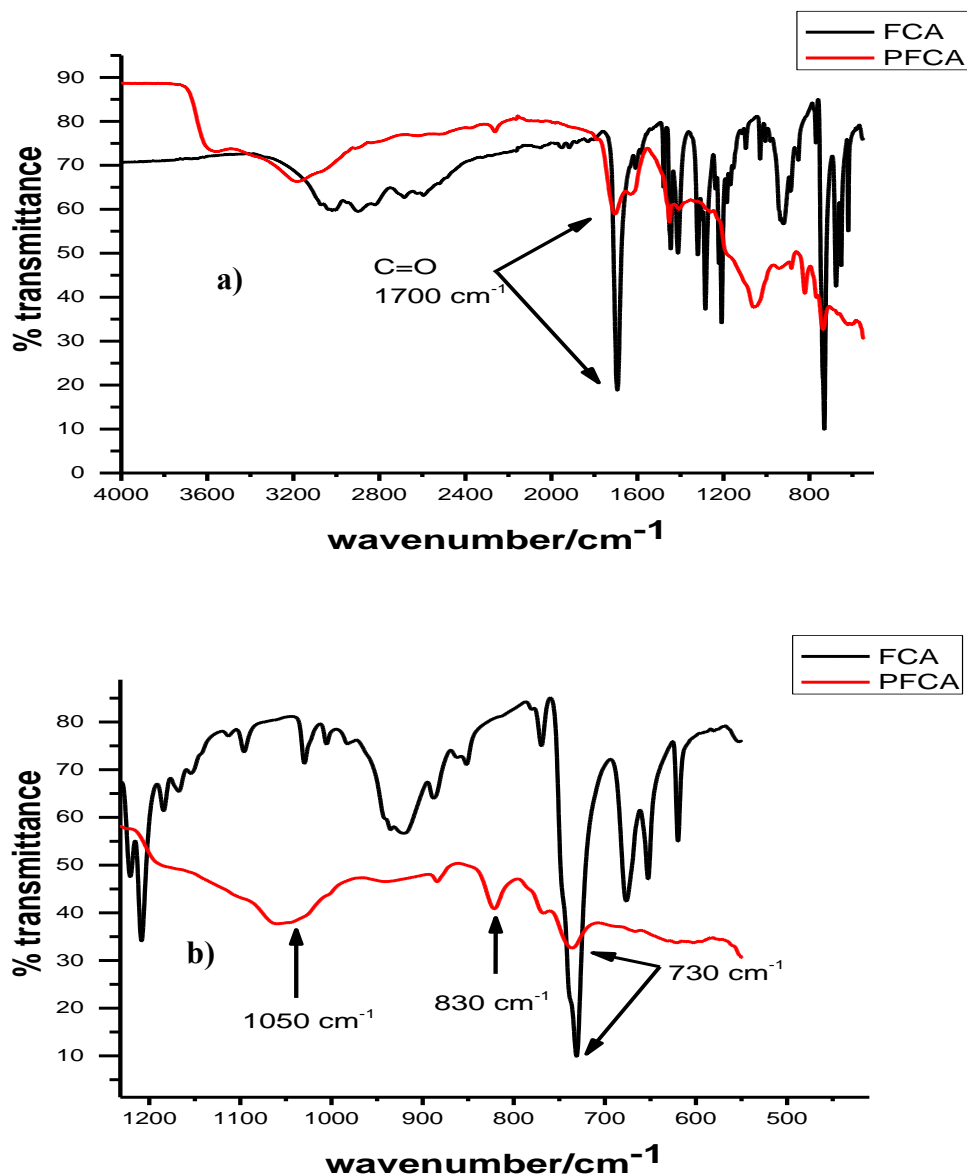


Figure 3.29. a) FT-IR spectra of FCA and PFCA. b) The region between 1200 cm⁻¹ and 550 cm⁻¹ of the spectra of FCA and PFCA is given in an enlarged scale.

3.9. Electrocatalytic Oxidation of DA in the Presence of AA at the PFCA/GCE

It is known that the electrochemical detection of **dopamine (DA)** in the presence of **ascorbic acid (AA)** is difficult due to the similar oxidation potentials of them and catalytic oxidation of AA by DA. However, the modification of glassy carbon

electrode (GCE) with **poly (9-fluorene carboxylic acid) (PFCA)** provided good resolution for their oxidation peaks and intense responses for **AA** and **DA** in this study.

3.9.1. Electrochemical Behavior of AA and DA on BARE/GCE and PFCA/GCE in Different Media

Calibration study at pH<1: Figure 3.30 displays the response of **BARE/GCE** to the mixture of **15 mM AA** and **3 mM DA** in 0.2 M H₂SO₄ solution. As seen from Figure 3.30 instead of separate oxidation peaks of **AA** and **DA**, an overlapping peak was observed at 577 mV. However, after the modification of GCE with **PFCA** film, two well resolved oxidation peaks appeared at 407 mV and 540 mV corresponding to electrochemical oxidation of **AA** and **DA**, respectively. The oxidation peak current signal increased upon increasing of **DA** concentration, on the other hand, the oxidation signal of **AA** was not affected by this change in the **DA** concentration. The peak separation was good enough to produce a calibration plot for **DA** from **0.3 mM** to **15 mM** in the presence of **15 mM AA**. The calibration plot shows good linearity for **DA** in pH<1 medium with a correlation coefficient of 0.994 (See Figure 3.31 (b)).

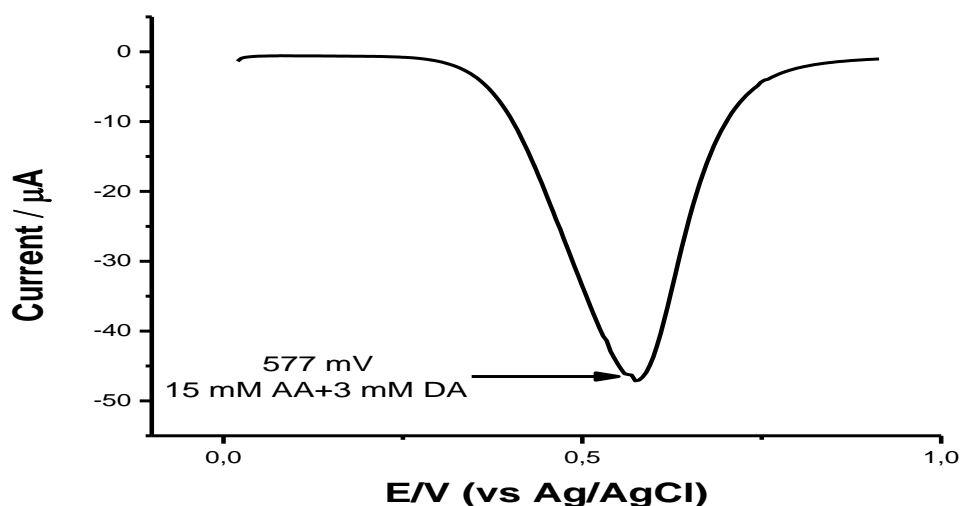


Figure 3.30. Differential pulse voltammogram of **15 mM AA** and **3 mM DA** mixture at **bare GCE** in 0.2 M H₂SO_{4(aq)} solution.

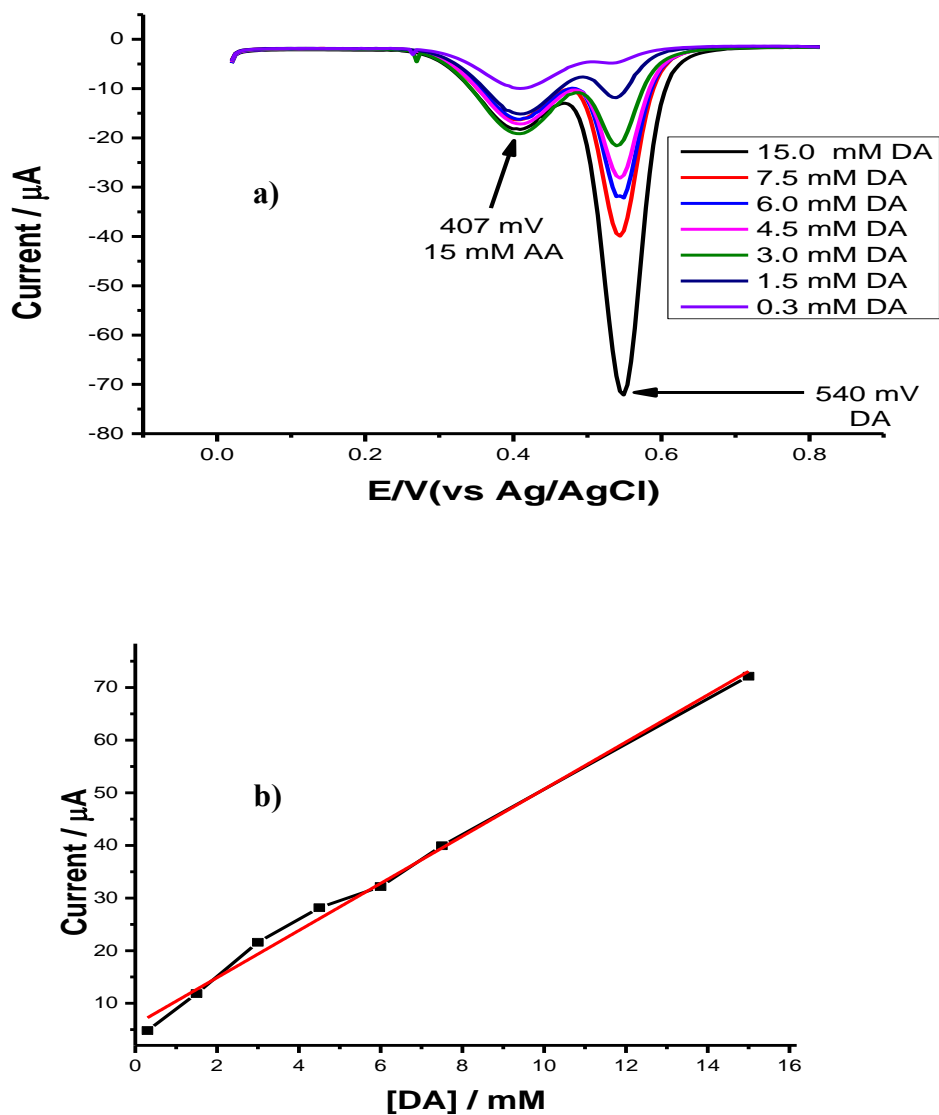


Figure 3.31. a) Differential pulse voltammogram of **0.3-15.0 mM DA** in the presence of **15.0 mM AA** in $0.2 \text{ M H}_2\text{SO}_{4(\text{aq})}$ solution. b) Calibration plot of **DA**.

Calibration study at pH=4: Figure 3.32 shows the response of **bare GCE** to the solution containing **15 mM AA** and **3 mM DA** in pH=4 phthalate buffer solution containing 0.1 M KCl . A broad overlapping peak at **468 mV** was observed indicating that **bare GCE** cannot resolve oxidation peaks of **AA** and **DA**. However, two well-defined oxidation peaks were observed at **206 mV** and **397 mV** for **AA** and **DA**,

respectively, on **PFCA/GCE** (Figure 3.33 (a)). The oxidation peak current signal increased with the increasing of **DA** concentration and the oxidation signal of **AA** was not affected by the changing of **DA** concentration. The separation was enough to produce **DA** calibration plot from **0.03 mM to 1.5 mM** in the presence of **15 mM AA**. The calibration plot shows good linearity for **DA** in pH=4 phthalate buffer solution containing 0.1 M KCl with correlation coefficient of 0.992 (See Figure 3.33 (b)). The limit of detection (LOD) for **DA** in pH=4 medium was calculated based on $3 s/m$ (s is the standard deviation of the lowest concentration response and m is the slope of the calibration curve) as $5.2 \mu\text{M}$.

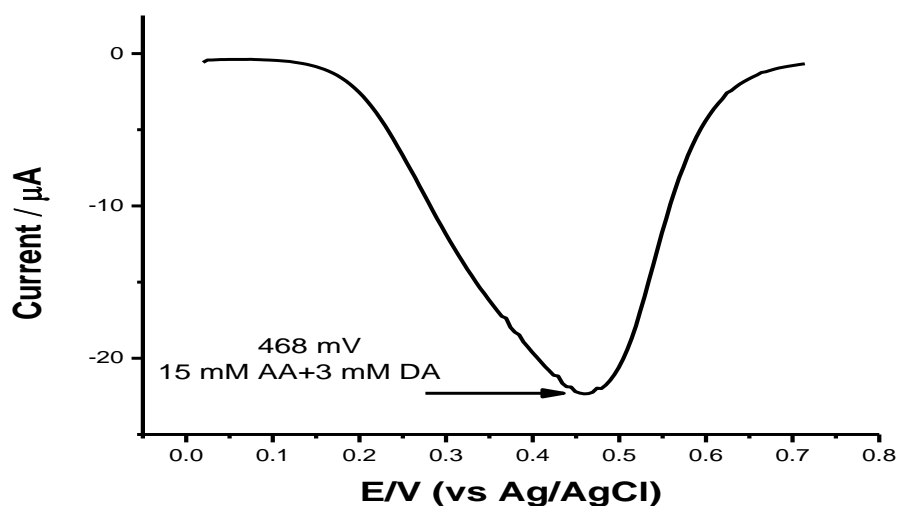


Figure 3.32. Differential pulse voltammogram of **15.0 mM AA** and **3.0 mM DA** mixture at **bare GCE** in pH=4 phthalate buffer containing 0.1 M $\text{KCl}_{(\text{aq})}$ solution.

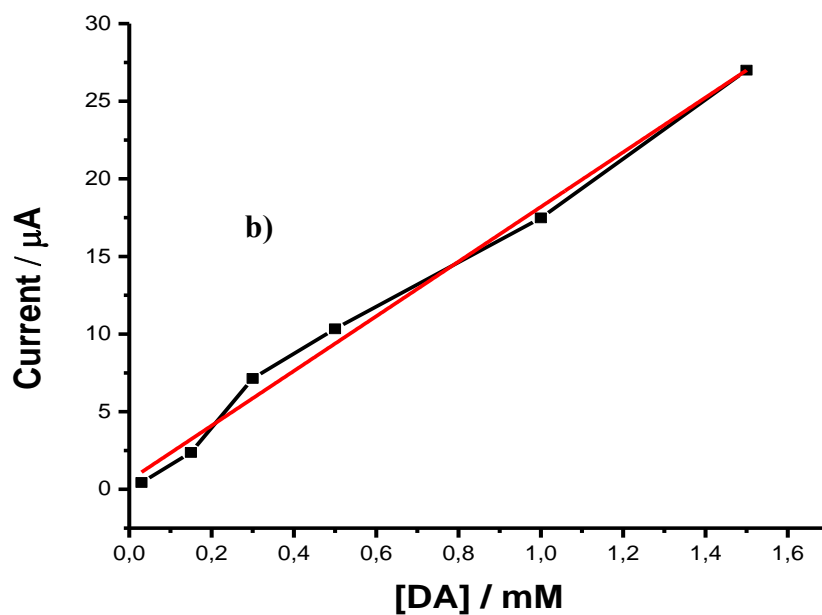
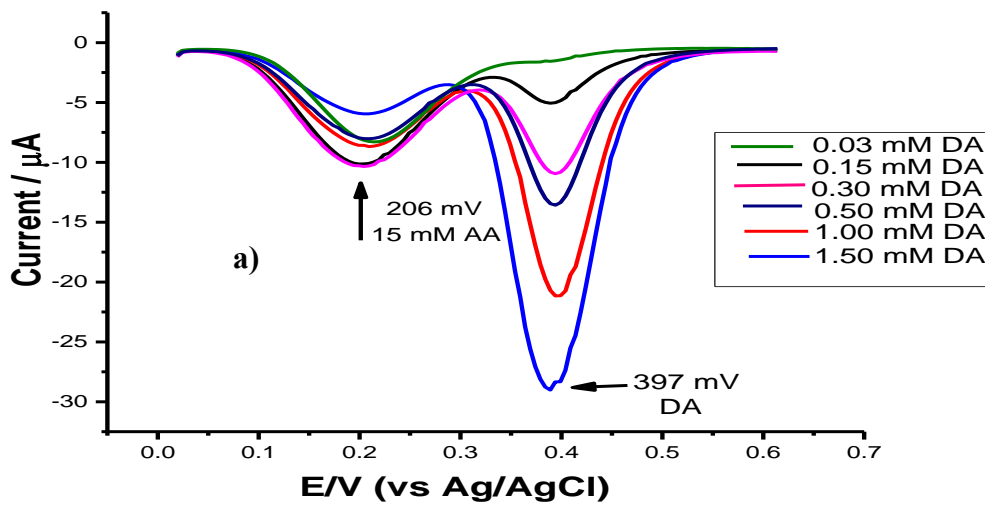


Figure 3.33. a) Differential pulse voltammogram of **0.03-1.50 mM DA** in the presence of **15.0 mM AA** in pH=4 phthalate buffer solution containing 0.1 M $KCl_{(aq)}$.
 b) Calibration plot of **DA**.

Calibration study at pH=5: As in the case of pH<1 and pH=4 studies **bare GCE** exhibited only a broad peak at 422 mV in Figure 3.34. Whereas for **PFCA/GCE** immersed in pH=5 phthalate buffer solution containing 0.1 M KCl, two well-defined oxidation peaks were observed at 153 mV and 372 mV for **AA** and **DA**, respectively, (Figure 3.35 (a)). It is also noted that oxidation peak current for **DA** oxidation increases linearly with increasing **DA** concentration without any noticeable change in the oxidation signal of **AA**. The **DA** calibration plot, prepared in the range of **0.015 mM to 3.0 mM** is given in Figure 3.35 (b). Good linearity for **DA** in pH=5 phthalate buffer solution containing 0.1 M KCl was obtained with correlation coefficient of 0.996.

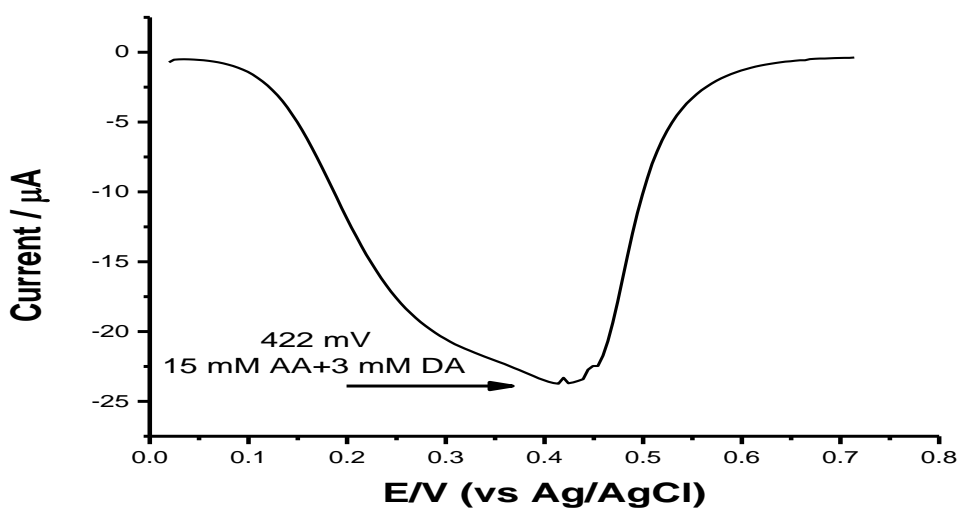


Figure 3.34. The differential pulse voltammogram of **15 mM AA** and **3 mM DA** mixture at **bare GCE** in pH=5 phthalate buffer solution containing 0.1 M $\text{KCl}_{(\text{aq})}$ solution.

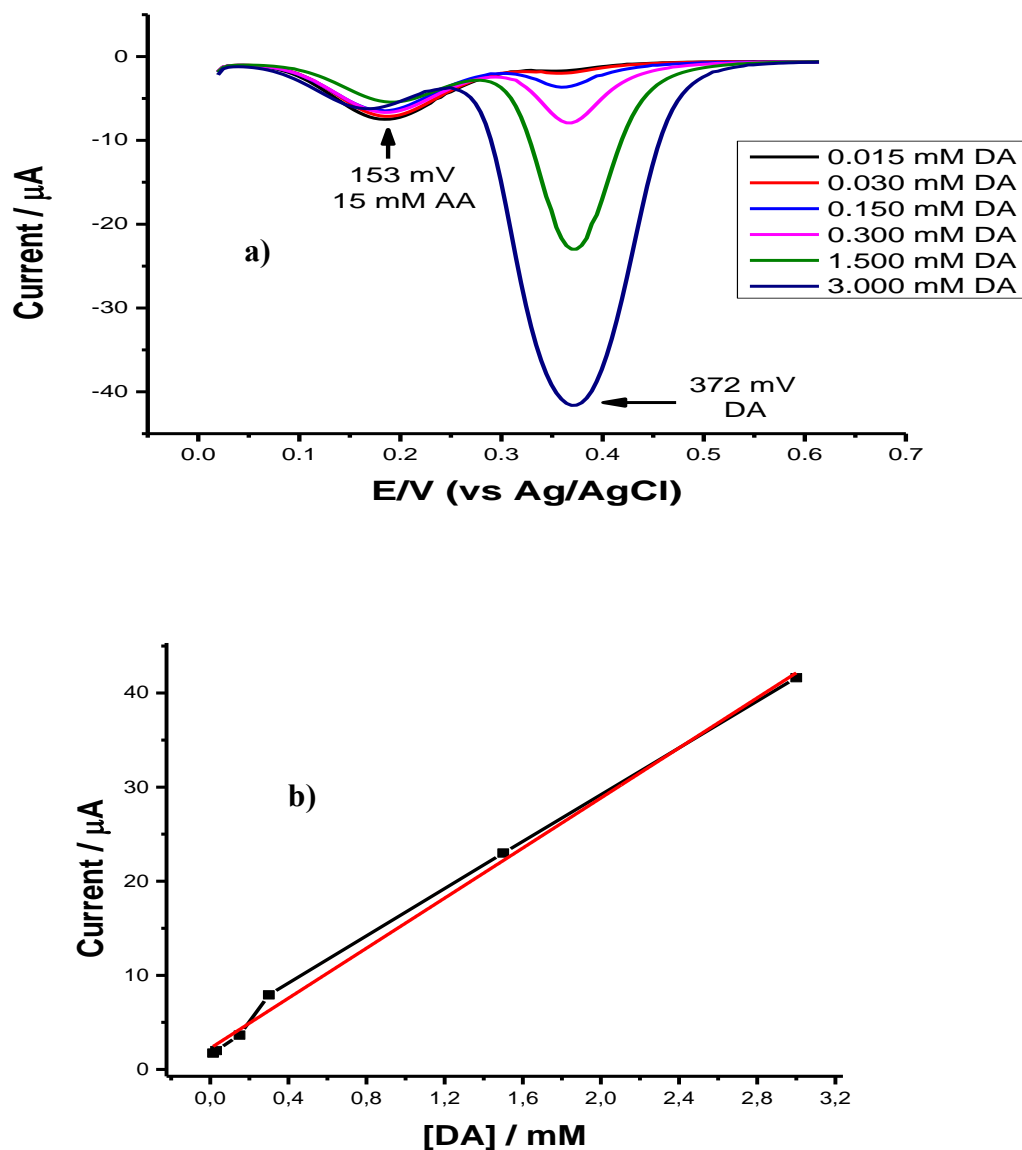


Figure 3.35. a) Differential pulse voltammogram of **0.015-3.0 mM DA** in the presence of **15.0 mM AA** in pH=5 phthalate buffer solution containing 0.1 M $\text{KCl}_{(\text{aq})}$ solution. b) Calibration plot of **DA**.

3.9.2. Effect of pH on the peak currents and peak potentials of DA and AA

The pH of the supporting electrolyte is very important to analyze the target molecules in electrochemical measurements. Figure 3.36 shows the peak currents and peak

potentials for **15.0 mM AA** and **0.30 mM DA** at different pH values. As it is seen from Figure 3.36, besides the shifts in the peak positions, the peak currents for **DA** and **AA** also changes. These changes are depicted in Figure 3.37 (a) and (b), respectively. As it is seen from Figure 3.37 (a) maximum peak current for **DA** was obtained in pH=4 phthalate buffer solution; therefore, this medium was used for further studies.

The pK_a value of FCA in aqueous medium is known as 3.61 [90]; therefore, surface of the electrode becomes negatively charged at pH=4.0 and pH=5.0 values. Ascorbic acid and dopamine pK_a values are 4.17 [56] and 8.87 [91], respectively. At pH=4, polymer carriers negative charge on carboxylic acid group (COO^-) and DA carriers positive charge as NH_3^+ form, Scheme 3.4. On the other hand, theoretically AA must be in positively charged form. In the solution, however, there might be some dissociation of AA at this pH so it might carry also negative charge. For this reason, the positive and negative charges of AA might be neutralized among themselves so negatively charged polymeric surface of the electrode might interact more strongly with the cationic form of DA at pH 4.0. When the pH was higher than 4 (such as pH=5), the peak response of DA sharply decreased because of totally negative form of AA. It might cause neutralization of DA (positively form at pH=5) because of excess amount of it. Therefore, the peak current of DA (Figure 3.37 (a)) decreased at pH=5. Scheme 3.4. shows the changing of DA species as function of pH.

In contrast to variation of oxidation current with pH, the oxidation potential of **DA** shifted linearly to more negative values with increasing of pH and the slope was found to be $-42 \text{ mV} \cdot \text{pH}^{-1}$ with the R^2 0.997 (Figure 3.37 (b)).

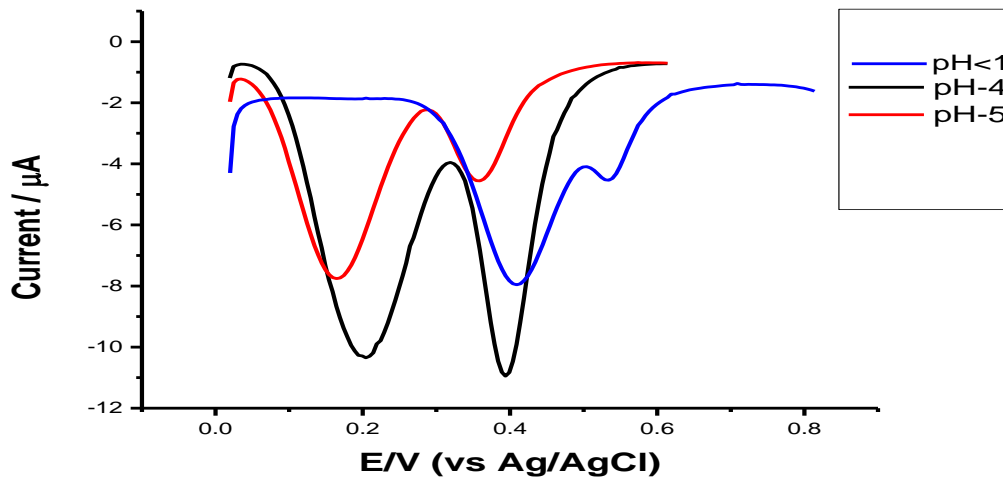


Figure 3.36. Differential pulse voltammograms mixture of **15.0 mM AA** and **0.30 mM DA** in different media.

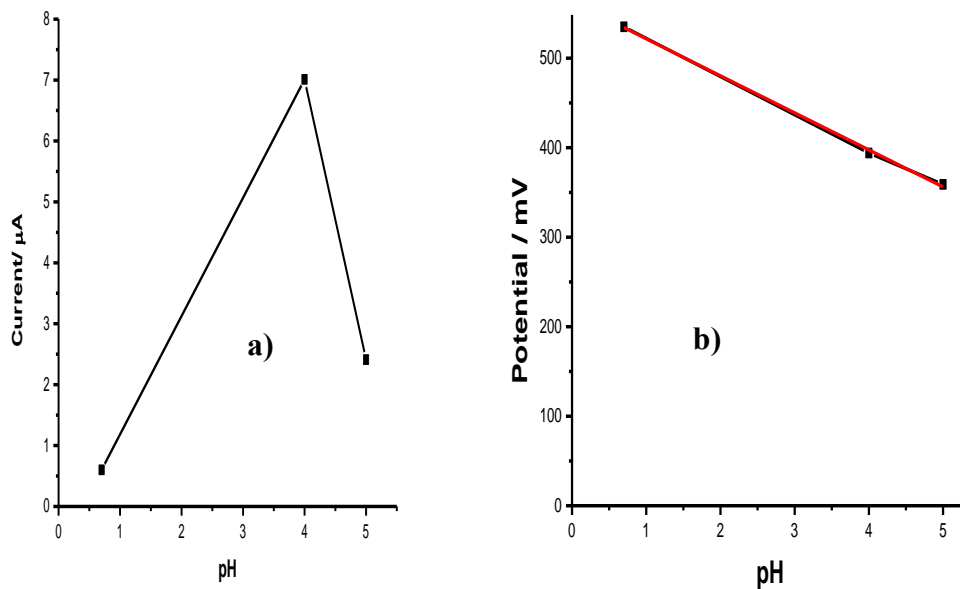
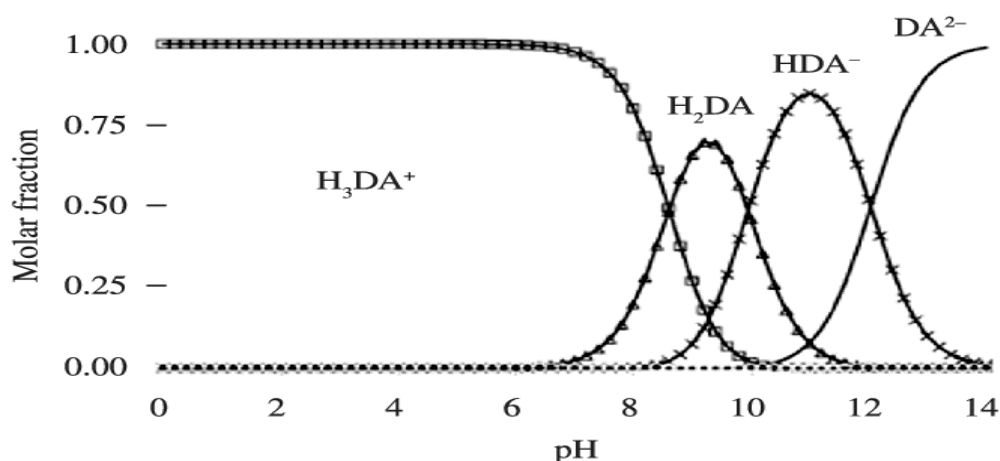
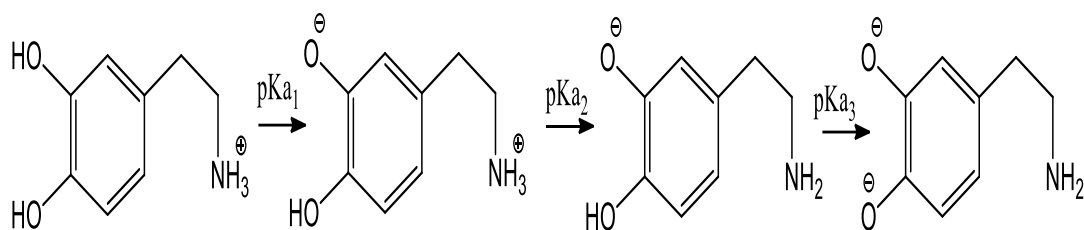


Figure 3.37. Effect of pH on (a) **0.30 mM DA** peak current and (b) **0.30 mM DA** peak potential.



Scheme 3.4. Various forms of **DA** as a function of pH [92].

3.9.3. Effect of Scan Rate

The effect of scan rate on the oxidation peak potential and peak current of **DA** was studied at the **PFCA/GCE** in pH=4 phthalate buffer solution containing 0.1 M KCl. Figure 3.38 (a) shows cyclic voltammograms of **1.0 mM DA** between 40 and 320 mV s^{-1} with increment of 20 mV s^{-1} . Anodic and cathodic peak currents of **DA** increased with the increasing of scan rate. When the oxidation peak current is plotted against square root of scan rate a straight line was obtained in accordance with Randles–Sevcik equation ($i_p = 2.69 \times 10^5 n^{3/2} A D^{1/2} C v^{1/2}$ at 25 °C) confirming that oxidation of **DA** at **PFCA/GCE** was a diffusion-controlled process (See Figure 3.38 (b)).

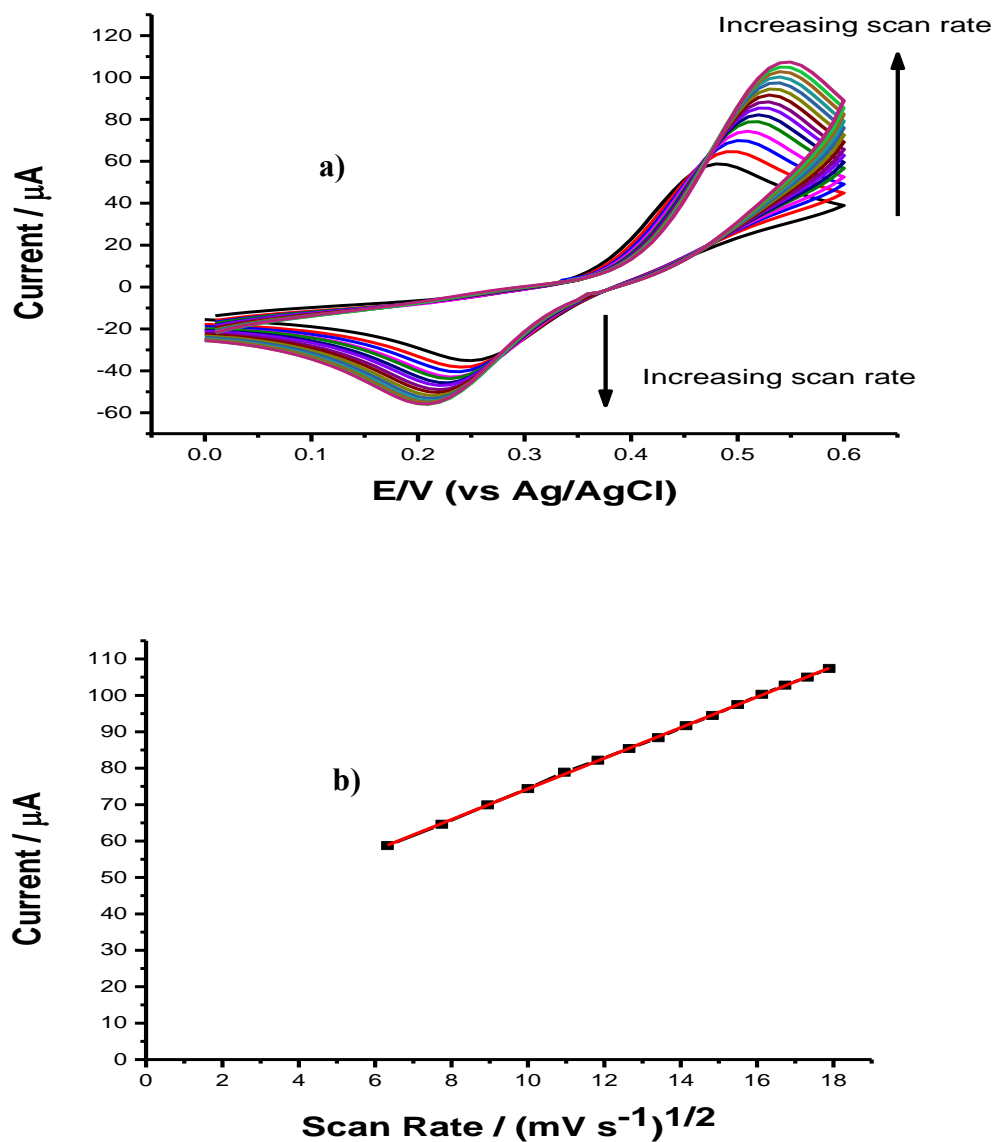


Figure 3.38. (a) Cyclic voltammograms of **1.0 mM DA** between 40 and 320 mV s^{-1} in $\text{pH}=4$ phthalate buffer containing $0.1 \text{ M KCl}_{(\text{aq})}$. (b) The plot of oxidation peak current vs square root of scan rate.

Although electrochemical oxidation of **DA** is found to be diffusion controlled, we have also noticed that a small amount of **DA** is remaining on the modified electrode surface due to adsorption of **DA**. To prove this adsorption, we kept the **PFCA** modified GCE in **1.0 mM DA** solution and recorded the CV in **DA** free electrolytic solution after 5

minute (See Figure 3.39). It is clearly noted that there is a reversible redox peak corresponding to **DA** oxidation and reduction on **PFCA/GCE** indicating the adsorption of **DA** on the modified electrode surface. It is important to mention that no such adsorption was noticed on **bare GCE**. Therefore, it can be concluded that the oxidation of **DA** at **PFCA/GCE** is not only diffusion controlled but also it has a little adsorption controlled character. For this reason, **PFCA/GCE** was refreshed prior to calibration studies by cycling the modified electrode in blank solutions until the loss of the **DA** signal.

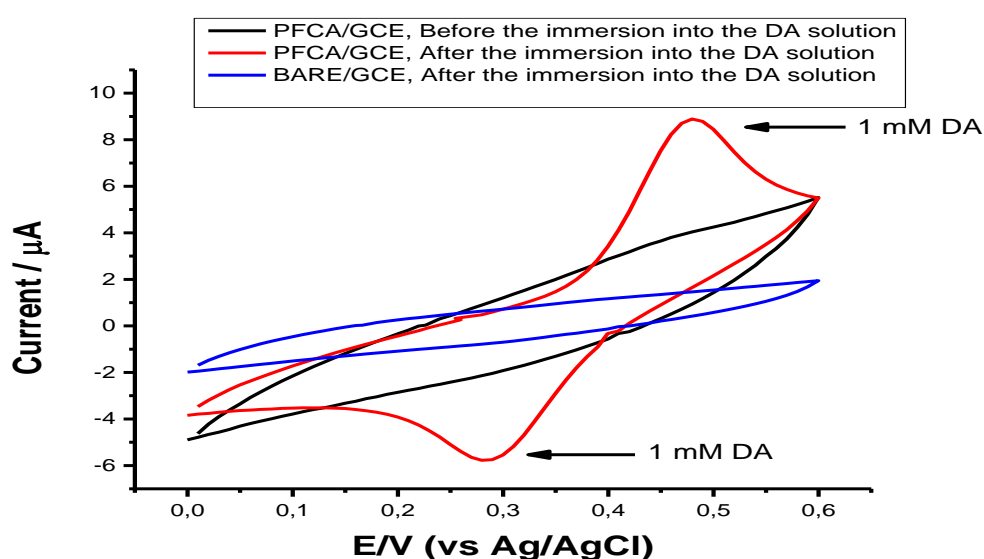


Figure 3.39. The comparison of cyclic voltammograms of **PFCA/GCE** and **BARE/GCE** before and after the immersion in **1.0 mM DA** solution. The CVs recorded in pH=4 phthalate buffer solution containing 0.1 M $\text{KCl}_{(\text{aq})}$. Scan rate is 100 mV/s.

3.9.4. Effect of Polymer Coating on Oxidation Potential of AA and DA Compared to that of Bare Electrode

As discussed earlier in part 3.9.1, it is not possible to resolve oxidation peaks of **AA** and **DA** in a solution containing both reagents with **BARE/GCE**. To investigate the reason for this observation, we have also recorded DPVs of **10.0 mM AA** and **1.0 mM**

DA solutions separately using **BARE/GCE** and the results are given in Figure 3.40. As can be seen from Figure 3.40, **AA** and **DA** oxidation peaks appeared at 454 mV and 390 mV, respectively. However, these oxidation peaks were observed at 206 mV and 397 mV for **AA** and **DA**, respectively on **PFCA/GCE** (See Figure 3.33 (a)). This cathodic shift in the oxidation potential of **AA** clearly shows the electrocatalytic effect of **PFCA** on **AA** oxidation. Due to this electrocatalytic effect, it was possible to resolve the oxidation peaks of **AA** and **DA** separately in the same solution.

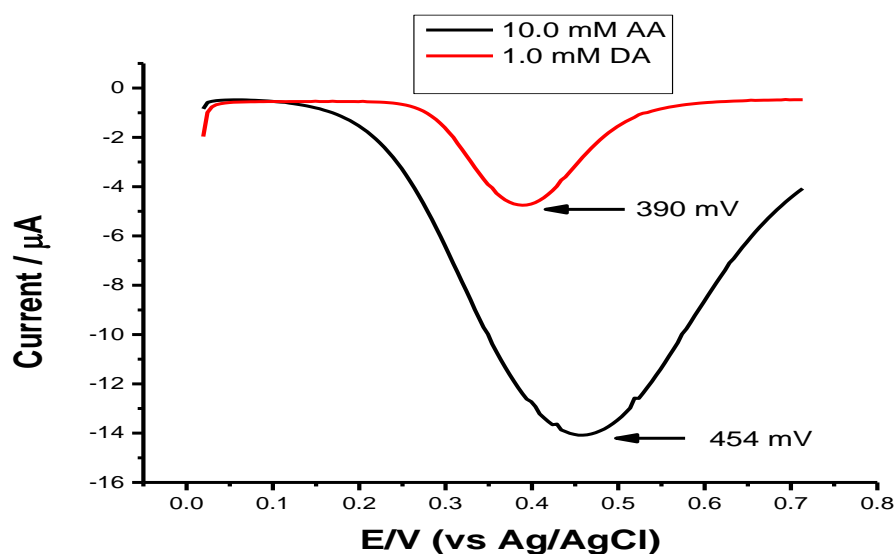


Figure 3.40. Differential pulse voltammograms of **10.0 mM AA** and **1.0 mM DA** in pH=4 phthalate buffer solution containing 0.1 M $\text{KCl}_{(\text{aq})}$ on **BARE/GCE**.

3.9.5. Stability of **PFCA/GCE**

Since the reusability of a modified electrode is very important for practical applications. The performance of the modified electrode was also tested after keeping the modified electrode under dry ambient condition for 3 days. From the DPVs given in Figure 3.41, only 7 % decrease was noted in the peak current for **DA**.

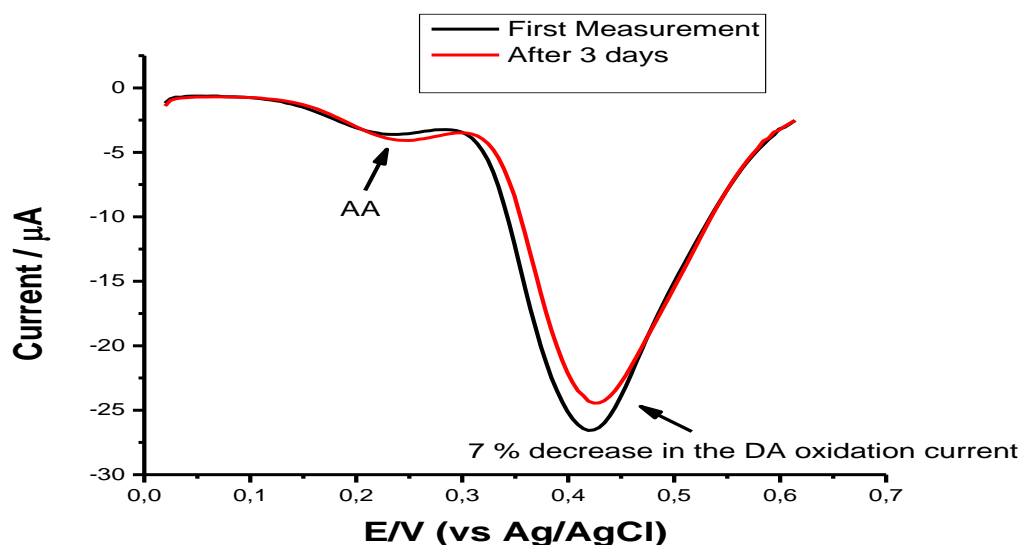


Figure 3.41. Stability test of the PFCA/GCE. The solution was **15.0 mM AA** and **1.5 mM DA** in pH=4 phthalate buffer solution containing 0.1 M $\text{KCl}_{(\text{aq})}$.

3.10. Comparison of the performances of PEDOT/GCE, P9AF/GCE and PFCA/GCE in terms of their electrochemical responses for AA and DA

As discussed earlier, **P9AF/GCE** could not resolve the oxidation potentials of **AA** and **DA** in acidic and neutral media in presence of both reagents (Figure 3.22). However, due to its electrocatalytic activity on **AA** oxidation, the peak separation was possible in solutions of pH=4 and pH=5. Therefore, comparison of **P9AF** and **PFCA** modified electrodes towards **AA** and **DA** oxidation is given in pH=5 medium in Figure 3.42. An inspection of Figure 3.42 reveals that both modified electrodes successfully separate the oxidation peaks of **AA** and **DA**. On the other hand, they showed different current responses for the oxidations. The much higher anodic currents obtained on **PFCA/GCE** might be due to better interaction of modified electrode surface with the reagents via lone pair electrons of carboxylic acid group in **PFCA**. This might contribute to electron transport process resulting in higher peak currents for **AA** and **DA** at **PFCA/GCE**.

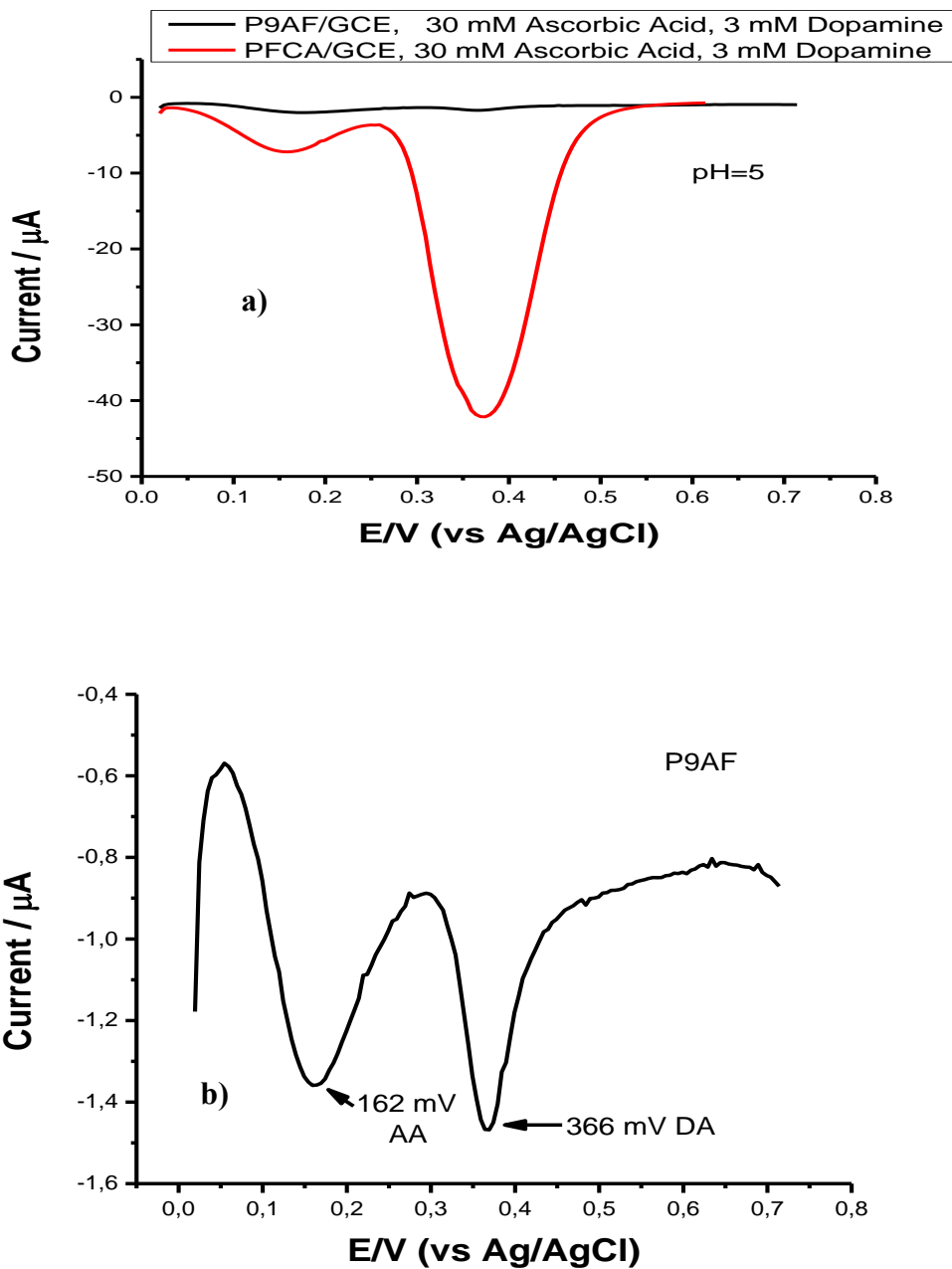


Figure 3.42. (a) The comparison of the responses of **P9AF/GCE** and **PFCA/GCE** to the **15.0 mM AA** and **3.0 mM DA** in pH=5 phthalate buffer solution containing 0.1 M $\text{KCl}_{(\text{aq})}$. (b) For clarity DPV of the **P9AF/GCE** is presented in a larger scale.

Although there are a number of reports in the literature on the detection of **DA** in the presence of **AA** using **PEDOT** modified electrodes [91,93-95], there is no report on

this issue using **PFCA** modified electrode. Therefore, we have also compared our results, obtained in this work, by using **PEDOT** and **PFCA** modified electrodes at pH=5 medium. Figure 3.43 shows that **PFCA/GCE** gave higher peak currents than that of **PEDOT/GCE** (about 2.5 times for **DA**). Peak separations for **AA** and **DA** were observed 194 mV and 274 mV at **PFCA/GCE** and **PEDOT/GCE**.

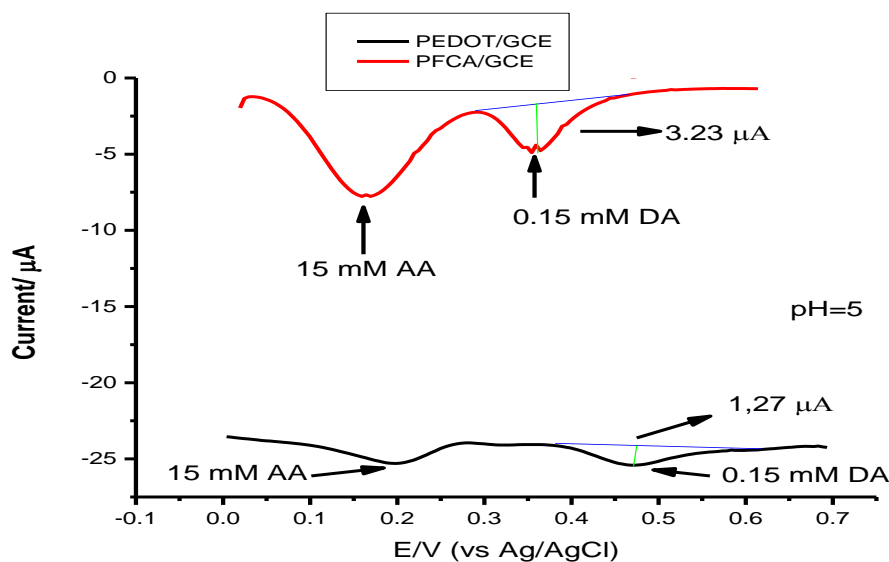


Figure 3.43. The comparison response of **PEDOT/GCE** and **PFCA/GCE** to the **15 mM AA** and **0.15 mM DA** in pH=5 phthalate buffer solution containing 0.1 M $\text{KCl}_{(\text{aq})}$.

Table 3.1 shows comparison the detection limit and linear range of this study for **DA** in the presence of **AA** with the other reported modified electrodes. These comparisons showed that our modified electrode has a reasonable linear range and the detection limit for **DA** in the presence of excess **AA**.

Table 3.1. Comparison of the response characteristics of different modified electrodes for the determination of **DA** in the presence of **AA**.

Electrode Materials	Linear Range (μM)	Detection Limit (μM)	Medium	Reference
Poly(p-nitrobenzenazo resorcinol)/GCE	5-25	0.3	pH=4	[72]
Polypyrrole-Ferrocyanide/CPE ^a	200-950	15.1	pH=6	[96]
Nafion [®] -Cobalt Hexacyanoferrate/GCE	12-500	8.9	1 M NaCl	[97]
Tyrosinase-SWCNT ^b -Polypyrrole/GCE	5-50	5.0	pH=6.5	[98]
Poly(9-fluorene carboxylic acid)/GCE	30-1500	5.2	pH= 4	This work

^a Carbon paste electrode

^b Single wall carbon nanotube

3.11. Analysis of DA in Real Sample

The analytical application of proposed method was tested using dopamine hydrochloride injection (40 mg mL^{-1}) (40000 ppm) ampoule. A calibration plot was produced from **DA** solutions and two different known concentrations of solution from dopamine hydrochloride injection ampoule were prepared. All dilutions were made using pH=4 phthalate buffer solution. The current responses from dopamine drug were measured and their concentrations were estimated by using the calibration plot. The results shown in Table 3.2 gave good recovery, indicating reliability of the method.

Table 3.2. Determination of **DA** in dopamine hydrochloride injection ampoule.

Sample No	DA Added (ppm)	DA Found (ppm)	Recovery (%)
1	9.45	8.88	94.0
2	17.0	16.44	96.7

CHAPTER 4

CONCLUSIONS

The main aim of this study was to prepare different modified GCEs and to investigate their electrocatalytic activities toward dopamine in the presence of excess amount of ascorbic acid. The unmodified GCEs showed one overlapped oxidation peak for AA and DA mixture in all media. For this reason, different monomers were electropolymerized on GCEs to prevent interference effect of AA in DA detection.

The first part of the study covered polyoxometalates (POMs) immobilization into the PEDOT matrix during electrochemical polymerization of EDOT. Electrocatalytic effect of POMs doped PEDOT/GCEs were investigated. The results showed that PEDOT-POM/GCEs showed higher peak currents for DA than that of PEDOT/GCE. However, the main limitation was that POMs gave more meaningful results only in acidic medium and only when one oxidation or reduction potential peaks of the POM superimposed with that of the analyte. Therefore, the usage of the POM did not make any contribution to dopamine determination in neutral conditions.

The second part of this thesis was related to the 9-amino fluorene (9AF) which was electropolymerized to form poly (9-amino fluorene) (**P9AF**) on GCE. Characterization of **P9AF** were achieved by using UV-VIS spectrophotometer and FT-IR spectroscopic techniques. Comparison of the FT-IR spectra of monomer and its corresponding polymer revealed that polymerization occurred via 2 (C) and 7 (C) positions. **P9AF/GCE** provided separation of **AA** and **DA** oxidation potentials at pH=4 and pH=5 medium. However, interference effect of **AA** could not be prevented in acidic and neutral pH values. Therefore, another polymer **PFCA**, having weak acid substituent group, was used to overcome interference problem. For this purpose, the monomer **FCA** was electropolymerized on GCE via potential cycling. The polymer

film obtained in BFEE-TFA (70/30; v/v) mixture was characterized using UV-VIS and FT-IR spectroscopic techniques. After finding that **PFCA/GCE** provided good separation of **AA** and **DA** oxidation potentials at all pH values, used in this study, the calibration studies for **DA** in the presence of excess **AA** were conducted at pH<1, pH=4 and pH=5. The highest peak current for **DA** was obtained at pH=4. For this reason, the rest of studies was performed at pH=4. The detection limit was calculated as 5.2 μ M for the concentration range 0.03 mM to 1.50 mM **DA** in the presence of 15.0 mM **AA** at pH=4 phthalate buffer solution containing 0.1 M KCl. Stability studies revealed that there was only 7% decrease in the **DA** oxidation current after 3 days keeping the electrode under ambient conditions.

The comparison of the results obtained utilizing three kinds of polymer to modify GCEs demonstrated that **PFCA** modified electrode gave higher peak currents for **DA** than that of **P9AF** and **PEDOT**. Moreover, **PFCA/GCE** showed good recovery values for DA in real samples.

REFERENCES

- [1] R. C. Alkire, D. M. Kolb, J. Lipkowski and P. N. Ross, *Chemically Modified Electrodes*, Weinheim: Wiley-VCH, 2009.
- [2] S. A. Wring and J. P. Hart, "Chemically modified, carbon-based electrodes and their application as electrochemical sensors for the analysis of biologically important compounds," *Analyst*, vol. 117, no. 8, pp. 1215-1229, 1992.
- [3] M. Gerard, A. Chaubey and B. D. Malhotra, "Application of Conducting Polymers to Biosensors," *Biosensors and Bioelectronics*, vol. 17, no. 5, pp. 345-359, 2002.
- [4] J. R. Fried, *Polymer Science and Technology*, Massachusetts: Prentice Hall Professional Technical Reference, 2007.
- [5] H. Shirakawa, E. J. Louis, A. G. MacDiarmid, C. K. Chiang and A. J. Heeger, "Synthesis of electrically conducting organic polymers: halogen derivatives of polyacetylene, $(CH)_x$," *Journal of the Chemical Society, Chemical Communications*, pp. 578-580, 1977.
- [6] U. Lange, N. V. Roznyatovskaya and V. M. Mirsky, "Conducting Polymers in Chemical Sensors and Arrays," *Analytica Chimica Acta*, vol. 614, no. 1, pp. 1-26, 2008.
- [7] N. K. Guimard, N. Gomez and C. E. Schmidt, "Conducting polymers in biomedical engineering," *Progress in Polymer Science*, vol. 32, no. 8-9, pp. 876-921, 2007.
- [8] G. Anguera and D. S. García, "Conjugated polymers: Synthesis and applications in optoelectronics," *Afinidad*, vol. 71, no. 568, pp. 251-262, 2014.
- [9] M. Ates, T. Karazehir and A. S. Sarac, "Conducting Polymers and their Applications," *Current Physical Chemistry*, vol. 2, no. 3, pp. 224-240, 2012.
- [10] N. J. Pinto, A. T. Johnson, A. G. MacDiarmid, C. H. Mueller, N. Theofylaktos, D. C. Robinson and F. A. Miranda, "Electrospun polyaniline/polyethylene oxide

nanofiber field-effect transistor," *Applied Physics Letters*, vol. 83, no. 20, pp. 4244-4246, 2003.

[11] A. C. Grimsdale, K. . L. Chan, R. E. Martin, P. G. Jokisz and A. B. Holmes, "Synthesis of Light-Emitting Conjugated Polymers for Applications in Electroluminescent Devices," *Chemical Reviews*, vol. 109, no. 3, pp. 897-1091, 2009.

[12] T. K. Das and S. Prusty, "Review on Conducting Polymers and Their Applications," *Polymer-Plastics Technology and Engineering*, vol. 51, no. 14, pp. 1487-1500, 2012.

[13] B. Adhikari and S. Majumdar, "Polymers in sensor applications," *Progress in Polymer Science*, vol. 29, no. 7, pp. 699-766, 2004.

[14] N. Gupta, S. Sharma, I. A. Mir and D. Kumar, "Advances in Sensors Based on Conducting Polymers," *Journal of Scientific and Industrial Research*, vol. 65, no. 7, pp. 549-557, 2006.

[15] J. L. Duvail, Y. Long, P. Retho, G. Louarn, L. Dauginet De Pra and S. Demoustier-Champagne, "Enhanced Electroactivity and Electrochromism in PEDOT Nanowires," *Molecular Crystals and Liquid Crystals*, vol. 485, no. 1, pp. 835-842, 2008.

[16] W. J. Sung and Y. H. Bae, "A Glucose Oxidase Electrode Based on Electropolymerized Conducting Polymer with Polyanion–Enzyme Conjugated Dopant," *Analytical Chemistry*, vol. 72, no. 9, pp. 2177-2181, 2000.

[17] G. Inzelt, "Applications of Conducting Polymers," in *Conducting Polymers*, Greifswald, Springer-Verlag Berlin Heidelberg, 2012, pp. 274-276.

[18] K. Kapur, "Conducting Polymer," 25 May 2018. [Online]. Available: <https://tr.scribd.com/doc/52588756/CONDUCTING-POLYMER>. [Accessed 26 June 2018].

- [19] L. B. Groenendaal, F. Jonas, D. Freitag, H. Pielartzik and J. R. Reynolds, "Poly(3,4-ethylenedioxythiophene) and Its Derivatives: Past, Present, and Future," *Advanced Materials*, vol. 12, no. 7, pp. 481-494, 2000.
- [20] H. Y. Byun, I. J. Chung, H. K. Shim and C. Y. Kim, "The Effects of Alkyl Side-Chain Length and Shape of Polyfluorenes on the Photoluminescence Spectra and the Fluorescence Lifetimes of Polyfluorene Blends with Poly(n-vinylcarbazole)," *Chemical Physics Letters*, vol. 393, no. 1-3, pp. 197-203, 2004.
- [21] T. Ouisse and O. Stéphan, "Electrical Bistability of Polyfluorene Devices," *Organic Electronics*, vol. 5, no. 5, pp. 251-256, 2004.
- [22] G. Nie, T. Cai, J. Xu and S. Zhang, "Low-Potential Facile Electrosyntheses of High-Quality Free-Standing Poly(fluorene-9-carboxylic acid) Films," *Electrochemistry Communications*, vol. 10, no. 2, pp. 186-189, 2007.
- [23] B. Bezgin, A. Cihaner and A. M. Önal, "Electrochemical Polymerization of 9-fluorencarboxylic Acid and its Electrochromic Device Application," *Thin Solid Films*, vol. 516, no. 21, pp. 7329-7334, 2008.
- [24] C. Fan, J. Xu, W. Chen and B. Dong, "Electrosynthesis and Characterization of Water-Soluble Poly(9-aminofluorene) with Good Fluorescence Properties," *The Journal of Physical Chemistry C*, vol. 112, no. 31, pp. 12012-12017, 2008.
- [25] M. Sadakane and E. Steckhan, "Electrochemical Properties of Polyoxometalates as Electrocatalysts," *Chemical Reviews*, vol. 98, no. 1, pp. 219-237, 1998.
- [26] C. E. Housecroft and A. G. Sharpe, "d-Block Metal Chemistry: The Second and Third Row Metals," in *Inorganic Chemistry*, Pearson Prentice Hall, 2004, pp. 660-662.
- [27] J. F. Keggin, "The Structure and Formula of 12-Phosphotungstic Acid," *The Royal Society*, vol. 144, no. 851, pp. 75-100, 1934.

- [28] K. N. Rao, C. Srilakshmi, K. M. Reddy, B. H. Babu, N. Lingaiah and P. S. Prasad, " Heteropoly Compounds as Ammoxidation Catalysts," in *Environmentally Benign Catalysts: For Clean Organic Reactions*, Baroda, Springer, 2013, pp. 11-55.
- [29] B. Dawson, "The Structure of the 9(18)-Heteropoly Anion in Potassium 9(18)-Tungstophosphate, $K_6(P_2W_{18}O_{62}) \cdot 14H_2O$," *Acta Crystallographica*, vol. 6, no. 2, pp. 113-126, 1953.
- [30] L. E. Briand, G. T. Baronetti and H. J. Thomas, "The State of the Art on Wells–Dawson Heteropoly-Compounds A Review of Their Properties and Applications," *Applied Catalysis A: General*, vol. 256, no. 1-2, pp. 37-50, 2003.
- [31] A. Malinauskas, "Electrocatalysis at Conducting Polymers," *Synthetic Metals*, vol. 107, no. 2, pp. 75-83, 1999.
- [32] D. E. Katsoulis, "A Survey of Applications of Polyoxometalates," *Chemical Reviews*, vol. 98, no. 1, pp. 359-388, 1998.
- [33] S. Dong and M. Liu, "Preparation and Properties of Polypyrrole Film Doped with a Dawson-Type Heteropolyanion," *Electrochimica Acta*, vol. 39, no. 7, pp. 947-951, 1994.
- [34] M. C. Pham, S. Bouallala, L. A. Lé, V. M. Dang and P. C. Lacaze, "Study of a Heteropolyanion-Doped Poly(5-amino-1-naphthol) Film Electrode and Its Catalytic Activity," *Electrochimica Acta*, vol. 42, no. 3, pp. 439-447, 1997.
- [35] T. P. Wijesekera, J. E. Lyons and P. E. Ellis, "Wells-Dawson Type Heteropolyacids, Their Preparation and Use as Oxidation Catalysts". United States Patent 6,060,419, 9 May 2000.
- [36] H. Wu, "Contribution to the Chemistry of Phosphomolybdic Acids, Phosphotungstic Acids, and Allied Substances," *Journal of Biological Chemistry*, vol. 43, pp. 189-220, 1920.

- [37] S. Gao, . R. Cao, W. Bi, X. Li and Z. Lin, "Porous Structures Constructed from [SiMo₁₂O₄₀] and [SiW₁₂O₄₀] Keggin Units," *Microporous and Mesoporous Materials*, vol. 80, no. 1-3, pp. 139-145, 2005.
- [38] X. Wang, Z. Kang, . E. Wang and C. Hu, "Preparation, Electrochemical Property and Application in Chemically Bulk-Modified Electrode of a Hybrid Inorganic–Organic Silicomolybdate Nanoparticles," *Material Letters*, vol. 56, no. 4, pp. 393-396, 2002.
- [39] L. Li and C. Sun, "Fabrication of Multilayer Films Containing 1:12 Molybdosilicate Anions Based on Electrostatic Interaction and Their Electrochemistry," *Materials Chemistry and Physics*, vol. 69, no. 1-3, pp. 45-52, 2001.
- [40] E. Itabashi, "Medium Effects on the Redox Properties of 12-Molybdophosphate and 12-Molybdosilicate," *Bulletin of the Chemical Society of Japan*, vol. 60, no. 4, pp. 1333-1336, 1987.
- [41] P. Wang, X. Wang, X. Jing and G. Zhu, "Sol–gel-Derived, Polishable, 1:12-Phosphomolybdic Acid-Modified Ceramic-Carbon Electrode and Its Electrocatalytic Oxidation of Ascorbic Acid," *Analytica Chimica Acta*, vol. 424, no. 1, pp. 51-56, 2000.
- [42] K. Unoura and N. Tanaka, "Comparative Study of the Electrode Reactions of 12-Molybdosilicate and 12-Molybdophosphate," *Inorganic Chemistry*, vol. 22, pp. 2963-2964, 1983.
- [43] K. C. Berridge and T. E. Robinson, "What is the role of dopamine in reward: hedonic impact, reward learning, or incentive salience?," *Brain Research Reviews*, vol. 28, no. 3, pp. 309-369, 1998.
- [44] J. Moncrieff, *The Myth of the Chemical Cure. A Critique of Psychiatric Drug Treatment*, New York: Palgrave Macmillan, 2008.

- [45] R. P. Nikolajsen and Å. . M. Hansen, "Analytical Methods for Determining Urinary Catecholamines in Healthy Subjects," *Analytica Chimica Acta*, vol. 449, no. 1-2, pp. 1-15, 2001.
- [46] K. Vuorensola, H. Siren and U. Karjalainen, "Determination of Dopamine and Methoxycatecholamines in Patient Urine by Liquid Chromatography with Electrochemical Detection and by Capillary Electrophoresis Coupled with Spectrophotometry and Mass Spectrometry," *Journal of Chromatography B*, vol. 788, no. 2, pp. 277-289, 2003.
- [47] H. X. Zhao, H. Mu, Y. H. Bai, H. Yu and Y. M. Hu, "A Rapid Method for the Determination of Dopamine in Porcine Muscle by Pre-Column Derivatization and HPLC with Fluorescence Detection," *Journal of Pharmaceutical Analysis*, vol. 1, no. 3, pp. 208-212, 2011.
- [48] H. R. Zare, N. Rajabzadeh, N. Nasirizadeh and M. M. Ardakani, "Voltammetric Studies of an Oracet Blue Modified Glassy Carbon Electrode and Its Application for the Simultaneous Determination of Dopamine, Ascorbic Acid and Uric Acid," *Journal of Electroanalytical Chemistry*, vol. 589, no. 1, pp. 60-69, 2006.
- [49] D. R. Shankaran, K. Iimura and T. Kato, "Simultaneous Determination of Ascorbic Acid and Dopamine at a Sol–Gel Composite Electrode," *Sensors and Actuators B: Chemical*, vol. 94, no. 1, pp. 73-80, 2003.
- [50] T. Selvaraju and R. Ramaraj , "Simultaneous Determination of Ascorbic acid, Dopamine and Serotonin at Poly(phenosafranin) Modified Electrode," *Electrochemistry Communications*, vol. 5, no. 8, pp. 667-672, 2003.
- [51] H. R. Zare, N. Nasirizadeh and M. M. Ardakani, "Electrochemical Properties of a Tetrabromo-p-Benzoquinone Modified Carbon Paste Electrode. Application to the Simultaneous Determination of Ascorbic acid, Dopamine and Uric Acid," *Journal of Electroanalytical Chemistry*, vol. 577, no. 1, pp. 25-33, 2005.

- [52] K. Iqbal, A. Khan and M. Khattak, "Biological Significance of Ascorbic Acid (Vitamin C) in Human Health – A Review," *Pakistan Journal of Nutrition*, vol. 3, no. 1, pp. 5-13, 2004.
- [53] S. Görög, "Vitamin C (ascorbic acid)," in *Ultraviolet-Visible Spectrophotometry in Pharmaceutical Analysis*, Boca Raton, CRC Press Taylor & Francis Group, 1995, pp. 351-354.
- [54] H. S. Mahmood and R. R. Ahmad, "High Performance Liquid Chromatographic Determination of Ascorbic Acid in Pharmaceutical Preparations, Fruit Juices and Human Serum," *Rafidain Journal of Science*, vol. 27, no. 3, pp. 79-92, 2018.
- [55] Z.-H. Sheng, X.-Q. Zheng, J.-Y. Xu, W.-J. Bao, F.-B. Wang and X.-H. Xia, "Electrochemical Sensor based on Nitrogen Doped Graphene: Simultaneous Determination of Ascorbic Acid, Dopamine and Uric Acid," *Biosensors and Bioelectronics*, vol. 34, no. 1, pp. 125-131, 2012.
- [56] C. R. Raj, K. Tokuda and T. Ohsaka, "Electroanalytical Applications of Cationic Self-Assembled Monolayers: Square-Wave Voltammetric Determination of Dopamine and Ascorbate," *Bioelectrochemistry*, vol. 53, no. 2, pp. 183-191, 2001.
- [57] D. A. Skoog, F. J. Holler and S. R. Crouch, "An Introduction to Electroanalytical Chemistry," in *Principles of Instrumental Analysis*, Belmont, Brooks/Cole, 2006, pp. 628-653.
- [58] D. A. Skoog, D. M. West, F. J. Holler and S. R. Crouch, "Electrochemical Methods," in *Fundamentals of Analytical Chemistry*, Belmont, Cengage Learning, 2003, pp. 487-743.
- [59] S. P. Kounaves, "Voltammetric Techniques," in *Handbook of Instrumental Techniques for Analytical Chemistry*, New Jersey, Prentice Hall PTR, 1997, pp. 711-729.
- [60] P. T. Kissinger and W. R. Heineman, "Cyclic Voltammetry," *Journal of Chemical Education*, vol. 60, no. 9, pp. 702-706, 1983.

- [61] J. Sochor, J. Dobes, O. Krystofova, P. Babula, M. Pohanka, T. Jurikova, O. Zitka, V. Adam, B. Klejdus and R. Kizek, "Electrochemistry as a Tool for Studying Antioxidant Properties," *International Journal of Electrochemical Science*, vol. 8, no. 6, pp. 8464-8489, 2013.
- [62] D. A. Skoog, F. J. Holler and S. R. Crouch, "Voltammetry," in *Principles of Instrumental Analysis*, Belmont, Brooks/Cole, 2006, pp. 716-753.
- [63] G. A. Edwards, A. J. Bergren and . M. D. Porter, "Chemically Modified Electrodes," in *Handbook of Electrochemistry*, Las Cruces, Elsevier, 2007, pp. 295-327.
- [64] R. A. Durst, A. J. Baumner, R. W. Murray, R. P. Buck and C. P. Andrieux, "Chemically Modified Electrodes: Recommended Terminology and Definitions," *Pure and Applied Chemistry*, vol. 69, no. 6, pp. 1317-1323, 1997.
- [65] W. Kutner, J. Wang, M. L'her and R. P. Buck, "Analytical Aspects of Chemically Modified Electrodes: Classification, Critical Evaluation and Recommendations," *Pure and Applied Chemistry*, vol. 70, no. 6, pp. 1301-1318, 1998.
- [66] M. Sajid, M. K. Nazal, M. Mansha, A. Alsharaa, S. M. Jillani and C. Basheer, "Chemically Modified Electrodes for Electrochemical Detection of Dopamine in the presence of Uric Acid and Ascorbic Acid: A Review," *Trends in Analytical Chemistry*, vol. 76, pp. 15-29, 2016.
- [67] F. Banica and G. Banica, "What are Chemical Sensors?," in *Chemical Sensors and Biosensors: Fundamentals and Applications*, Trondheim, John Wiley & Sons, 2012, pp. 1-20.
- [68] M. Ates, A. S. Sarac, C. M. Turhan and N. E. Ayaz, "Polycarbazole Modified Carbon Fiber Microelectrode: Surface Characterization and Dopamine Sensor," *Fibers and Polymers*, vol. 10, no. 1, pp. 46-52, 2009.
- [69] R. M. Wightman, L. J. May and A. C. Michael, "Detection of Dopamine Dynamics in the Brain," *Analytical Chemistry*, vol. 60, no. 13, pp. 769A-779A, 1988.

- [70] J. Maciejewska, K. Pisarek, I. Bartosiewicz, P. Krysinski, K. Jackowska and A. T. Bieganski, "Selective Detection of Dopamine on Poly(indole-5-carboxylic acid)/Tyrosinase Electrode," *Electrochimica Acta*, vol. 56, no. 10, pp. 3700-3706, 2011.
- [71] A. Balamurugan and S.-M. Chen, "Poly(3,4-ethylenedioxythiophene-co-(5-amino-2-naphthalenesulfonic acid)) (PEDOT-PANS) Film Modified Glassy Carbon Electrode for Selective Detection of Dopamine in the presence of Ascorbic Acid and Uric Acid," *Analytica Chimica Acta*, vol. 596, no. 1, pp. 92-98, 2007.
- [72] X. Lin, Y. Zhang, W. Chen and P. Wu, "Electrocatalytic Oxidation and Determination of Dopamine in the presence of Ascorbic Acid and Uric Acid at a Poly (p-nitrobenzenazo resorcinol) Modified Glassy Carbon Electrode," *Sensors and Actuators B: Chemical*, vol. 122, no. 1, pp. 309-314, 2007.
- [73] M. D. Rubianes and G. A. Rivas, "Highly Selective Dopamine Quantification Using a Glassy Carbon Electrode Modified with a Melanin-type Polymer," *Analytica Chimica Acta*, vol. 440, no. 2, pp. 99-108, 2001.
- [74] P. . R. Roy, T. Okajima and T. Ohsaka, "Simultaneous Electroanalysis of Dopamine and Ascorbic Acid using Poly (N,N-dimethylaniline)-modified Electrodes," *Bioelectrochemistry*, vol. 59, no. 1-2, pp. 11-19, 2003.
- [75] X. Zheng, X. Zhou, X. Ji, R. Lin and W. Lin, "Simultaneous Determination of Ascorbic Acid, Dopamine and Uric Acid using Poly(4-aminobutyric acid) Modified Glassy Carbon Electrode," *Sensors and Actuators B: Chemical*, vol. 178, pp. 359-365, 2013.
- [76] E. A. Khudaish, F. Al-Nofli, J. A. Rather, M. Al-Hinaai, K. Laxman, H. H. Kyaw and S. Al-Harthy, "Sensitive and Selective Dopamine Sensor based on Novel Conjugated Polymer Decorated with Gold Nanoparticles," *Journal of Electroanalytical Chemistry*, vol. 761, pp. 80-88, 2016.

- [77] G. . Turdean, A. Curulli, I. C. Popescu, C. Rosu and G. Palleschi, "Electropolymerized Architecture Entrapping a Trilacunary Keggin-Type Polyoxometalate for Assembling a Glucose Biosensor," *Electroanalysis*, vol. 14, no. 22, pp. 1550-1556, 2002.
- [78] A. Balamurugan and S.-M. Chen, "Silicomolybdate-Doped PEDOT Modified Electrode: Electrocatalytic Reduction of Bromate and Oxidation of Ascorbic *Electroanalysis*, vol. 19, no. 15, pp. 1616-1622, 2007.
- [79] Zhang, G. Lai, A. Yu and H. Zhang, "A Glassy Carbon Electrode Modified with a Polyaniline Doped with Silicotungstic Acid and Carbon Nanotubes for the Sensitive Amperometric Determination of Ascorbic Acid," *Microchimica Acta*, vol. 180, no. 5-6, pp. 437-443, 2013.
- [80] J. Xu, S. Xu, S. Feng, Y. Hao and J. Wang, "Electrochemical Sensor for Detecting both Oxidizing and Reducing Compounds based on Poly(ethyleneimine)/Phosphotungstic Acid Multilayer Film Modified Electrode," *Electrochimica Acta*, vol. 174, pp. 706-711, 2015.
- [81] Y.-T. Chang, K.-C. Lin and S.-M. Chen, "Preparation, Characterization and Electrocatalytic Properties of Poly(luminol) and Polyoxometalate Hybrid Film Modified Electrode," *Electrochimica Acta*, vol. 51, no. 3, pp. 450-461, 2005.
- [82] D. Thirumalai, D. Subramani, J.-H. Yoon, J. Lee, H.-J. Paik, S.-C. Chang, "De-Bundled Single-Walled Carbon Nanotube Modified Sensors for Simultaneous Differential Pulse Voltammetric Determination of Ascorbic Acid, Dopamine, and Uric Acid," *New Journal of Chemistry*, vol. 42, no. 4, pp. 2432-2438, 2018.
- [83] A. H. Ismail, M. N. Mustafa, A. H. Abdullah, R. M. Zawawi and Y. Sulaiman, "Effect of Electropolymerization Potential on the Properties of PEDOT/ZnO Thin Film Composites," *Journal of The Electrochemical Society*, vol. 163, no. 2, pp. G7-G14, 2016.

- [84] M. Lira-Cantú and P. Gómez-Romero, "Electrochemical and Chemical Syntheses of the Hybrid Organic-Inorganic Electroactive Material Formed by Phosphomolybdate and Polyaniline. Application as Cation-Insertion Electrodes," *Chemistry of Materials*, vol. 10, no. 3, pp. 698-704, 1998.
- [85] C. Sun and J. Zhang, "Fabrication and Electrochemical Behavior of Multilayer Films Containing 1:12 Phosphomolybdic Anions and Their Electrocatalytic Oxidation of Ascorbic Acid," *Electrochimica Acta*, vol. 43, no. 8, pp. 943-950, 1998.
- [86] G. Nie, Q. Guo, Y. Zhang and S. Zhang, "Direct Electrosynthesis and Characterization of A New Soluble Polyfluorene Derivative Containing Carboxyl Group in Boron Trifluoride Diethyl Etherate," *European Polymer Journal*, vol. 45, no. 9, pp. 2600-2608, 2009.
- [87] S. Soyleyici, M. Karakus and M. Ak, "Transparent-Blue Colored Dual Type Electrochromic Device: Switchable Glass Application of Conducting Organic-Inorganic Hybrid Carbazole Polymer," *Journal of The Electrochemical Society*, vol. 163, no. 8, pp. H679-H683, 2016.
- [88] A. Cihaner, S. Tirkeş and A.M. Önal, "Electrochemical Polymerization of 9-Fluorenone," *Journal of Electroanalytical Chemistry*, vol. 568, pp. 151-156, 2004.
- [89] R. L. Hunt and B. S. Ault, "Spectroscopic Influences of Ion Pairing: Infrared Matrix Isolation Spectra of the $M^+ BF_4^-$ Ion Pair and Its Chlorine-Fluorine Analogs," *Spectrochimica Acta Part A: Molecular Spectroscopy*, vol. 37, no. 2, pp.63-69, 1981.
- [90] A. J. Kresge, I. G. Pojarlieff and E. M. Rubinstein, "The Acidity Constant of Fluorene-9-Carboxylic Acid in Aqueous Solution. Determination of the pK_a of a Sparingly Soluble Substance," *Canadian Journal of Chemistry*, vol. 71, no. 2, pp.227-229, 1993.
- [91] V. S. Vasantha and S.M. Chen, "Electrocatalysis and Simultaneous Detection of Dopamine and Ascorbic Acid using Poly(3,4-ethylenedioxy)thiophene Film Modified Electrodes," *Journal of Electroanalytical Chemistry*, vol. 592, no. 1, pp.77-87, 2006.

- [92] C. A. Martinez-Huitle, M. Cerro-Lopez and M. A. Quiroz, "Electrochemical Behaviour of Dopamine at Covalent Modified Glassy Carbon Electrode with L-Cysteine: Preliminary Results, " *Materials Research*, vol. 12, no. 4, pp.375-384, 2009.
- [93] S. S. Kumar, J. Mathiyarasu, K.L. Phani and V. Yegnaraman, "Simultaneous Determination of Dopamine and Ascorbic Acid on Poly (3,4-ethylenedioxythiophene) Modified Glassy Carbon Electrode, " *Journal of Solid State Electrochemistry*, vol. 10, no. 11, pp. 905-913, 2006.
- [94] G. Xu, B. Li, X.T. Cui, L. Ling and X. Luo, "Electrodeposited Conducting Polymer PEDOT Doped with Pure Carbon Nanotubes for the Detection of Dopamine in the Presence of Ascorbic Acid, " *Sensors and Actuators B: Chemical*, vol. 188, pp. 405-410, 2013.
- [95] F. S. Belaidi, A. Civelas, V. Castagnola, A. Tsopela, L. Mazonq, P. Gros, J. Launay and P. Temple-Boyer, "PEDOT-Modified Integrated Microelectrodes for the Detection of Ascorbic Acid, Dopamine and Uric Acid, " *Sensors and Actuators B: Chemical*, vol. 214, pp. 1-9, 2015.
- [96] J.-B. Raoof, R. Ojani and S. Rashid-Nadimi, "Voltammetric Determination of Ascorbic Acid in the Same Sample at the Surface of a Carbon Paste Electrode Modified with Polypyrrole/Ferrocyanide Films, " *Electrochimica Acta*, vol. 50, no. 24, pp. 4694-4698, 2005.
- [97] S. L. Castro, R. J. Mortimer, M. F. De Oliveira and N. R. Stradiotto, "Electrooxidation and Determination of Dopamine Using a Nafion[®]-Cobalt Hexacyanoferrate Film Modified Electrode, " *Sensors*, vol. 8, no. 3, pp. 1950-1959, 2008.
- [98] K. Min and Y. J. Yoo, "Amperometric Detection of Dopamine based on Tyrosinase-SWNTs-Ppy Composite Electrode, " *Talanta*, vol. 80, no. 2, pp. 1007-1011, 2009.